NAVAL POSTGRADUATE SCHOOL

MONTEREY, CALIFORNIA

THESIS

HYBRID HARD AND SOFT DECISION DECODING OF REED-SOLOMON CODES FOR *M*-ARY FREQUENCY-SHIFT KEYING

by

Konstantinos Spyridis

June 2010

Thesis Advisor: Clark Robertson
Second Reader: Frank Kragh
                                                    Roberto Cristi

Approved for public release; distribution unlimited

THIS PAGE INTENTIONALLY LEFT BLANK

REPORT DOCUMENTATION PAGE		*Form Approved OMB No. 0704-0188*

Public reporting burden for this collection of information is estimated to average 1 hour per response, including the time for reviewing instruction, searching existing data sources, gathering and maintaining the data needed, and completing and reviewing the collection of information. Send comments regarding this burden estimate or any other aspect of this collection of information, including suggestions for reducing this burden, to Washington headquarters Services, Directorate for Information Operations and Reports, 1215 Jefferson Davis Highway, Suite 1204, Arlington, VA 22202-4302, and to the Office of Management and Budget, Paperwork Reduction Project (0704-0188) Washington DC 20503.

1. AGENCY USE ONLY *(Leave blank)*	2. REPORT DATE June 2010	3. REPORT TYPE AND DATES COVERED Master's Thesis	
4. TITLE AND SUBTITLE Hybrid Hard and Soft Decision Decoding of Reed–Solomon Codes for *M*-ary Frequency-Shift Keying		5. FUNDING NUMBERS	
6. AUTHOR(S) Konstantinos Spyridis			
7. PERFORMING ORGANIZATION NAME(S) AND ADDRESS(ES) Naval Postgraduate School Monterey, CA 93943-5000		8. PERFORMING ORGANIZATION REPORT NUMBER	
9. SPONSORING /MONITORING AGENCY NAME(S) AND ADDRESS(ES) N/A		10. SPONSORING/MONITORING AGENCY REPORT NUMBER	

11. SUPPLEMENTARY NOTES The views expressed in this thesis are those of the author and do not reflect the official policy or position of the Department of Defense or the U.S. Government. IRB Protocol number _____.

12a. DISTRIBUTION / AVAILABILITY STATEMENT Approved for public release; distribution unlimited	12b. DISTRIBUTION CODE

13. ABSTRACT (maximum 200 words)

All modern communication systems use some form of forward error correction coding. Generally, coding gain is improved when soft decision decoding is used instead of hard decision decoding. While soft decision decoding is a mature technology for convolutional codes, practical soft decision decoding for the commonly used Reed-Solomon (RS) non-binary block code has only recently been developed and is currently limited to use with bandwidth efficient modulation schemes such as *M*-ary phase-shift keying. Since JTIDS/Link-16 uses quasi-orthogonal, cyclic code-shift keying (CCSK), in this thesis, soft decision decoding of RS encoded symbols is extended to *M*-ary frequency-shift keying, a power efficient modulation scheme. In addition, the soft decision decoding scheme recently developed, actually a hybrid hard decision-soft decision (HD SD) decoding scheme, is improved for both bandwidth efficient and power efficient modulation schemes. Finally, the effect of the hybrid HD SD decoding technique on signals corrupted by additive white Gaussian noise (AWGN) and other interference, including Pulse Noise Interference (PNI), is examined. The performances of various systems using the hybrid HD SD decoding technique were investigated using both analysis and simulation. It was found that HD SD decoding is generally effective in minimizing the degradation in system performance due to PNI but has only a small benefit when only AWGN is present.

14. SUBJECT TERMS Hybrid Reed-Solomon (RS) coding, Orthogonal signaling, Additive White Gaussian Noise (AWGN), Pulse-Noise Interference (PNI), coherent detection, noncoherent detection.			15. NUMBER OF PAGES 129
			16. PRICE CODE
17. SECURITY CLASSIFICATION OF REPORT Unclassified	18. SECURITY CLASSIFICATION OF THIS PAGE Unclassified	19. SECURITY CLASSIFICATION OF ABSTRACT Unclassified	20. LIMITATION OF ABSTRACT UU

THIS PAGE INTENTIONALLY LEFT BLANK

HYBRID HARD AND SOFT DECISION DECODING OF REED-SOLOMON CODES FOR *M*-ARY FREQUENCY-SHIFT KEYING

Konstantinos Spyridis
Lieutenant, Hellenic Navy
B.S., Hellenic Naval Academy, 1999

Submitted in partial fulfillment of the
requirements for the degrees of

ELECTRICAL ENGINEER
and
MASTER OF SCIENCE IN ELECTRICAL ENGINEERING

from the

NAVAL POSTGRADUATE SCHOOL
June 2010

Author: Konstantinos Spyridis

Approved by: R. Clark Robertson
Thesis Advisor

Frank Kragh
Second Reader

Roberto Cristi
Second Reader

R. Clark Robertson
Chairman, Department of Electrical and Computer Engineering

iii

THIS PAGE INTENTIONALLY LEFT BLANK

ABSTRACT

All modern communication systems use some form of forward error correction coding. Generally, coding gain is improved when soft decision decoding is used instead of hard decision decoding. While soft decision decoding is a mature technology for convolutional codes, practical soft decision decoding for the commonly used Reed-Solomon (RS) non-binary block code has only recently been developed and is currently limited to use with bandwidth efficient modulation schemes such as M-ary phase-shift keying. Since JTIDS/Link-16 uses quasi-orthogonal, cyclic code-shift keying (CCSK), in this thesis, soft decision decoding of RS encoded symbols is extended to M-ary frequency-shift keying, a power efficient modulation scheme. In addition, the soft decision decoding scheme recently developed, actually a hybrid hard decision-soft decision (HD SD) decoding scheme, is improved for both bandwidth efficient and power efficient modulation schemes. Finally, the effect of the hybrid HD SD decoding technique on signals corrupted by additive white Gaussian noise (AWGN) and other interference, including Pulse Noise Interference (PNI), is examined. The performances of various systems using the hybrid HD SD decoding technique were investigated using both analysis and simulation. It was found that HD SD decoding is generally effective in minimizing the degradation in system performance due to PNI but has only a small benefit when only AWGN is present.

THIS PAGE INTENTIONALLY LEFT BLANK

TABLE OF CONTENTS

LIST OF FIGURES

x

THIS PAGE INTENTIONALLY LEFT BLANK

LIST OF TABLES

EXECUTIVE SUMMARY

System performance, including maximization of throughput, is a continuing concern of communications systems engineers. In the modern era of information systems, those needs have increased significantly. Forward error correction (FEC) techniques can dramatically improve the reliability of a communication system.

Error detection and correction codes were invented to improve communication across noisy channels. Shannon, in his 1948 paper, proved that there exists error detection and correction codes that can achieve a small probability of information bit error given that the rate of the code falls below the channel's capacity. For many years, researchers have focused their attention on FEC codes, resulting in the invention of a multitude of code families. Of all the code families discovered, one that has been applied to a wide array of real-world, engineering problems is the Reed-Solomon (RS) family of nonbinary codes. One advantage of RS codes is their ability to correct burst errors when binary modulation is used. Many of the applications are for storage devices such as CDs, DVDs, hard drives, telecommunication satellite links, Tactical Data Information Links (TADIL) and Digital Video Broadcasting (DVB). The most common RS decoding technique is algebraic hard decision (HD) decoding that utilizes either the Berlekamp–Massey (BM) algorithm or the Euclidean algorithm. For a RS (n, k) code of length n and dimension k, those algorithms are guaranteed to recover the transmitted codeword within an error radius of $(n-k+1)/2$ symbols, providing an error correction capability of $t_{BM} = (n-k)/2$ symbols when the BM algorithm is used.

While soft decision decoding is a mature technology for convolutional codes, practical soft decision decoding for the commonly used RS non-binary block code has only recently been developed. Generally, coding gain is improved when soft decision (SD) decoding is used instead of hard decision decoding. Guruswami and Sudan presented a new algebraic decoding method for RS codes that can correct errors beyond the BM decoding radius. This algorithm requires construction of a bivariate polynomial with zeros of multiplicity and estimation polynomials in the Galois field based on the received symbols. The polynomial can then be factored to give a list of possible valid

codewords. A Guruswami-Sudan (GS) decoder can successfully decode a codeword if the error is within a radius of $n - \sqrt{nk}$ symbols and provides an error correction capability of $t_{\text{GS}} = n - \sqrt{nk}$ symbols (upper bound). However, for code rates $r > 1/3$, the GS algorithm does not improve error correction capability over traditional HD decoding. Additionally, the increased complexity of the GS algorithm makes it impractical for real-time communications. A hybrid hard decision-soft decision (HD SD) decoding scheme was recently developed for use with bandwidth efficient modulation schemes such as M-ary phase-shift keying (MPSK). This novel decoding scheme does not significantly increase decoding complexity as does the GS SD algorithm.

Network-centric warfare (NCW) is an emerging theory of war applied to modern military operations in order to improve their effectiveness. To achieve this, NCW applies information age concepts to speed communications and increase situational awareness through networking. As a result, NCW transforms the efficient flow of information into combat power by linking allied forces across the battlefield, thus enabling them to employ more effective decision making during military operations. One of the most demanding requirements for the developers of NCW is to achieve communications interoperability within a multinational coalition. Interoperability is achieved with the integration of communication systems such as the digital datalinks Joint Tactical Information Distribution System (JTIDS/Link–16) and Automatic Link Establishment (ALE), the Single Channel Ground and Airborne Radio System (SINCGARS), which is a combat net radio (CNR), and satellite communications (MILSTAR). If interoperability is effectively applied, the preceding systems are significant tools in implementing NCW theory.

Since JTIDS/Link-16 uses quasi-orthogonal modulation, cyclic code-shift keying, and MILSTAR uses a noncoherent M-ary frequency-shift keying (MFSK) modulation, the hybrid hard decision-soft decision decoding scheme developed for bandwidth efficient modulation is extended in this thesis to M-ary frequency-shift keying (MFSK), a power efficient modulation scheme. In addition, the recently developed hybrid hard decision-soft decision (HD SD) decoding scheme is improved for both bandwidth efficient and power efficient modulation schemes. Finally, how noise other than additive

white Gaussian noise (AWGN), such as pulse-noise interference (PNI), is affected by hybrid HD SD decoding is examined. The performances of various systems using hybrid HD SD decoding were investigated using both analysis and simulation.

Specifically, the performance analysis and simulation of a signal encoded with a RS code and either coherently or noncoherently detected MFSK for M = 8, 16, and 32 were examined in this thesis. The simulations were performed in AWGN and PNI. For the analysis and simulations with PNI, fractions of interference time $\rho = 1, 0.4$ and 0.2 were used. Additionally, the performance of increased block lengths attained by using two channel symbols to transmit one code symbol, referred to as double-symbol modulation, were investigated. Performance obtained with hybrid HD SD decoding was compared to that obtained with HD decoding. HD SD decoding was found to be a powerful tool that provides significant coding gains and increased error correction capabilities compared to traditional HD decoding when PNI is present. The advantages of hybrid HD SD decoding are minimal when only AWGN is present. Lastly, double-symbol transmission of MFSK significantly improves performance compared to single-symbol transmission with only a small penalty in decoding time.

THIS PAGE INTENTIONALLY LEFT BLANK

LIST OF ACRONYMS AND ABBREVIATIONS

ALE	Automatic Link Establishment
ARES	Amateur Radio Emergency Service
ARQ	Automatic Request
ASD	Algebraic Soft Decision Decoding
AWGN	Additive White Gaussian Noise
BER	Bit Error Rate
BCH	Bose Chaudhuri Hocquenghem
BM	Berlekamp Massey
CalEMA	California Emergency Management Agency
CCSK	Cyclic Code Shift Keying
CNR	Combat Net Radio
DS	Direct Sequence
DSL	Digital Line Subscriber
DVB	Digital Video Broadcasting
EDAC	Error Detection and Correction
FEC	Forward Error Correction
FH	Frequency Hopped
FPGA	Field Programmable Gate Arrays
ITU	International Telecommunications Union
JTIDS	Joint Tactical Information Distribution System
JTRS	Joint Tactical Radio System
GS	Guruswami - Sudan
HD	Hard Decision
MILSTAR	Military Strategic and Tactical Relay
MFSK	M-ary Frequency Shift Keying
MHPSK	M-ary Hyper Phase Shift Keying
MPSK	M-ary Phase Shift Keying
MQAM	M-ary Quadrature Amplitude Modulation

NATO   North Atlantic Treaty Organization

NCW   Network Centric Warfare

NRZ   Non Return to Zero

PDF   Probability Distribution Function

PNI   Pulse Noise Interference

PSD   Power Spectral Density

RS   Reed Solomon

SD   Soft Decision

TADIL   Tactical Data Link

SINCGARS   Single Channel Ground and Airborne Radio System

ACKNOWLEDGMENTS

I would like to deeply thank my advisor, Professor Clark Robertson, for his invaluable guidance during this journey to knowledge and exploration. This thesis is a product of our collaboration. By adopting his attention to detail, I learned the importance of composing a technical document that is both concise and precise.

I would also like to express my appreciation to Professor Frank Kragh and Professor Roberto Cristi for evaluating this work and giving me an additional insight.

I dedicate this work to my parents, Georgio and Eleni, for the educational enlightenment that they offered me and all their support throughout my educational and professional career. Their morals and principles have always been an inspiration for my development. I would like, also, to thank my lovely sisters, Chrisa and Evi, for their continuous, loving support.

THIS PAGE INTENTIONALLY LEFT BLANK

I.   INTRODUCTION

A.   OVERVIEW

Performance and maximization of throughput is an ongoing concern of military communications systems engineers. In the modern era of information systems, those needs have increased significantly. Error detection and correction (EDAC) techniques can improve both the reliability and the performance of a communication system.

EDAC codes were invented to improve communication across noisy channels. Shannon, in his 1948 paper [1], proved that there exist EDAC codes that can achieve a small probability of error given the rate of the code is less than the channel's capacity. Since 1948 researchers have focused their attention on finding such code constructions, resulting in the invention of a multitude of code families. Of all the code families discovered, none has been applied to such a wide array of real-world, engineering problems as Reed-Solomon (RS) codes. RS codes are widely used because of their ability to correct burst errors when used with binary modulation schemes. Many of the applications that are used are in storage devices such as CDs, DVDs, and hard drives, as well as telecommunication lines, such as satellite links, Tactical Data Information Links (TADIL), Digital Video Broadcasting (DVB), Wimax, and in data transmission technologies such as Digital Signature Lines (DSL).

All modern communication systems use some form of forward error correction (FEC) coding. Generally, coding gain is improved when soft decision (SD) decoding is used instead of hard decision (HD) decoding. While soft decision decoding is a mature technology for convolutional codes, practical soft decision decoding for Reed-Solomon non-binary block codes has only recently been developed and is currently limited to use with bandwidth efficient modulation schemes such as M-ary phase-shift keying (MPSK). In [2], [3] a novel hybrid hard and soft decision decoding algorithm for RS codes was presented. This novel decoding scheme does not increase significantly the decoding complexity as does SD decoding of RS codes.

1

Network-centric warfare (NCW) is an emerging concept applied to modern military operations in order to improve their effectiveness. To achieve this, NCW applies information age concepts to increase the speed of communications and increase situational awareness through networking. As a result, NCW transforms the efficient flow of information into combat power by linking allied forces across the battlefield, thus enabling them to employ more effective decision making during military operations [4], [5].

One of the most demanding requirements for the developers of NCW is to achieve communications interoperability within a multinational coalition. Interoperability is achieved with the integration of communication systems such as the Joint Tactical Information Distribution System (JTIDS/Link–16), Automatic Link Establishment (ALE), Single Channel Ground and Airborne Radio System (SINCGARS), and satellite communications (MILSTAR).

Since JTIDS/Link-16 uses quasi-orthogonal, cyclic code-shift keying (CCSK), SINCGARS is a frequency hopping (FH) system and MILSTAR uses noncoherent M-ary frequency-shift keying (MFSK) modulation, it is of considerable interest to extend soft decision decoding of RS encoded symbols to CCSK as well as orthogonal modulation schemes such as M-ary frequency-shift keying (MFSK). In addition, the soft decision decoding scheme recently developed, actually a hybrid hard decision-soft decision (HD SD) decoding scheme, has not been developed for power efficient modulation schemes. It is also of interest to determine how noise other than additive white Gaussian noise (AWGN), such as pulse-noise interference (PNI), affects the hybrid HD SD decoding technique. The performance of various systems using hybrid HD SD decoding will be investigated using both analysis and simulation.

B.   LITERATURE REVIEW

Since 1948, when Shannon published his famous information theory paper, researchers have focused their attention on finding code constructions in order to improve the performance of communication systems. In 1960, Irving Reed and Gus Solomon presented a new class of error correcting codes that are well known as Reed Solomon

(RS) codes. Although they are a subclass of nonbinary Bose − Chauduri − Hocquengen (BCH) codes, they were constructed independently using an independent approach. One advantage of RS codes is the capability to correct random symbol errors and random burst errors [6], [7].

The first decoding algorithms for RS codes were presented by Gorenstein and Zierler (1961) [8], Chien (1964) [9] and Forney (1965) [10]. Because these decoding algorithms only corrected a few errors, they could not exploit the capabilities of RS codes. 1967 was a milestone for RS codes, when Berlekamp presented a decoding algorithm [11] that efficiently corrected many errors. Berlekamp proved the power of RS codes for the first time. The following year, Massey demonstrated [12] a fast shift-register implementation of the Berlekamp decoding algorithm. The classical Berlekamp and Massey algorithm (BM algorithm) has been employed for decoding in most cases.

In 1975, a new approach for decoding RS codes was presented by Sugiyama, Kasahara, Hirasawa and Namekawa. The Euclidean algorithm, named by its discoverer for the great ancient Greek mathematician, finds the greatest common divisor of two polynomials. The performance of the BM and Euclidean algorithms is exactly the same for all RS code rates. The above mentioned decoding algorithms are implemented in the time domain. A RS code can also be decoded in the frequency domain [6]. However, the BM algorithm for many decades has been the most widely used decoding technique for RS codes.

In the following years, much effort was concentrated on reducing the complexity of hard decision decoders that used the BM algorithm. In the last decade, the rapid development of internet, wireless links and the transformation to the information era made this need imperative. Nowadays, the acceleration of computation is more practical due to the growing capabilities of Field Programmable Gate Arrays (FPGAs). Since the mid-1990s, the BM algorithm seemed to be irreplaceable.

Soft decision decoding techniques had not been developed for RS codes until 1997. Sudan presented a decoding capability beyond the error correction bound $t = (n-k)/2$ [13]. Guruswami and Sudan presented an improved RS decoding algorithm

based on list decoding [14]. This decoding algorithm is referred to herein as GS SD decoding. Koetter and Vardy developed and implemented the GS SD algorithm [15]. However, the complexity of this SD decoding algorithm is a restricting factor, especially for real-time communication systems.

In [2] and [3], a novel hybrid hard decision-soft decision decoding algorithm was introduced. This decoding algorithm has a greater improvement in the correction capabilities of RS codes and better performance than GS SD decoding with much less complexity. The lower complexity allows actual implementation in real-time communication systems.

C.   THESIS OBJECTIVE

All modern communication systems use some form of forward error correction coding to reduce the received signal power required to close the link. RS codes are widely used in such military and commercial link systems. Improving the robustness of such systems is always a concern of communications engineers. Until recently, RS SD decoding was practically unrealizable due to the complexity of the SD algorithms that were presented [16], [17], [18], [19]. The use of a hybrid HD SD RS decoding technique to improve the performance of bandwidth efficient modulation schemes such as M-ary hyper phase-shift keying (MHPSK), MPSK, and MQAM has been implemented in previous research [2], [3]. The practicality of using hybrid hard decision-soft decision decoding to improve the performance for the power efficient modulations used by systems such as JTIDS/Link-16 and ALE by extending the correction capability of the existing HD decoder that is based on the BM algorithm are investigated in this thesis for the first time. Specifically, this thesis presents for the first time the performance simulation and analysis of MFSK with RS encoding, hybrid HD SD decoding, and both coherent and noncoherent demodulation. In addition to AWGN, the effects of pulse-noise interference (PNI) in conjunction with hybrid HD SD decoding are examined for the first time. The systems considered for this investigation use MFSK modulation for $M = 8, 16$ and 32 with RS encoding for different block lengths and code rates. The effects of both AWGN and PNI are

4

investigated. Also, the use of longer block lengths is implemented by using two channel symbols to transmit one code symbol, referred to herein as double-symbol transmission.

D.   THESIS OUTLINE

This thesis is organized as follows. The first chapter is the introduction and explains the importance of this research. Additionally, a literature review of the RS decoding schemes that have been developed is discussed. The background that is necessary to understand the concepts, simulations and analysis that are presented in this thesis is presented in Chapter II. The results of the performance simulation and analysis for MFSK with RS encoding, hybrid HD SD decoding, and coherent demodulation in AWGN are discussed in Chapter III. In Chapter IV, the analysis is extended for both AWGN and PNI. The performance simulation and analysis for MFSK with RS encoding, hybrid HD SD decoding, and noncoherent demodulation in AWGN is examined in Chapter V. The investigation of the previous chapter is extended to include PNI in Chapter VI. The results derived in this thesis are used to improve the performance of two existing communication systems in Chapter VII. Finally, the conclusions based on the results derived from the analysis in the previous chapters are presented in Chapter VIII.

THIS PAGE INTENTIONALLY LEFT BLANK

II.   BACKGROUND

The intent of this chapter is to provide the reader with the basic background and concepts required to understand the analysis and simulations that are presented in the following sections. A block diagram of the communication system that is examined is illustrated in Figure 1.
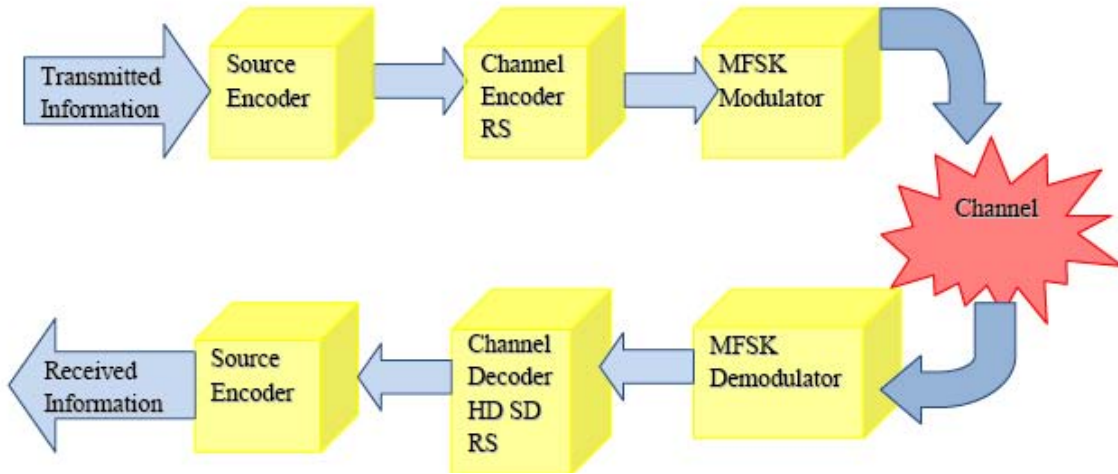
Figure 1.   Communication system with FEC coding.

*M*FSK modulation and RS channel encoding are assumed. At the demodulator, coherent / noncoherent demodulation is assumed, and hybrid HD SD decoding is used in order to maximize coding gain.

A.   *M*–ARY FREQUENCY SHIFT KEYING (MFSK)

*M*FSK is a modulation scheme that is widely used in communications systems such as ALE because *M*FSK provides highly reliable and robust communications with low signal strength. *M*FSK is less sensitive to noise than bandwidth efficient modulation schemes due to the small receiver bandwidth (relative to the overall signal bandwidth) for each specific signaling frequency. Additionally, *M*FSK is less sensitive to ionospheric effects such as Doppler, fading and multi-path. The main disadvantages of *M*FSK modulation are related to the narrow tone spacing, the

requirement for accurate synchronization, and the bandwidth requirement, which increases significantly with the order of modulation, *M*.

MFSK belongs to the class of *M*-ary orthogonal signals. For *M*-ary signaling the processor considers q coded information bits at a time. Consequently, the modulator transmits those information bits with $M = 2^q$ distinct waveforms $s_m(t)$, $m = 1, 2, ..., M$ in order to represent *M* different symbols. For $q > 1$, *M*-ary orthogonal signaling improves the performance of a communications system for a given signal-to-noise ratio [20] as can be seen in Figure 2.
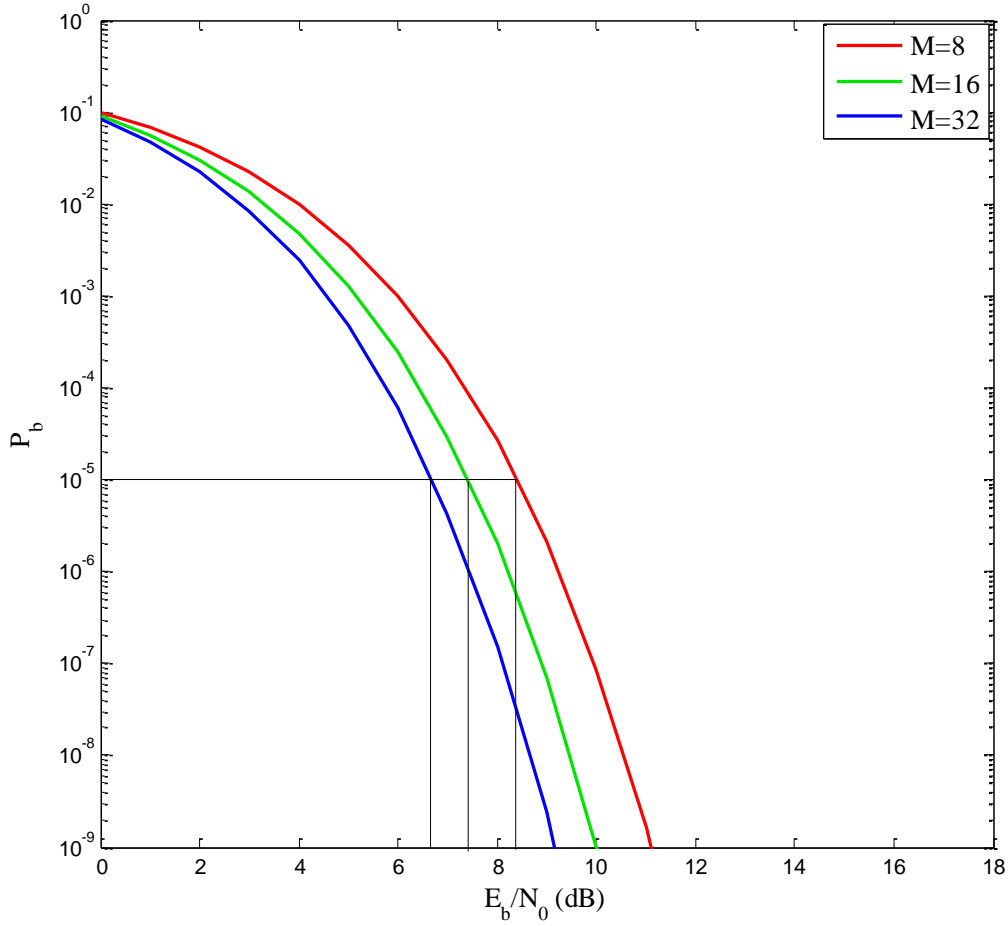
Figure 2.   Performance of 8, 16, and 32 coherent *M*FSK in AWGN.

Orthogonal signals are defined as a set of equal energy signals $s_m(t), \; m = 1, 2, ..., M$, such that [21]

$$\langle s_m(t), \; s_n(t) \rangle = \int_{-\infty}^{\infty} s_m(t) s_n^*(t) dt = \begin{cases} E_s, & m=n \\ 0, & m \neq n \end{cases} \quad 1 \leq m, n \leq M . \tag{2.1}$$

The channel waveform of the MFSK signal in AWGN environment is represented by

$$s_T(t) = \sqrt{2} A_c \cos\left(2\pi f_m t + \theta_i\right) + n(t) \text{ for } 0 \leq t \leq T_s \tag{2.2}$$

where E_s is the average symbol energy, A_c is the signal amplitude, $n(t)$ is AWGN with two-sided power spectral density (PSD) $N_0 / 2$ and θ_i is the ith symbol's phase. An MFSK waveform can be received either coherently, as shown in Figure 3, (the receiver requires the phase of the received signal) or noncoherently, as shown in Figure 4 (the receiver does not require the phase of received signal) [22]. This type of receiver can be implemented either with a bank of M correlation detectors or with a bank of M matched filters [22].

The PSD of MFSK with simple non return to zero (NRZ) pulse shapes can be expressed as

$$S_{MFSK}(f) = \frac{A_c^2 T_s}{2M^2} \sum_{m=1}^{M} \left\{ \frac{1}{T_s} \left[\delta(f - f_m) + \delta(f + f_m) \right] + \text{sinc}^2 \left[(f - f_m) T_s \right] + \text{sinc}^2 \left[(f + f_m) T_s \right] \right\} \tag{2.3}$$

where T_s is the symbol duration. The minimum null-to-null channel waveform bandwidth for coherent and noncoherent orthogonal MFSK is

$$B_{nn} = (M-1)\Delta f + 2R_s , \tag{2.4}$$

where $\Delta f = p R_s / 2$ for coherent detection, $\Delta f = p R_s$ for noncoherent detection and p is an integer. Thus, noncoherent detection requires more bandwidth than coherent.

Spectral efficiency is a very important figure of merit for evaluating how a specific modulation technique uses bandwidth to transmit information. MFSK spectral efficiency is defined as [20], [21], [22]

$$\eta = \frac{R_b}{B_{eq}} = \frac{R_b}{(M-1)\Delta f + R_S} \tag{2.5}$$

The spectral efficiency of MFSK decreases as the order of modulation increases.

1. Coherent Demodulation of *M*FSK

For coherent demodulation of an *M*FSK waveform, a receiver as shown in Figure 3 is required. The transmitted waveform is given by (2.2), where phase θ_i is known to the receiver.
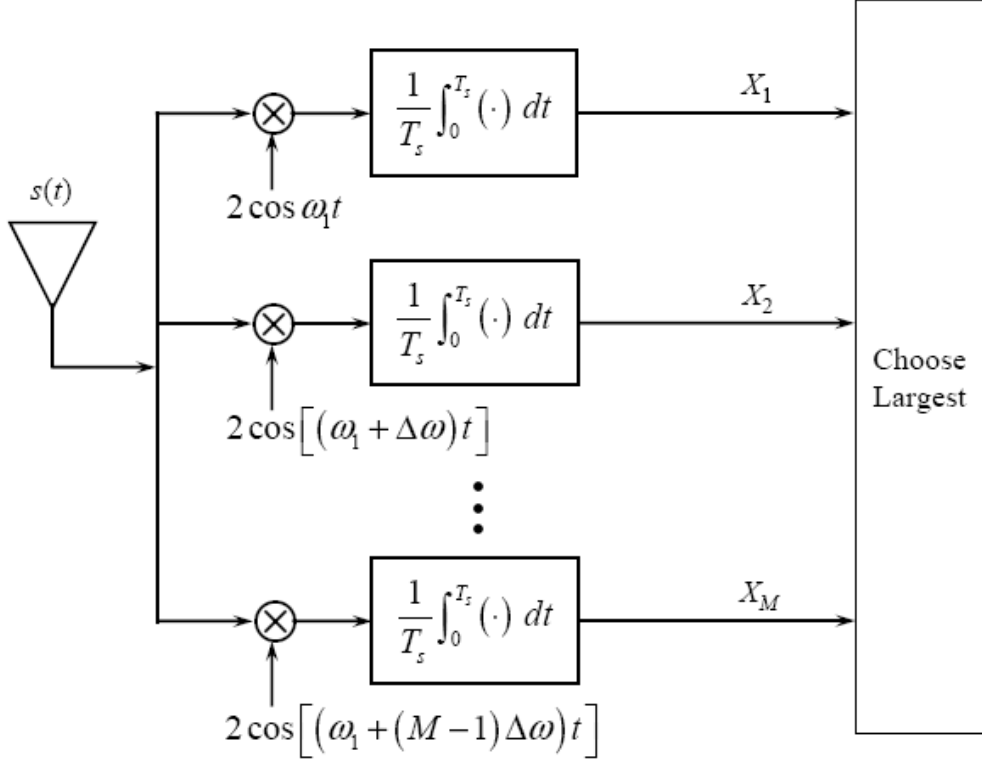
Figure 3.   Block diagram of a coherent *M*FSK receiver. From [22]

It can be shown that the integrator outputs $x_m(iT_S)$ for each branch of the receiver are independent Gaussian random variables $X_m, m = 1, 2, ..., M$. For orthogonal signaling, the X_m s are all independent random variables with mean value

$$\overline{X_m} = \frac{2\sqrt{2}A_c}{T_s} \int_0^{T_s} \cos(2\pi f_m t + \theta_i) \cos(2\pi f_n t + \theta_i) dt = \begin{cases} \sqrt{2}A_c & \text{for, } n=m \\ 0 & \text{for, } n \neq m \end{cases} \qquad (2.6)$$

where symbol n was transmitted and the noise powers at the integrator outputs are given by the variances of $X_m, m = 1, 2, ..., M$ and expressed as [23]

10

$$\sigma_{X_1}{}^2 = \sigma_{X_2}{}^2 = ... = \sigma_{X_M}{}^2 = \sigma^2 = N_0 / T_s.$$ (2.7)

The conditional probability density functions (PDFs) for the random variables X_m, $m = 1, 2, ..., M$, that represent the integrator outputs when the noise is modeled as Gaussian, are [22]

$$f_{X_m}\left(x_m \mid m = n\right) = \frac{1}{\sqrt{2\pi}\sigma_{x_m}} \exp\left[\frac{-\left(x_m - \sqrt{2}A_c\right)^2}{2\sigma_{x_m}{}^2}\right] u(v_m)$$ (2.8)

and

$$f_{X_m}\left(x_m \mid n \neq m\right) = \frac{1}{\sqrt{2\pi}\sigma_{x_m}} \exp\left[\frac{-x_n^2}{2\sigma_{x_m}{}^2}\right] u(v_m).$$ (2.9)

2. Noncoherent Demodulation of *M*FSK

For noncoherent demodulation of an *M*FSK waveform, a receiver as shown in Figure 4 is required. The transmitted waveform is the same for noncoherent detection, but the phase difference is not known.

From [23], when AWGN is present, it can be shown that the integrator outputs $x_m\left(iT_S\right)$ for each branch of the receiver can be represented as the independent Gaussian random variables $X_{m_i}, X_{m_q}, m = 1, 2, ..., M$, where for the in-phase integrator outputs the expected values are

$$\overline{X_{m_i}} = \frac{2\sqrt{2}A_c}{T_s} \int_0^{T_s} \cos\left(2\pi f_m t + \theta_i\right) \cos\left(2\pi f_n t\right) dt$$
$$= \begin{cases} \sqrt{2}A_c \cos\theta_i \ for, n=m \\ 0 \qquad\qquad for, n \neq m \end{cases}$$ (2.10)

and for the quadrature integrator outputs

11

$$\overline{X_{m_q}} = \frac{2\sqrt{2}A_c}{T_s} \int_0^{T_s} \cos\left(2\pi f_m t + \theta_i\right) \sin\left(2\pi f_n t\right) dt$$

$$= \begin{cases} -\sqrt{2}A_c \sin\theta_i \; for, n=m \\ 0 \qquad\qquad for, n\neq m \end{cases}$$

(2.11)

where symbol n was transmitted.

The noise power at the integrator outputs are given by the variances of X_{m_i} and X_{m_q}, $m = 1, 2, ..., M$, and the variances are expressed as

$$\sigma_{X_{1_i}}^2 = \sigma_{X_{2_i}}^2 = ... = \sigma_{X_{M_i}}^2$$

$$= \sigma_{X_{1q}}^2 = \sigma_{X_{2q}}^2 = ... = \sigma_{X_{Mq}}^2 = \sigma^2 = N_0 / T_s$$

(2.12)
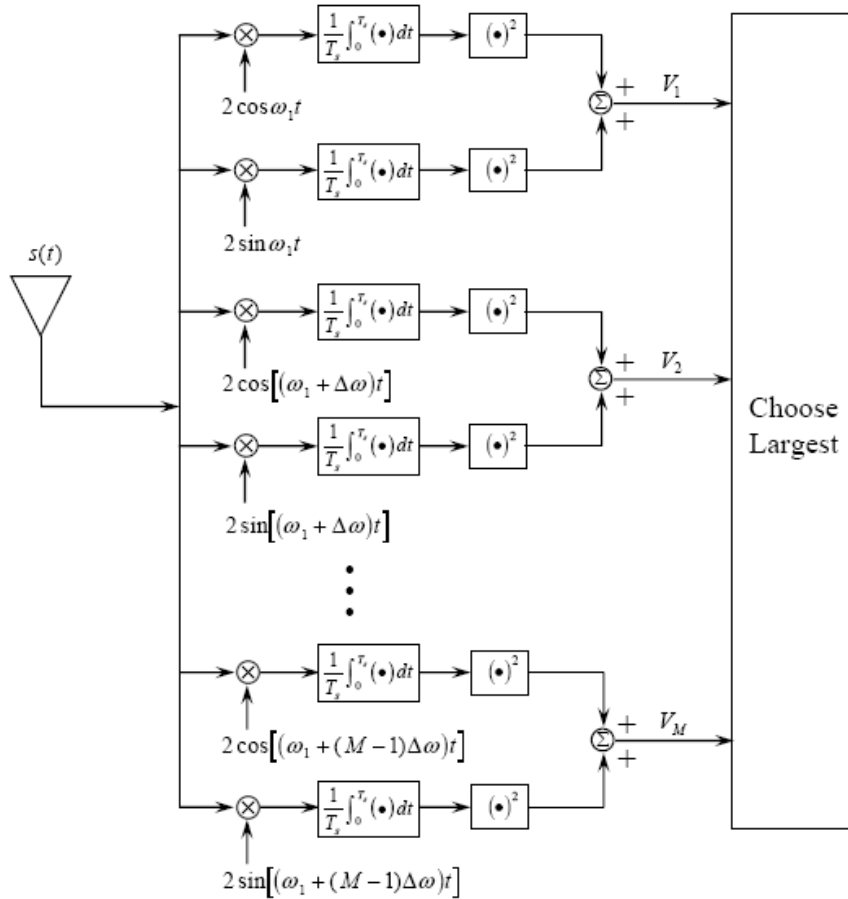
Figure 4.   Block diagram of a noncoherent MFSK receiver. From [22]

The conditional PDFs for the random variables V_m, $m = 1, 2, ..., M$, that represent the output of the mth branch when the signal corresponding to symbol n is transmitted are given by the non-central chi-squared PDF with two degrees of freedom when the noise is modeled as Gaussian. Hence,

$$f_{V_m}\left(v_m \mid m = n\right) = \frac{1}{2\sigma^2} \exp\left[\frac{-\left(v_m + 2A_c^2\right)}{2\sigma^2}\right] I_0\left(\frac{A_c\sqrt{2v_m}}{\sigma^2}\right) u(v_m) \qquad (2.13)$$

where $I_0(\bullet)$ is the modified Bessel function of the first kind and order zero, $u(\bullet)$ is the unit step function, and

$$f_{V_n}\left(v_m \mid n \neq m\right) = \frac{1}{2\sigma^2} \exp\left[\frac{-v_n}{2\sigma^2}\right] u(v_m) \qquad (2.14)$$

since $I_0(0) = 1$.

B.   PERFORMANCE OF *M*FSK

In this section, the performance of an *M*FSK waveform in AWGN and as well as AWGN and PNI is presented for both coherent and noncoherent demodulation.

1.   Performance of *M*FSK in AWGN

The probability of channel symbol error for coherent *M*FSK in AWGN is [22]

$$p_s = \frac{1}{\sqrt{2\pi}} \int_{-\infty}^{\infty} e^{\left(\frac{-u^2}{2}\right)} \times \left\{1 - \left[1 - Q\left(u + \sqrt{\frac{2rE_s}{N_0}}\right)\right]^{M-1}\right\} du \qquad (2.15)$$

In the preceding, r is the code rate of the FEC code, E_s is the average energy per channel symbol, $E_s = A_c^2 T_s$, A_c^2 is the average received signal power, T_s is the symbol duration, and $Q(\bullet)$ is the complementary cumulative distribution function for the standard normal random variable. T

An alternate and simplified expression for the performance of coherent *M*FSK in AWGN is the union bound [22]

13

$$p_s \leq (M-1)Q\left(\sqrt{\frac{rE_s}{N_0}}\right). \tag{2.16}$$

Similarly, the performance of noncoherent MFSK in AWGN is given by [22]

$$p_s = \sum_{n=1}^{M-1} \frac{(-1)^{n+1}}{n+1}\binom{M-1}{n}\exp\left[\frac{-nrE_s}{(n+1)N_o}\right], \tag{2.17}$$

with the upper bound

$$p_s \leq \frac{M-1}{2}\exp\left(\frac{-rE_s}{2N_0}\right). \tag{2.18}$$

the union bounds are accurate only for the case of large E_s/N_0. Throughout this thesis, (2.15) and (2.17) are used and are compared with the results obtained by simulation.

2.   Performance of MFSK in AWGN and PNI

The term interference can be used to describe both the intentional and unintentional disruption of communications. However, we distinguish between the deliberate use of noise or signals to disrupt communications, which is widely known as jamming, and the unintentional disruption of communications known as interference. Both of these are of interest for all modern military communication systems. The need for highly robust communication systems in the theatre of operations requires that the performance should be evaluated for an interference environment. Since the intent of this thesis is to examine the use of MFSK in military datalink systems, the performance in both AWGN and PNI is considered.

In military applications, hostile interference, or jamming, may be encountered. Barrage noise interference is when a jammer spreads his noise power uniformly across the bandwidth of the communication system at all times. This technique can be effective when the jammer is capable of delivering high noise power to the receiver.   An alternative jamming technique is pulsed-noise interference, where the jammer is turned on only for a specific fraction of time ρ. Since ρ represents the fraction of time that the PNI is on, then $(1-\rho)$ represents the fraction of time that the PNI is turned off, where $0 < \rho \leq 1$. In this kind of noisy environment, received symbols are affected by

two different levels of noise power because some of the symbols are affected only by AWGN and the rest by both AWGN and PNI. If the one-sided PSD of the AWGN is N_0 and the one-sided PSD of pulsed-noise interference is N_I when $\rho = 1$, then N_I/ρ is the PSD of the PNI since we assume that the average interference power is independent of ρ. The performance of both coherent and noncoherent MFSK in AWGN and PNI for various ρ is examined in this thesis.

When a channel is affected by AWGN, the noise signal that arrives at the receiver is assumed to be uniformly spread across the receiver bandwidth and time-independent, but these assumptions may not be valid when PNI is present. In this thesis, the AWGN and the PNI are assumed to be statistically independent, and the PNI is modeled as Gaussian noise. When AWGN and PNI are both present, the total noise power at the receiver integrator outputs is given by

$$\sigma_X^2 = \sigma_{WG}^2 + \sigma_I^2 \tag{2.19}$$

where $\sigma_{WG}^2 = N_0/T_s$ and $\sigma_I^2 = N_I/\rho T_s$, and ρ is a fraction of time that an interferer is switched on. When $\rho = 1$, the interferer is continuously on and the interference is referred to as barrage noise interference.

When PNI is present, the probability of symbol error is given by

$$P_s = \rho\, p_s(\text{AWGN+PNI}) + (1-\rho)\, p_s(\text{AWGN}), \tag{2.20}$$

where $p_s(x)$ is the conditional probability of symbol error, and we assume that each symbol is either completely free of PNI or that the entire symbol is affected by PNI [23].

C.   ERROR DETECTION AND CORRECTION

The landmark paper by [1] in 1948 offered new capabilities to designers of communication systems. The existence of error detection and correction codes increased the potential of sustaining highly reliable communications across noisy channels. Error detection and correction codes use redundancy to improve reliability; that is, extra code symbols are added to the transmitted message to provide the necessary detection and

15

correction information [24]. EDAC can improve the robustness and performance of communications. There are two basic error control strategies [7], automatic repeat request (ARQ) and forward error correction (FEC) coding. All ARQ systems require the transmission of data in packets. The receiver checks for errors in each received data packet. Hence, ARQ systems require only error detection. If no errors are detected in a received packet, the receiver sends the transmitter a positive acknowledgment; else the receiver sends the transmitter a negative acknowledgement and requests retransmission of the specific packet. Thus, all ARQ systems require a noise-free feedback channel from the receiver to the transmitter in order to function properly [7]. On the other hand, FEC coding consists of adding a certain number of redundant bits to the actual data bits in a particular pattern such that the recovery of the actual data bits is enhanced. In a system utilizing FEC coding, for every k information data symbols, n coded symbols are transmitted where $n > k$ [7].

FEC codes are very popular because they have the capability to correct and reconstruct erroneous transmitted messages without requiring a feedback channel. The two most common FEC codes are convolutional and block codes. This thesis investigates one of the most widely used block codes, Reed Solomon codes, in conjunction with hybrid HD SD decoding.

1. Reed Solomon Codes

Reed Solomon codes are a special class of q-ary Bose-Chaudhuri-Hocquenghem (BCH) codes and are linear and systematic [6], [7]. For nonbinary codes, m bits at a time are combined to form a symbol, and $M = 2^m$ symbols are required to represent all possible combinations of m bits. An (n, k) RS encoder takes k information symbols and generates n coded symbols. RS codes are systematic, since $(n-k)$ redundant symbols are embedded in the original k information symbols as shown in Figure 5.
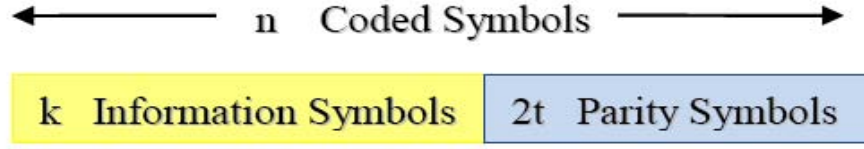
Figure 5.   RS systematic encoding.

RS codes have the largest possible minimum distance for each combination of n and k. A t-error correcting RS code with symbols from Galois Field ($GF(2^m)$) is characterized by [7]

$$
\begin{aligned}
n &= 2^m - 1 \\
n - k &= 2t \\
d_{m\min} &= 2t + 1
\end{aligned}
\tag{2.21}
$$

where m is the number of information bits per symbol, n is the number of coded symbols per codeword, k the number of information symbols per codeword, t the number of symbol errors that can be corrected within a block of n coded symbols, and $d_{\min}$ is the minimum distance between the codewords. A $(255, 231)$ RS code implies that $m = 8$, $k = 231$ and $t = 12$.

2.   Reed Solomon Encoding

The generator polynomial for a t-error correcting RS code has coefficients from $GF(2^m)$ and is [8]

$$
g(X) = (X + a)(X + a^2)...(X + a^{2t}) = \prod_{i=1}^{2t}\left(X + a^i\right)
\tag{2.22}
$$

where a is a primitive element in $GF(2^m)$. The code generated by $g(X)$ is an (n,k) cyclic code and consists of polynomials of degree $n-1$ or less with coefficients from $GF(2^m)$. As with all binary cyclic codes, all code words are multiples of $g(X)$. A message is encoded as a RS code in manner analogous to that used for binary cyclic codes. The information polynomial is

$$
a(X) = a_0 + a_1 X + a_2 X^2 + ... + a_{k-1}X^{k-1}
\tag{2.23}
$$

17

where the coefficients a_i are from $GF(2^m)$. For systematic encoding, we obtain the product $X^{2t}a(X)$, and the parity check symbols are given by the coefficients of the polynomial

$$b(X) = b_0 + b_1 X + b_2 X^2 + ... + b_{2t-1}X^{2t-1} \qquad (2.24)$$

where

$$X^{2t}a(X) = c(X)g(X) + b(X) \qquad (2.25)$$

As with binary cyclic codes, $b(X)$ is the remainder obtained when $X^{2t}a(X)$ is divided by $g(X)$ and $c(X)$ is the quotient. The difference is that the arithmetic operations are performed in $GF(2^m)$ rather than $GF(2)$. The encoding of RS codes is performed by a circuit as shown in Figure 6.
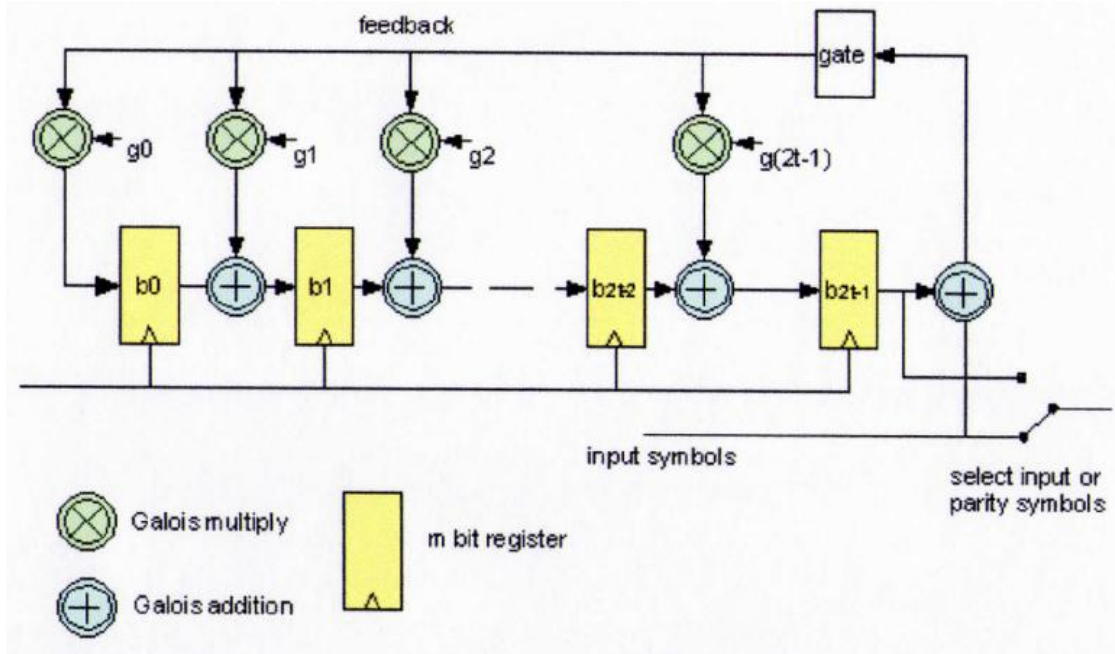
Figure 6.   Encoding circuit for RS code. From [25]

3.   Reed Solomon Hard Decision Decoding

RS hard decision decoding is based on syndrome $s(X)$ detection. The received codeword can be represented as a polynomial of degree $n-1$ or less [7]

18

$$r(X) = r_0 + r_1 X + r_2 X^2 + ... + r_{n-1} X^{n-1}, \tag{2.26}$$

and the syndrome can be computed from the following equation

$$r(X) = a(X)g(X) + s(X). \tag{2.27}$$

When the RS decoder receives a codeword, it first computes the syndrome in order to determine if the received codeword is valid, in which case the syndrome $s(X) = 0$. If $s(X) \neq 0$, errors have occurred during the transmission of the codeword through the communication channel. At this point, error detection has been completed and the decoder proceeds to error correction.

RS decoding consists of the following four steps [6]

- Compute the syndrome $(s_1, s_2, ..., s_{2t})$.

- Determine the error location polynomial $\sigma(X)$.

- Determine the error value evaluator.

- Evaluate error location numbers and error values and perform error correction.

The most complicated part of RS decoding is the second step, error location. The most commonly used hard decision decoding algorithms are the Berlekamp-Massey and Euclidean algorithms. The advantage of HD decoding is the decoding speed.

4.   Reed Solomon Soft Decision Decoding

In the last two decades, significant research has been conducted in the field of soft decision decoding of RS codes. Scientists were interested in extending the error correction capability of traditional HD decoding. In this section, the Guruswami Sudan (GS) SD algorithm, the algebraic SD (ASD) algorithm, and the novel hybrid HD SD decoding algorithm are reviewed.

a.   *Guruswami Sudan Algorithm*

Sudan first discussed the possibility of decoding RS codes where t exceeded the traditional $t = (n-k)/2$ obtained for HD decoding [14].   In 1999 Guruswami and Sudan presented the GS SD algorithm [13], a new algebraic decoding method for RS codes that is able to correct errors beyond the BM decoding radius. This algorithm requires constructing a bivariate polynomial with zeros of multiplicity and estimation polynomials in the Galois field based on the received symbols. The polynomial can then be factored to give a list of possible valid codewords. A GS SD decoder can successfully decode a codeword if the error is within a radius of $n - \sqrt{nk}$. The computational complexity of the list-based GS SD RS decoding algorithm is proportional to $n^2 l^4$ where n is the block length of the code and l is the required multiplicity of the polynomial, which refers to the number of zero crossings by the polynomial in the Galois field (an example multiplicity number could be 120) [2], [16], [17], [18], [27].

The GS SD algorithm has larger error correction capabilities than HD decoding and can correct [26]

$$t = n - \sqrt{nk} \tag{2.28}$$

symbol errors per block of n symbols. Equation (2.28) is valid for large values of multiplicity.

For a (255,191) RS code, the GS SD algorithm can correct up to approximately 34 symbol errors per block, while traditional HD decoding corrects up to 32 symbol errors per block. But for a $(255, 231)$ RS code, the GS SD algorithm can correct up to 12 symbols errors per block, the same as HD decoding. Generally, the GS SD algorithm outperforms traditional HD decoding correction capabilities for low to medium code rates, but this is translated to only a small improvement in a communication system's performance in terms of required E_b/N_0. As it is stated in [13] "For codes rate greater than $1/3$, however, this algorithm does not improve over the

algorithm [21]" ([21] in [13] is [28] in this thesis). Furthermore, the complexity of the GS SD algorithm is a limiting factor for many communications systems.

b. *Algebraic Soft Decision Decoding*

Kotter and Vardy [15] modified the Guruswami-Sudan algorithm to use soft information from the communication channel to help improve decoding performance. Their algorithm translates the probabilistic reliability information into a set of interpolation points, along with their multiplicities. In this manner the ASD algorithm increases the list of candidate codewords during the decoding procedure. Kotter and Vardy claimed that their algorithm was less complex than GS SD. However, using the channel reliability information to increase the decoding list requires greater receiver complexity in order to supersede the GS decoding list. Additionally, most of the reviewed literature for ASD was for low-to-medium rates codes and for channels far from q - ary symmetric, as illustrated in Figure 7 [26].
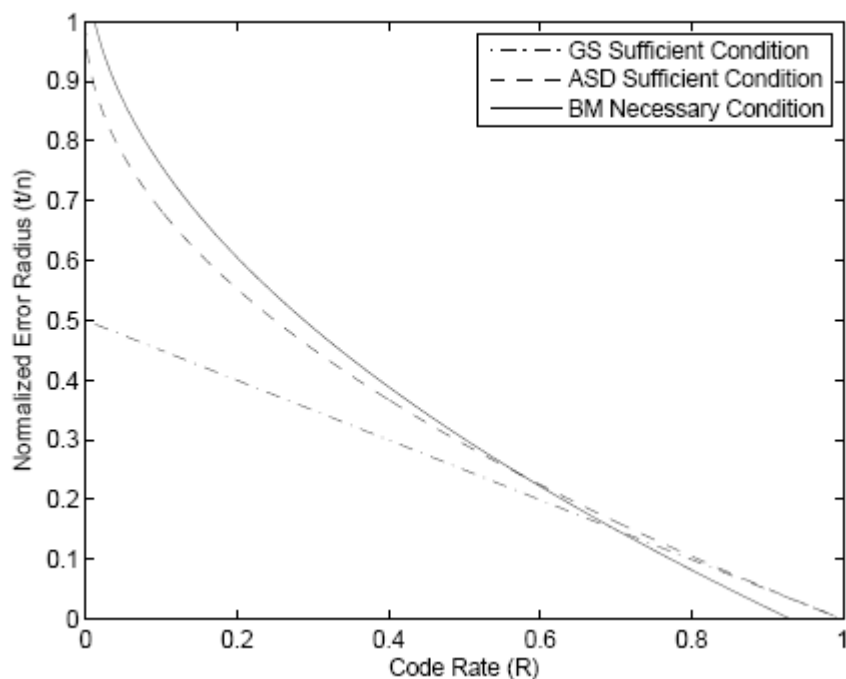
Figure 7.   Decoding radius of ASD compared to GS SD and BM HD decoding for "two error channel." From [26]

5.   Reed Solomon Hybrid Hard Decision-Soft Decision Decoding

A novel decoding technique for RS codes, hybrid HD SD decoding, was introduced in [2], [3] that extends the error correction capability of traditional RS HD decoding with less complexity than the GS SD algorithm. Hybrid HD SD decoding can significantly improve the error correction capability even for high code rates.

Hybrid HD SD decoding utilizes traditional hard decision RS decoding. If a decoding failure occurs, then SD reliability information from the channel is used to estimate the received code symbols' conditional probabilities. The hybrid HD SD algorithm selects up to ten symbols that were received with low probabilities. Next, new code symbol estimates are used in the HD decoding algorithm. From those selected symbol positions, the symbols received with the second highest conditional probabilities are chosen. Then, a matrix with 2^w columns is created, where w is the number of selected symbols. Each column is a possible codeword and each of them is passed through the RS decoder. Most of the decoding failures occur for only a few errors in excess of the error correction capability of the HD decoder. Thus, the correction of a small number of errors leads to successfully decoding the received block. The computational complexity of hybrid HD SD is significantly less than that of the GS SD algorithm [2, 3, 27].

SD reliability information is computed as a matrix for all possible symbols at each code symbol location where each matrix element is given by [2]

$$P_r(T = t_a \mid R = r_\beta) = \frac{f\left(r_\beta \mid t_a\right)}{\sum_{t \in S} f\left(r_\beta \mid t\right)} \tag{2.29}$$

where T is the M-ary signal that represents a transmitted symbol and is selected from the set $S = \{t_1, t_2, ..., t_M\}$, R is a random variable that models the received signal, $f\left(r_\beta \mid t_a\right)$ is a conditional probability density function, a varies from 1 to M, and β varies from 1 to n, the block length of the code. The algorithm for hybrid HD SD decoding is described in [3] , [4].

6.   Performance of Reed Solomon Codes for Hard Decoding

The probability of decoder, or block, error for a t-symbol error correcting, nonbinary block code with maximum likelihood decoding is upper bounded by [7]

or
$$P_E \leq \sum_{i=t+1}^{n} \binom{n}{i} p_s^i (1-p_s)^{n-i} = 1 - \sum_{i=0}^{t} \binom{n}{i} p_s^i (1-p_s)^{n-i} \qquad (2.30)$$

where the equality holds for either a perfect code or a bounded distance decoder, and p_s is the probability of coded, or channel, symbol error.

Furthermore, (2.30) is a very accurate approximation for a maximal likelihood decoder when p_s is sufficiently small. The probability of information symbol error is approximately

$$P_s \approx \sum_{i=t+1}^{n} \frac{\delta_i}{k} \binom{n}{i} p_s^i (1-p_s)^{n-i} \qquad (2.31)$$

where δ_i is the number of information symbol errors that occur when i of n symbols are in error. Hence, δ_i/k is the conditional probability of symbol error given that a block error is caused by i code symbols errors, and from [29]

$$\frac{\delta_i}{k} \approx \frac{i}{n}. \qquad (2.32)$$

For orthogonal signaling, the relationship between P_s and P_b is given by [20]

$$P_b = \frac{n+1}{2n} P_s. \qquad (2.33)$$

Substituting (2.31) and (2.32) in (2.33), we get the information bit error rate for hard decision coding,

$$P_b \approx \frac{n+1}{2n^2} \sum_{i=t+1}^{n} i \binom{n}{i} p_s^i (1-p_s)^{n-i}. \qquad (2.34)$$

In the following chapters, the performance of MFSK with RS HD SD decoding is examined. In this case, (2.34) is used find the equivalent error correction capability t for hard decision decoding that yields the same information BER as the simulation results of HD SD decoding.

The performance of RS HD SD decoding for increased block lengths is also examined in this thesis. In this case, the channel symbol error probability p_s in (2.34) is given by [30]

$$p_{sDouble} = 2p_s - p_s^2 \tag{2.35}$$

where $p_{sDouble}$ is the channel error probability for double-symbol transmission.

D.   CHAPTER SUMMARY

In this chapter, the basic concepts required to understand this thesis, such as MFSK and Reed Solomon codes, were introduced. The performance equations that are utilized throughout this thesis were presented and the novel hybrid HD SD RS decoding algorithm was briefly discussed. In the next chapter, the performance simulation and analysis for MFSK with RS encoding, hybrid HD SD decoding and coherent demodulation in AWGN is examined.

III. PERFORMANCE SIMULATION AND ANALYSIS OF *M*FSK WITH RS ENCODING, HYBRID HD SD DECODING, AND COHERENT DEMODULATION IN AWGN

In this chapter, we examine the performance of *M*FSK for $M = 8$, 16 and 32 with RS encoding, coherent demodulation, and hybrid HD SD decoding in AWGN. The results are presented two sections. Initially, the simulation and analytical results are presented for single-symbol transmission, and the error correction capabilities of hybrid HD SD and GS SD decoding are compared. Next, results are presented for longer RS block lengths by specifying double-symbol transmission.

A. SINGLE-SYMBOL TRANSMISSION

For this section, a block diagram of the receiver is shown in Figure 8.
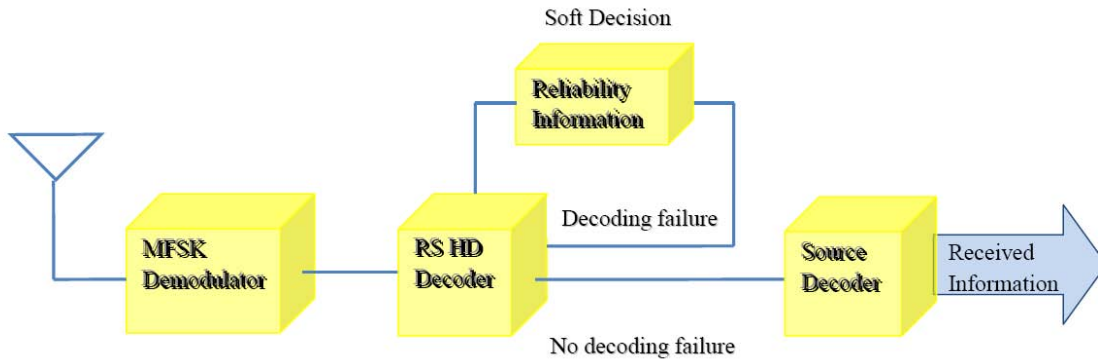
Figure 8.   *M*FSK demodulation with HD SD RS decoding for single symbol transmission

The channel symbol error probability is given by [22]

$$p_s = \frac{1}{\sqrt{2\pi}} \int_{-\infty}^{\infty} e^{\left(\frac{-u^2}{2}\right)} \times \left\{ 1 - \left[1 - Q\left(u + \sqrt{\frac{2rE_s}{N_0}} \right) \right]^{M-1} \right\} du \,, \tag{3.1}$$

and the probability of information bit error for HD decoding is given by [7]

$$P_b \approx \frac{n+1}{2n^2} \sum_{i=t+1}^{n} i \binom{n}{i} p_s^{\,i} (1-p_s)^{n-i} \tag{3.2}$$

where t is a function of n, k,

1. 8-FSK

For $M = 8$, we examined only a (7, 5) RS code. The performance of 8-FSK with (7, 5) RS is shown in Figure 9. The simulation results for HD SD decoding are represented by the red line, the blue line represents the HD decoding analytical results where the t error correction capability is one, and the green line represents the HD SD analytical results. This representation is followed throughout this thesis. Hybrid HD SD decoding does not significantly improve the performance in this case. For $P_b = 10^{-5}$ the E_b / N_0 required with HD SD decoding is 7.3 dB, almost the same as for HD at 7.5 dB. The HD SD algorithm corrects approximately one error per block like traditional HD decoding. For the "Analytical HD SD results" plot, (2.34) is used find the equivalent error correction capability t for hard decision decoding that yields the same information BER as the simulation results of HD SD decoding.
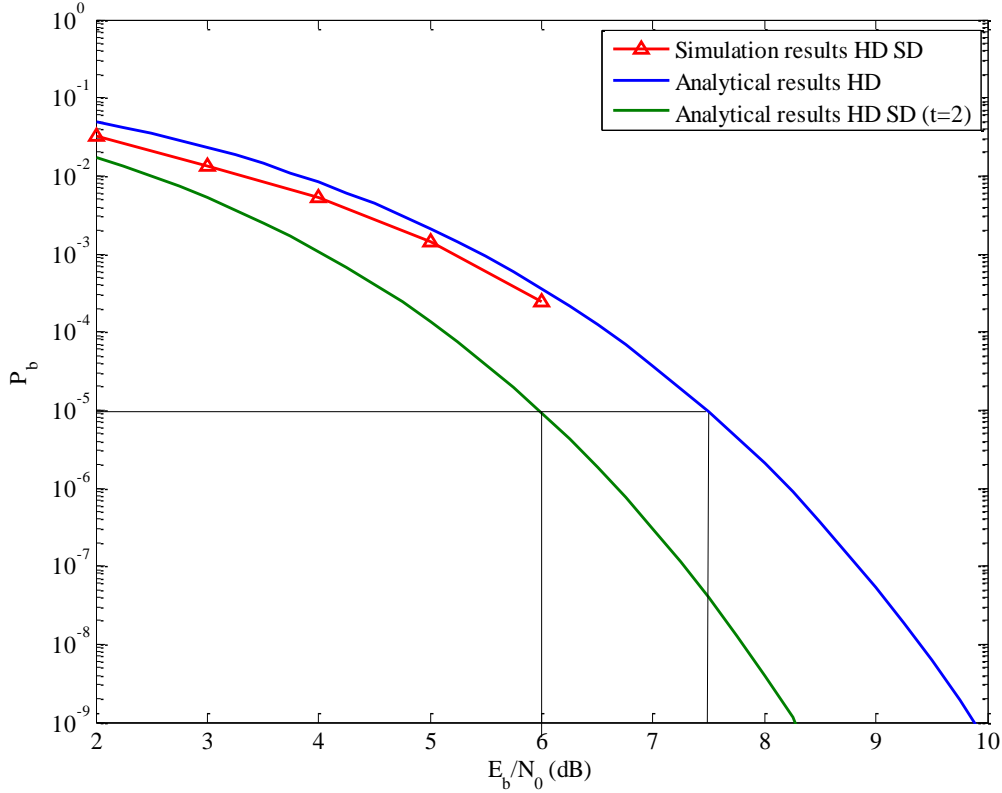
Figure 9.   Probability of bit error for single-symbol 8-FSK with (7, 5) RS encoding and hybrid HD SD decoding.

If the code was able to correct two errors per block, it would achieve a coding gain of 1.5 dB as obtained using equation (3.2). The results for a (7, 5) RS code when $P_b = 10^{-5}$ are summarized in Table 1.

Table 1.   Performance of single-symbol 8-FSK with (7, 5) RS encoding when $P_b = 10^{-5}$.

P_b	8-FSK RS (7, 5) $r = 5/7 = 0.71$	E_b / N_0 (dB)	Error Correction Capability t
10^{-5}	Simulation HD SD	7.3	1
10^{-5}	Analytical HD SD	6	2
10^{-5}	Analytical HD	7.5	1

The inadequate performance with HD SD decoding is due to the small block length. Even traditional HD decoding of a (7, 5) RS code has only a small improvement compared to uncoded 8-FSK, as can be seen in Figure 10. Another explanation has to do with the soft decision reliability information matrix first introduced in equation (2.29). The maximum dimension of the matrix for 8-FSK is 8×7. In Table 2, the simulation data from a decoding failure are presented. In the first line we observe the transmitted symbols; in the second line we observe the HD received symbols. The second and fifth positions were decoded incorrectly; thus, there is a decoding failure with HD decoding since only a single error can be corrected within a block. HD SD decoding corrected the second symbol but created one more error at the fourth position to again result in a decoding failure. Table 3 is the reliability information matrix for this decoding example.
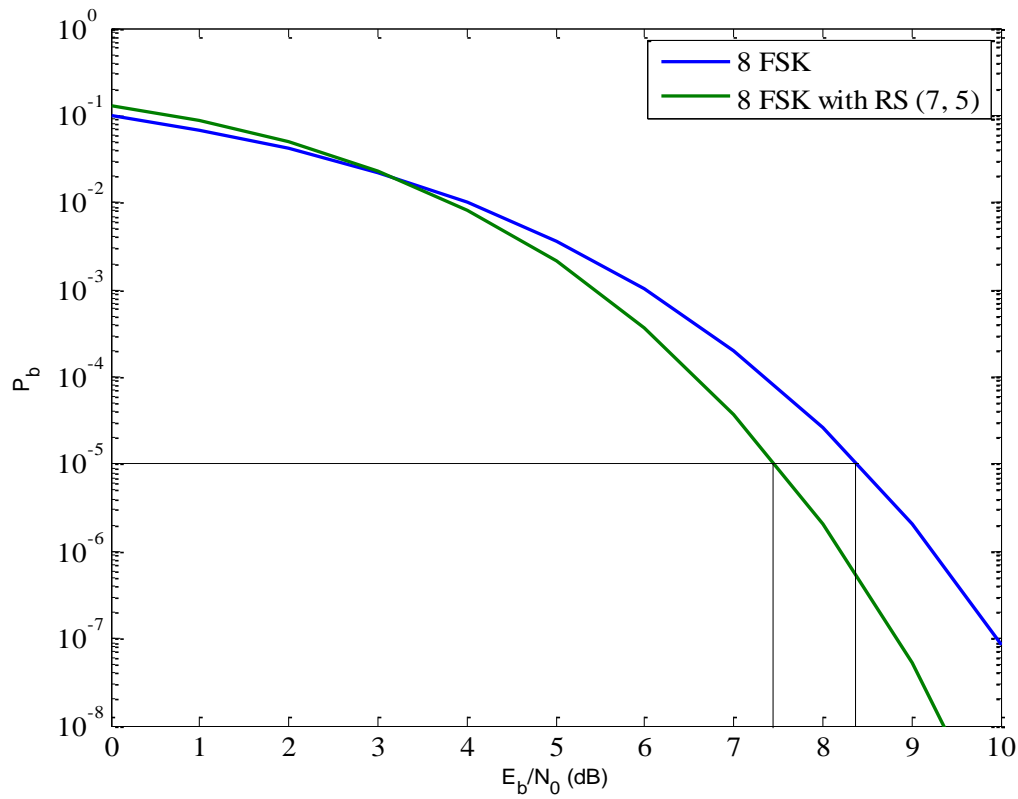
Figure 10.   Probability of bit error for both uncoded 8-FSK and 8-FSK with (7, 5) RS encoding and HD decoding.

Table 2.   RS (7, 5) Decoding Failure Data.

Transmitted Symbols	7	5	1	5	8	8	6
HD Received Symbols	7	3	1	5	7	8	6
HD SD Received Symbols	7	5	1	8	3	8	6

The HD SD algorithm selects the symbols received with the smallest conditional probabilities (for 8-FSK, the maximum number is eight) and finds those positions where the code symbols are received with the second highest conditional probabilities. In this way, it creates 2^7 permutations of possible decoding sequences from a total of 8^7 available permutations. A decoding failure occurs when the actual symbol sequence is not included among the 2^7 permutations. In the example, the transmitted sequence in Table 2 was not included in the HD SD decoding matrix.

Table 3.   Example reliability information matrix for 8-FSK with (7, 5) RS encoding.

Symbol/Symbol Position	1	2	3	4	5	6	7
1	0.0000	0.0000	1.0000	0.0002	0.0000	0.0000	0.0000
2	0.0000	0.0001	0.0000	0.0002	0.0000	0.0000	0.0000
3	0.0000	**0.0066**	0.0000	0.0004	**0.0088**	0.0064	0.0000
4	0.0000	0.0001	0.0000	0.0002	0.0000	0.0000	0.0000
5	0.0000	**0.3567**	0.0000	**0.9750**	0.0000	0.0000	0.0000
6	0.0000	0.0000	0.0000	0.0001	0.0000	0.0008	1.0000
7	1.0000	0.6356	0.0000	0.0015	**0.0000**	0.8660	0.0000
8	0.0	0.0010	0.0000	**0.0217**	**0.9911**	0.1267	0.0000

2.   16-FSK

For single-symbol transmission, 16-FSK modulation was examined for various code rates ranging from high to low. The simulation and analysis results for three different code rates are shown in Figures 11, 12, 13 and 14. As can be seen from Figure 11, HD SD decoding for a (15, 11) RS code requires $E_b/N_0 = 5.3\,\text{dB}$ for $P_b = 10^{-5}$, and the performance is improved by only 0.3 dB as compared to HD decoding. In this case, t is only increased by about one symbol per block (that is, in some cases t was increased by one, but in many cases remained the same as HD). The results for a (15, 11) RS code when $P_b = 10^{-5}$ are summarized in Table 4.

Table 4.   Performance of single-symbol 16-FSK with (15, 11) RS encoding when $P_b = 10^{-5}$.

P_b	16-FSK RS (15, 11) $r = 11/15 = 0.73$	E_b / N_0 (dB)	Error Correction Capability t
10^{-5}	Simulation HD SD	5.3	1
10^{-5}	Analytical HD SD	4.8	2
10^{-5}	Analytical HD	5.6	1
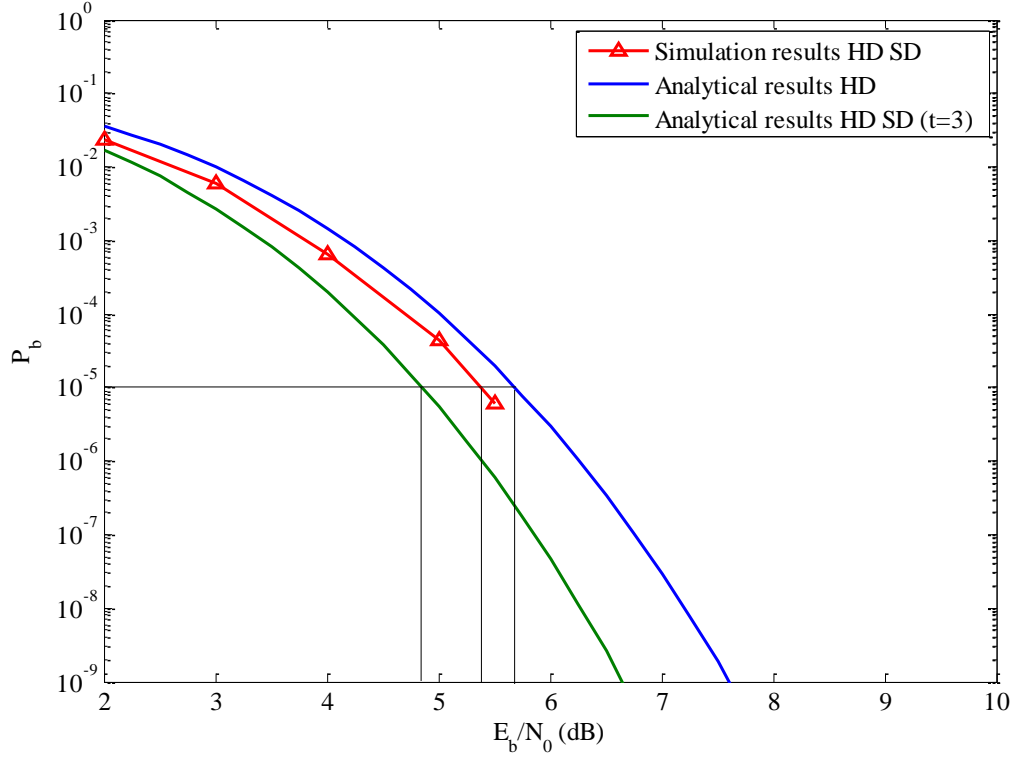
Figure 11.   Probability of bit error for single-symbol 16-FSK with (15, 11) RS encoding and hybrid HD SD decoding.

For a (15, 9) RS code, hybrid HD SD decoding can correct one more symbol error per block as compared to traditional HD decoding. As can be seen in Figure 12, a coding gain of 0.7 dB is achieved for $P_b = 10^{-5}$. The analytical approximation for HD SD decoding matches very well with the simulation results, which are summarized in Table 5.

Table 5.   Performance of single-symbol 16-FSK with (15, 9) RS encoding when $P_b = 10^{-5}$.

P_b	16-FSK RS (15, 9) $r = 9/15 = 0.6$	E_b / N_0 (dB)	Error Correction Capability t
10^{-5}	Simulation HD SD	5.1	4
10^{-5}	Analytical HD SD	5.1	4
10^{-5}	Analytical HD	5.8	3
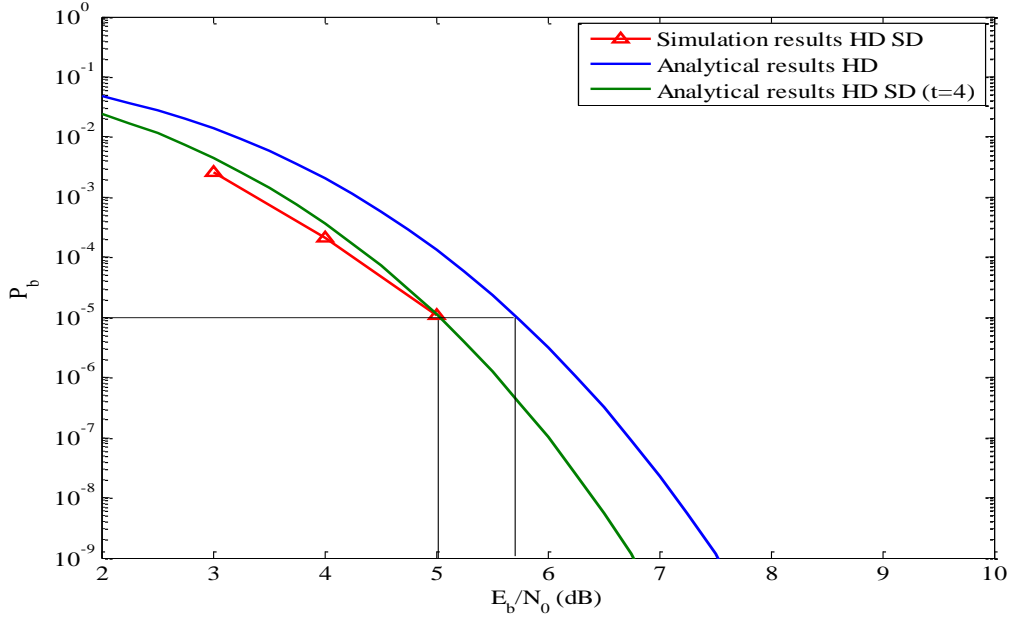
Figure 12.   Probability of bit error for single-symbol 16-FSK with (15, 9) RS encoding and hybrid HD SD decoding.

The results for a (15, 7) RS code are shown in Figure 13, where we see that $P_b = 10^{-5}$ requires $E_b/N_0 = 4.9\,\text{dB}$ when hybrid HD SD decoding is used. In this case, the coding gain as compared to HD decoding is 1.2 dB, and the error correction capability is increased by two symbols per block. While the (15, 9) RS code with HD decoding has better performance than that of a (15, 7) RS code with HD decoding, when HD SD decoding is used, the opposite is true because of the increased value of t. The results for a (15, 7) RS code when $P_b = 10^{-5}$ are summarized in Table 6.

Table 6.   Performance of single-symbol 16-FSK with (15, 7) RS encoding when $P_b = 10^{-5}$.

P_b	16-FSK RS (15, 7) $r = 7/15 = 0.47$	E_b / N_0 (dB)	Error Correction Capability t
10^{-5}	Simulation HD SD	4.9	6
10^{-5}	Analytical HD SD	4.9	6
10^{-5}	Analytical HD	6.1	4

31
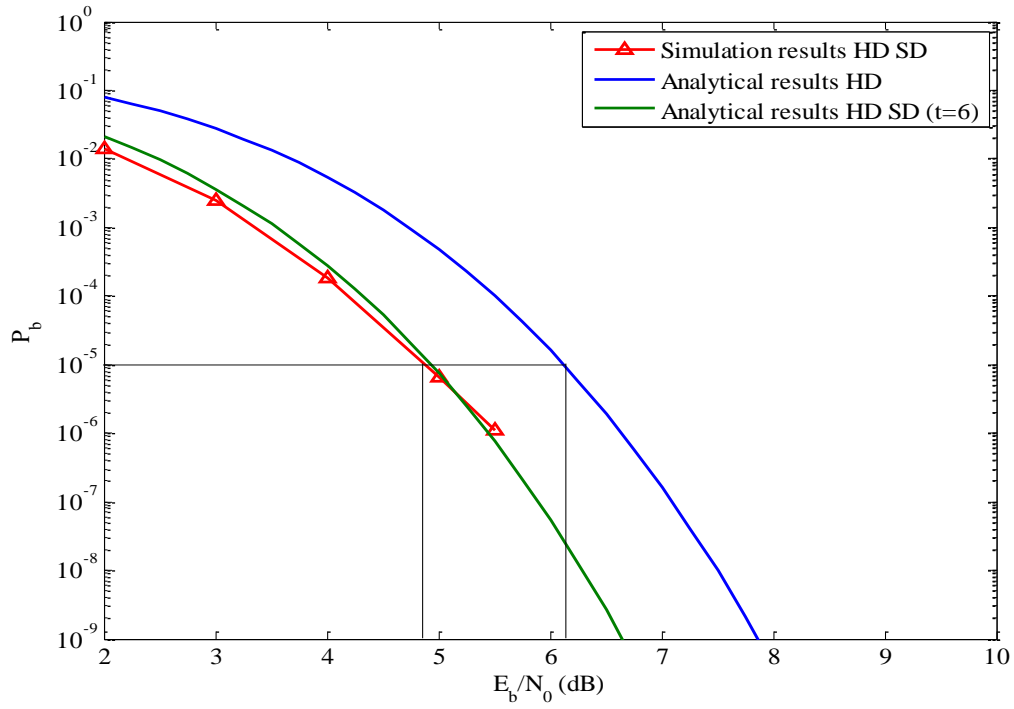
Figure 13. Probability of bit error for single-symbol 16-FSK with (15, 7) RS encoding and hybrid HD SD decoding.

Finally, in Figure 14, the probability of bit error for a (15, 5) RS code is presented. HD SD decoding requires $E_b / N_0 = 5.8$ dB for $P_b = 10^{-5}$. A (15, 5) RS code has a coding gain of 1.2 dB and increases t by two units. Analytical and simulation results match very well for HD SD decoding, but the absolute performance worsens, which is expected for decreasing code rates when the code rate is low. The results are summarized in Table 7.

Table 7. Performance of single-symbol 16-FSK with (15, 5) RS encoding when $P_b = 10^{-5}$.

P_b	16-FSK RS (15, 5) $r = 5/15 = 0.33$	E_b / N_0 (dB)	Error Correction Capability t
10^{-5}	Simulation HD SD	5.8	7
10^{-5}	Analytical HD SD	5.8	7
10^{-5}	Analytical HD	7	5
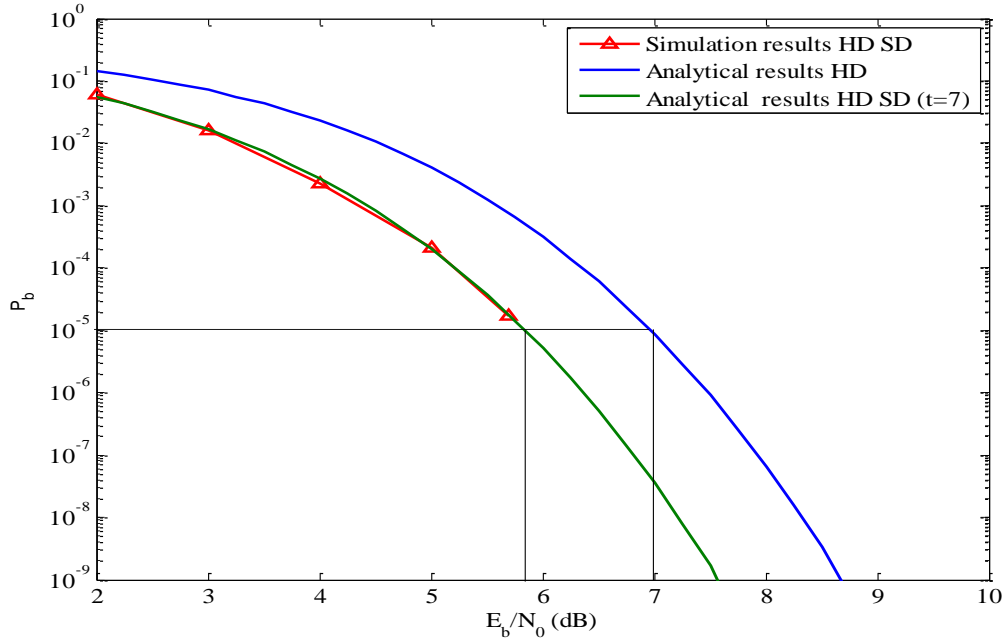
Figure 14.   Probability of bit error for single-symbol 16-FSK with (15, 5) RS encoding and hybrid HD SD decoding.

For single-symbol transmission with 16-FSK modulation in AWGN, hybrid HD SD decoding improves the performance and the error correction capability of the RS code, but the performance improvement is slight. In this case, the lower the code rates, up to a point, resulted in greater improvement. However, higher code rates are preferred in order to maximize throughput. The results for a (15, 9) RS code with HD SD decoding are better than for a (15, 11) RS code with HD decoding by 0.5 dB with little degradation in code rate. Furthermore, HD SD extends the error correction capability more than the GS SD algorithm. As already discussed, the GS SD algorithm provides better error correction capability than traditional HD decoding only for medium to low code rates. The error correction capability of HD SD decoding is compared to that of GS SD decoding in Table 8.

Table 8.   Comparison of error corrections capabilities.

RS	HD SD t Error Correction	GS SD t Error Correction	HD t Error Correction
(15, 7)	6	4.75	4
(15, 5)	7	6.33	5

33

3. 32-FSK

Lastly, 32-FSK is examined for single-symbol transmission. As seen in Figure 15, HD SD decoding for a (31, 15) RS code does not improve the performance over traditional HD decoding. The reason is the increased number of dimensions of the orthogonal modulation. Unfortunately, the probability that the actual transmitted symbol does not have the greatest or second greatest conditional probability has become significant. Thus, when the HD SD algorithm selects for the same position, the symbol that was received with the second highest conditional probability cannot correct any mistake that occurs because most of the time the correct symbol is one of the others 30 symbols. Thus, in the following chapters, 32-FSK with single-symbol transmission will not be examined.
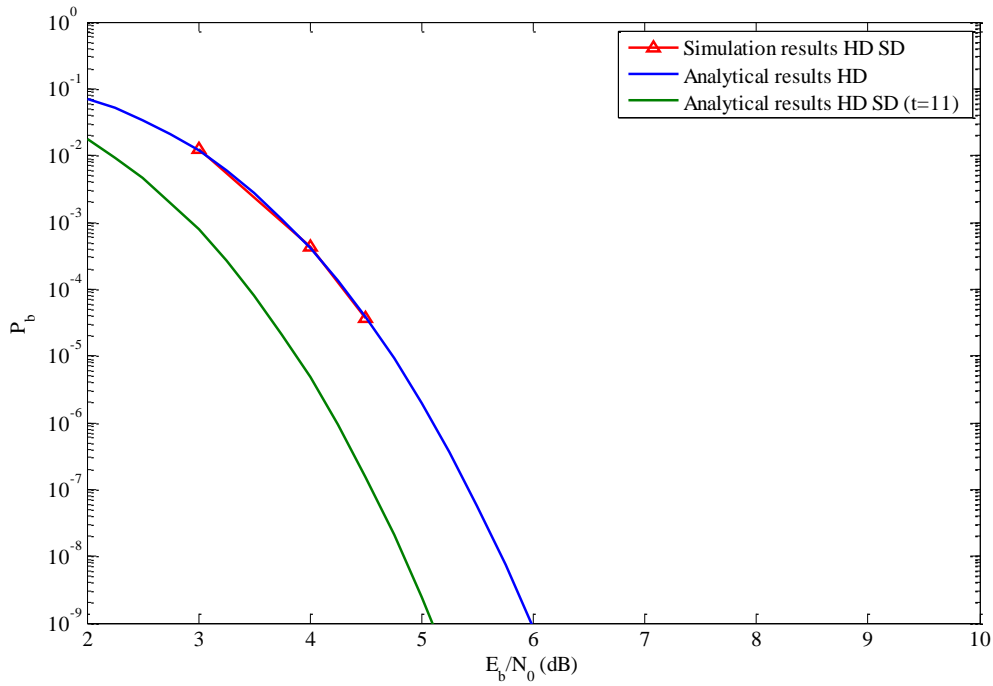
Figure 15.   Probability of bit error for single-symbol 32-FSK with (31, 15) RS encoding and hybrid HD SD decoding.

B.   DOUBLE-SYMBOL TRANSMISSION

The simulation results and the performance analysis for coherent MFSK for longer block length RS codes, implemented by transmitting two channel symbols per code symbol, are presented in this section. Specifically, the RS encoder encodes $2m$ bits per symbol and generates $n = 2^{2m} - 1$ coded symbols per block. The difference in the HD analysis is that (2.32) is used in (3.2).

The block diagram of the receiver with HD SD RS decoding is shown in Figure 16.
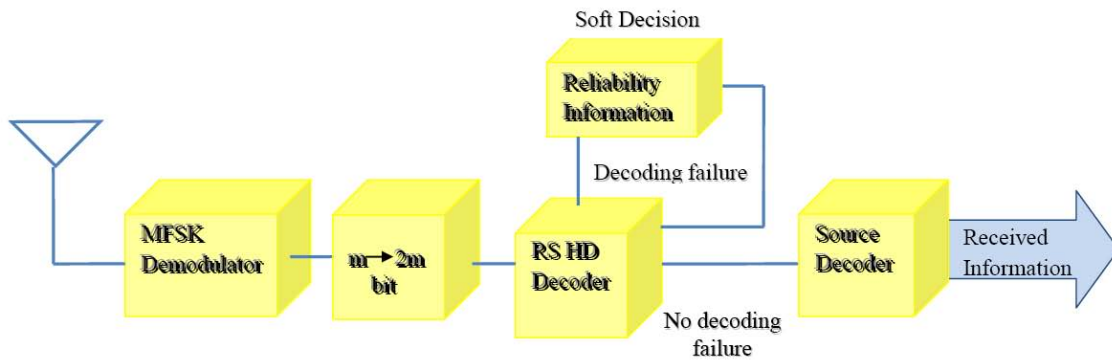
Figure 16. MFSK demodulation with HD SD RS decoding for double-symbol transmission.

1.   8-FSK

The probabilities of bit error for double-symbol 8-FSK for (63, 55), (63, 47) and (63, 39) RS codes are shown in Figures 17, 18 and 19, respectively. For a (63, 55) RS code, HD SD decoding requires $E_b/N_0 = 5.5$ dB for $P_b = 10^{-5}$, which equates to a coding gain of 3.5 dB relative to HD decoding. The error correction capability is increased by one error per block. The results for (63, 55) RS encoding when $P_b = 10^{-5}$ are summarized in Table 9.
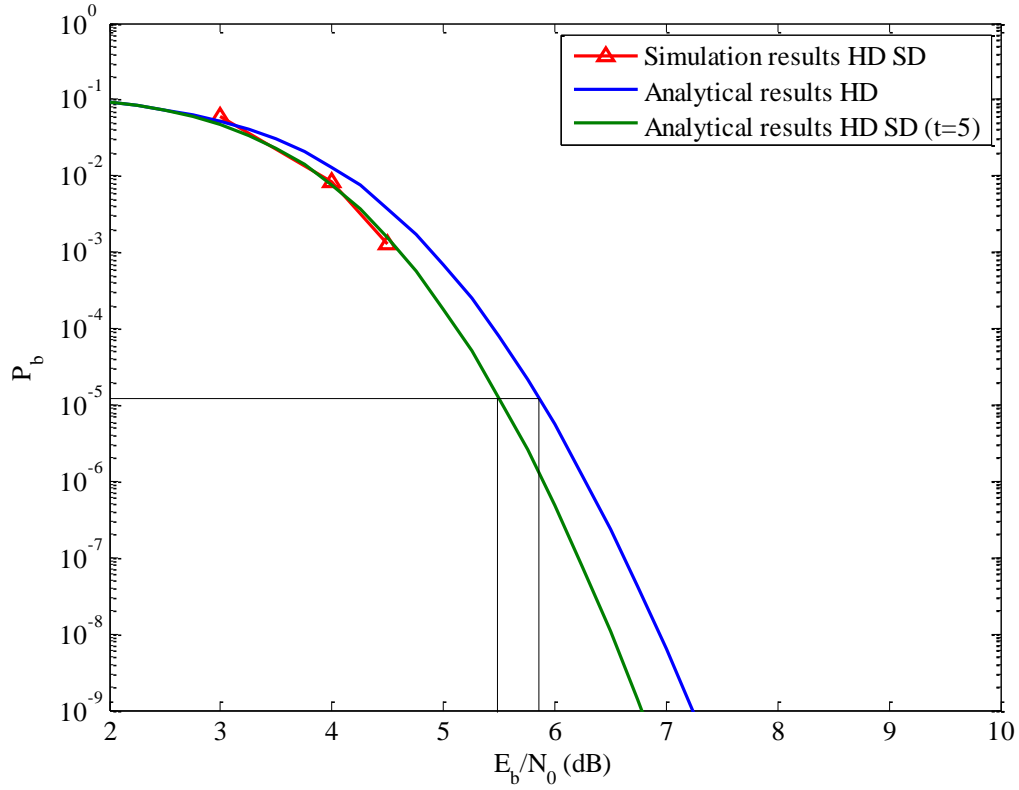
Figure 17.   Probability of bit error for double-symbol 8-FSK with (63, 55) RS encoding and hybrid HD SD decoding.

Table 9.   Performance of double-symbol 8-FSK with (63, 55) RS encoding when $P_b = 10^{-5}$.

P_b	8-FSK RS (63, 55) $r = 55/63 = 0.87$	E_b / N_0 (dB)	Error Correction Capability t
10^{-5}	Simulation HD SD	5.5	5
10^{-5}	Analytical HD SD	5.5	5
10^{-5}	Analytical HD	5.9	4

The performance for double-symbol transmission with a (63, 47) RS code is shown in Figure 18. Note that by utilizing a lower code rate, approximately 0.75, performance is improved for HD decoding but is improved much more for HD SD decoding. For $P_b = 10^{-5}$, $E_b/N_0 = 4.6$ dB is required, resulting in a coding gain of 0.8 dB. In this case, there is a significant improvement in the error correction capability of

36

the code with HD SD, where four errors more than with HD decoding can be corrected. The results for (63, 47) RS encoding when $P_b = 10^{-5}$ are summarized in Table 10.
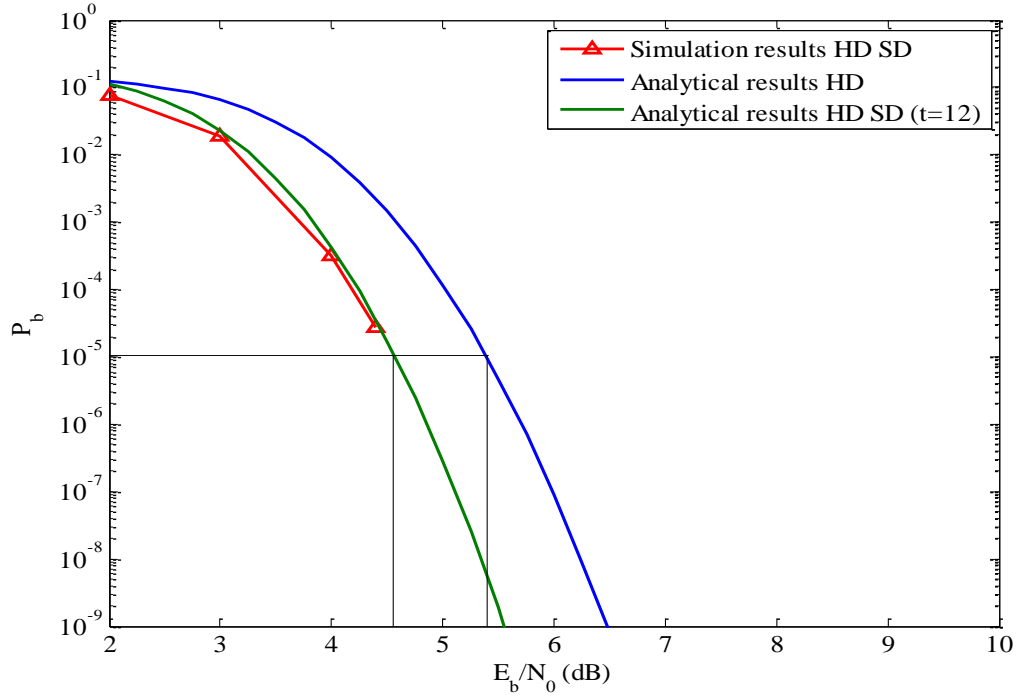
Figure 18.　　Probability of bit error for double-symbol 8-FSK with (63, 47) RS encoding and hybrid HD SD decoding.

Table 10.　Performance of double-symbol 8-FSK with (63, 47) RS encoding when $P_b = 10^{-5}$.

P_b	8-FSK RS (63, 47) $r = 47/63 = 0.75$	E_b / N_0 (dB)	Error Correction Capability t
10^{-5}	Simulation HD SD	4.6	12
10^{-5}	Analytical HD SD	4.6	12
10^{-5}	Analytical HD	5.4	8

Lastly, we examine double-symbol 8-FSK with a (63, 21) RS code. From Figure 19, we can see that for this low code rate, performance is degraded. Nevertheless, the performance with HD SD decoding is better than with HD decoding, and HD SD

decoding can correct four symbol errors per block more than HD decoding alone. The results for (63, 21) RS encoding when $P_b = 10^{-5}$ are summarized in Table 11.
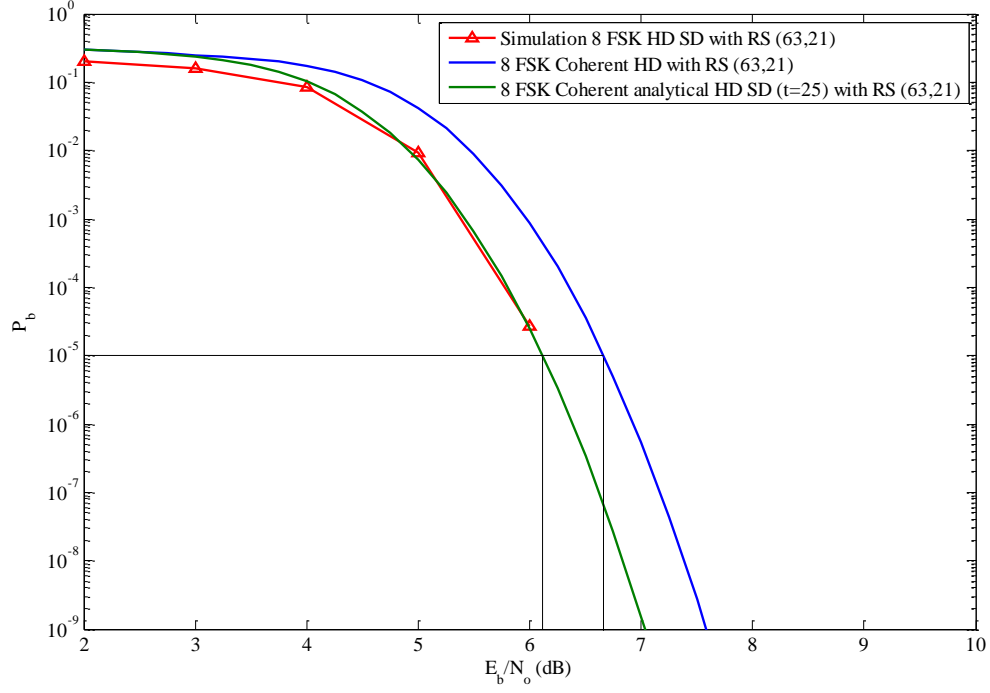
Figure 19.   Probability of bit error for double-symbol 8-FSK with (63, 21) RS encoding and hybrid HD SD decoding.

Table 11.   Performance of double-symbol 8-FSK with (63, 21) RS encoding when $P_b = 10^{-5}$.

P_b	8-FSK RS (63, 21) $r = 21/63 = 0.33$	E_b / N_0 (dB)	Error Correction Capability t
10^{-5}	Simulation HD SD	6.1	25
10^{-5}	Analytical HD SD	6.1	25
10^{-5}	Analytical HD	6.6	21

Double-symbol transmission and RS encoding generally improves significantly the performance of communication systems as compared with single-symbol transmission. If double-symbol transmission is combined with HD SD decoding, both the performance and the error correction capability are improved even more. A further

38

advantage of HD SD decoding is that it can be utilized with higher code rates as compared to the GS SD decoding scheme. For example, GS SD decoding of a (63, 47) RS code can correct approximately 8.5 symbol errors per block, while HD SD decoding can correct up to twelve errors per block.

2.   16-FSK

In this section, the performance of three code rates with double-symbol 16-FSK are examined. The probability of bit error for a (255, 223) RS code is shown in Figure 20.
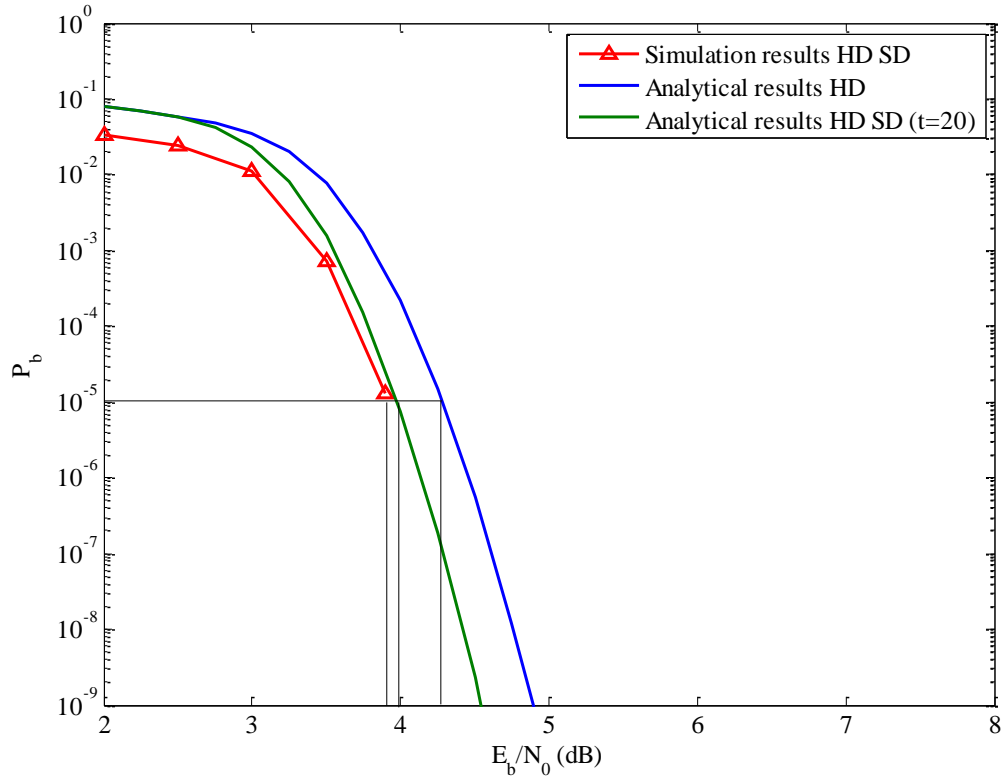
Figure 20.   Probability of bit error for double-symbol 16-FSK with (255, 223) RS encoding and hybrid HD SD decoding.

For a (255, 233) RS code, HD SD decoding requires $E_b/N_0 = 3.9$ dB for $P_b = 10^{-5}$. A small coding gain of 0.4 dB is observed, and the error correction capability

of the code was increased by four errors per block. The results for (255, 223) RS encoding when $P_b = 10^{-5}$ are summarized in Table 12.

Table 12. Performance of double-symbol 16-FSK with (255, 223) RS encoding when $P_b = 10^{-5}$.

P_b	16-FSK RS (255, 223) $r = 223/255 = 0.87$	E_b / N_0 (dB)	Error Correction Capability t
10^{-5}	Simulation HD SD	3.9	20
10^{-5}	Analytical HD SD	4	20
10^{-5}	Analytical HD	4.3	16

Next, a (255, 191) RS code was examined, and the performance is shown in Figure 21.
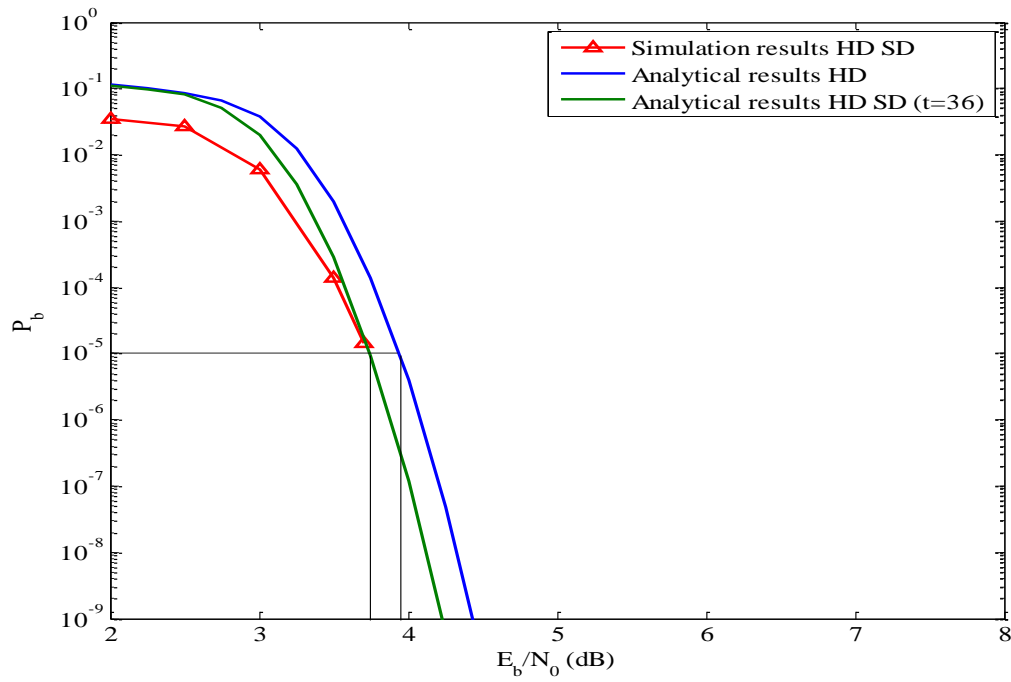
Figure 21. Probability of bit error for double-symbol 16-FSK with (255, 191) RS encoding and hybrid HD SD decoding.

As can be seen, a code rate of approximately 2/3 performs better than a higher code rate. For $P_b = 10^{-5}$, $E_b/N_0 = 3.8$ dB is required with HD SD decoding. The results suggest that the point of diminishing returns has been reached for the performance of double-symbol 16-FSK. The performance is analogous to a concatenated code [7]. The (255, 191) RS code has the best performance of all code rates examined for double-symbol 16-FSK. The results for (255, 191) RS encoding when $P_b = 10^{-5}$ are summarized in Table 13.

Table 13.   Performance of double-symbol 16-FSK with (255, 223) RS encoding when $P_b = 10^{-5}$.

P_b	16-FSK RS (255, 191) $r = 191/255 = 0.74$	E_b / N_0 (dB)	Error Correction Capability t
10^{-5}	Simulation HD SD	3.75	36
10^{-5}	Analytical HD SD	3.8	35
10^{-5}	Analytical HD	3.95	32

We conclude our examination of double-symbol 16-FSK by presenting the probability of bit error for a low rate (255, 83) RS code in Figure 22.
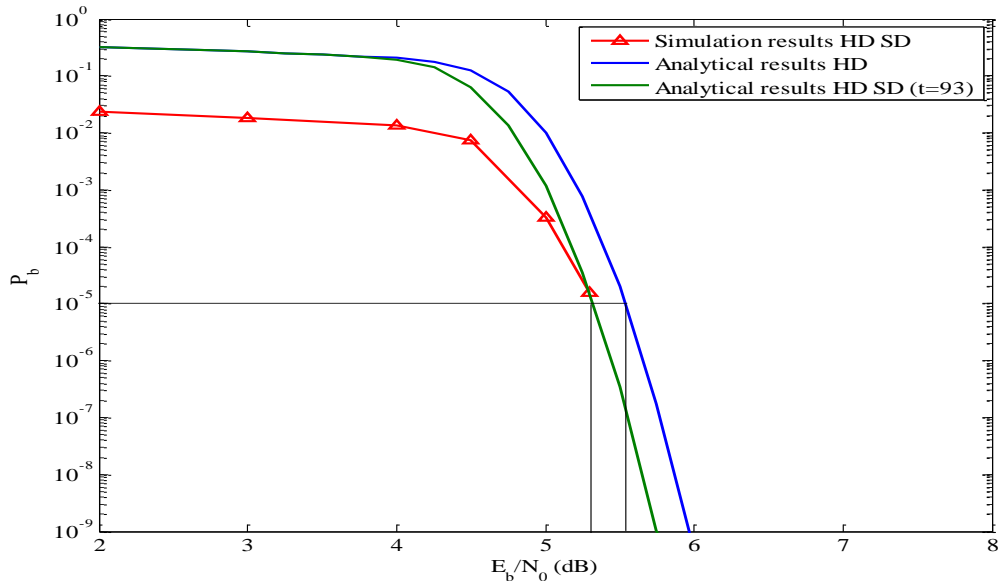
Figure 22.   Probability of bit error for double-symbol 16-FSK with (255, 191) RS encoding and hybrid HD SD decoding.

As was expected, the performance is degraded significantly, but HD SD decoding performs better than traditional HD decoding. $E_b/N_0 = 5.4$ dB is required for $P_b = 10^{-5}$, and the code corrects seven more errors per block. The results for (255, 83) RS encoding when $P_b = 10^{-5}$ are summarized in Table 14.

Table 14. Performance of double-symbol 16-FSK with (255, 83) RS encoding when $P_b = 10^{-5}$.

P_b	16-FSK RS (255, 83) $r = 83/255 = 0.33$	E_b / N_0 (dB)	Error Correction Capability t
10^{-5}	Simulation HD SD	5.4	93
10^{-5}	Analytical HD SD	5.4	93
10^{-5}	Analytical HD	5.6	86

From the preceding results, we conclude that double-symbol 16-FSK improves the performance, but HD SD decoding cannot achieve coding gains similar to that obtained with double-symbol 8-FSK. HD SD decoding corrects four additional errors per block, but from our analysis a coding gain of 1 dB requires correction of approximately 20 additional errors. On the other hand, if we compare HD SD error correction capability with the GS SD algorithm for medium and low code rates (see Table 15), we observe that the GS SD algorithm for a low code rate has better error correction capability, but for a medium code rate has a similar error correction capability but with a higher order of decoding complexity.

Table 15. Comparison of error corrections capabilities.

RS	HD SD t Error Correction	GS SD t Error Correction	HD t Error Correction
(255, 191)	35	34.3	32
(255, 83)	93	109.5	86

3. 32-FSK

In this thesis, HD SD decoding for double-symbol 32-FSK is not simulated for three reasons. First, for HD SD decoding, the size of the reliability matrix would be 32×1023, and the decoding procedure would be very computationally intensive. Second, as has already been stated for single-symbol 32-FSK, the probability that the actual transmitted symbol is not the one with the second highest conditional probability is high. Lastly, double-symbol transmission improves the performance of 32-FSK significantly, as can been seen in Figure 23. The improvement in coding gain is comparable to that which can be obtained with turbo codes [6, 7].
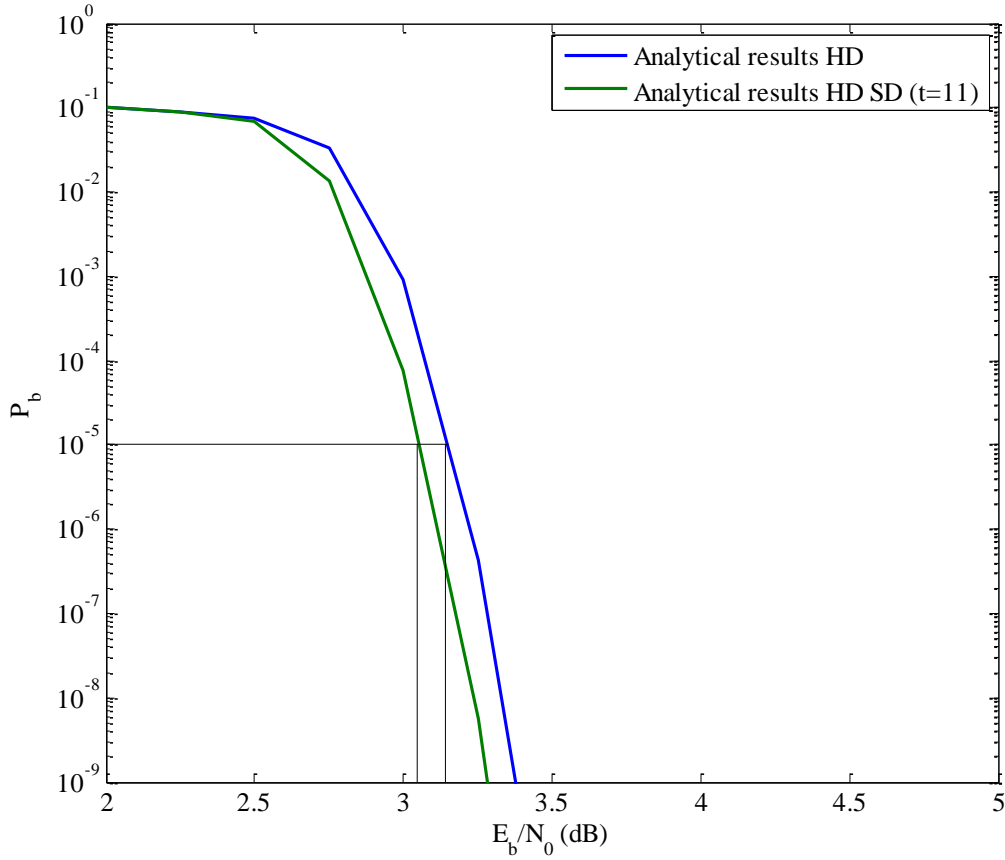
Figure 23.   Probability of bit error for double-symbol 32-FSK with (1023, 759) RS encoding and HD SD decoding.

C.   CHAPTER SUMMARY

In this chapter, the performance of MFSK with RS encoding and hybrid HD SD decoding was examined for AWGN environment with coherent demodulation. From the simulation and analysis results it was shown that, for 8-FSK and single-symbol transmission, a (7, 5) RS code with HD SD decoding does not significantly improve performance. 16-FSK modulation with HD SD decoding achieved a coding gain of 1.2 dB for medium to low code rates. The HD SD algorithm does not improve the performance of 32-FSK for either single-symbol or double-symbol transmission. On the other hand, for longer block lengths, HD SD decoding improves the performance of double-symbol 8-FSK and 16-FSK, but the coding gain is very small for 16-FSK. As was expected, the error correction capability is significantly better than that of the GS SD algorithm in many cases, especially for code rates $> 1/3$. The next chapter presents the performance simulation and analysis for MFSK with RS encoding, hybrid HD SD decoding, and coherent demodulation in both AWGN and PNI.

IV. PERFORMANCE SIMULATION AND ANALYSIS OF *M*FSK WITH RS ENCODING, HYBRID HD SD DECODING, AND COHERENT DEMODULATION IN AWGN AND PNI

In this section, for first time since it was developed in [2], the performance of hybrid HD SD decoding in conjunction with power efficient modulations techniques, such as *M*FSK, is evaluated when both pulsed-noise interference and AWGN are present.

With PNI, we assume that the communications system is attacked by a noise-like signal that is turned on and off sporadically [31], as discussed in Chapter II. The effect of PNI for $\rho = 1$ (barrage noise), $\rho = 0.4$ and 0.2 are investigated in this thesis.

When PNI is present, the SD reliability information is obtained from [2]

$$P_r(T = t_a \mid R = r_\beta) = \frac{f\left(r_\beta \mid t_a\right)}{\sum_{t \in S} f\left(r_\beta \mid t\right)}, \tag{4.1}$$

where the conditional probabilities are Gaussian PDFs . In this chapter, when we calculate the Gaussian PDFs the variances are computed using only AWGN and not the PNI while the mean values are the ones of the received signal either corrupted by PNI or not. In this case, the symbols received with PNI will have lower conditional probabilities than the other symbols, and the HD SD decoding algorithm, which selects the ten symbols received with the smallest conditional probabilities, will most likely choose those corrupted by PNI and correct them. As is seen in the following section, HD SD decoding provides significantly greater coding gains than when utilized with only AWGN.

The simulation and analytical results are first presented for single-symbol transmission. Next, results for longer block lengths, obtained by invoking double-symbol transmission, are presented.

A. SINGLE-SYMBOL TRANSMISSION

The performance analysis is obtained by using

$$p_s(AWGN) = \frac{1}{\sqrt{2\pi}} \int_{-\infty}^{\infty} e^{\left(\frac{-u^2}{2}\right)} \times \left\{ 1 - \left[1 - Q\left(u + \sqrt{\frac{2rE_s}{N_0}} \right) \right]^{M-1} \right\} du$$

$$p_s(AWGN + PNI) = \frac{1}{\sqrt{2\pi}} \int_{-\infty}^{\infty} e^{\left(\frac{-u^2}{2}\right)} \times \left\{ 1 - \left[1 - Q\left(u + \sqrt{\frac{2rE_s}{N_0 + \frac{N_I}{\rho}}} \right) \right]^{M-1} \right\} du \qquad (4.2)$$

in (2.20) and using that result in [7,31]

$$P_b \approx \frac{n+1}{2n^2} \sum_{i=t+1}^{n} i \binom{n}{i} P_s^i (1 - P_s)^{n-i}. \qquad (4.3)$$

For analysis purposes, the increased error correction capability provided by the hybrid HD SD decoding algorithm is utilized in (4.3) in order to verify the simulation results. Furthermore, in this section only the performance for single-symbol 16-FSK is presented for the reasons mentioned in the previous chapter.

For single-symbol transmission, we examine the probability of bit error for (15, 9) RS encoding and $\rho = 1$, 0.4, and 0.2. The results for $E_b/N_0 = 6.3\,\text{dB}$ that yields $P_b = 10^{-8}$ when only AWGN is present are shown in Figures 24, 25, and 26. The results when $P_b = 10^{-5}$ are summarized in Table 16.

Table 16.   Performance of single-symbol 16-FSK with (15, 9) RS in both AWGN and PNI for $E_b/N_0 = 6.3\,\text{dB}$ when $P_b = 10^{-5}$.

P_b	16-FSK RS (15, 9) $r = 9/15 = 0.6$	E_b/N_I (dB) $\rho = 1$	E_b/N_I (dB) $\rho = 0.4$	E_b/N_I (dB) $\rho = 0.2$	Error Correction Capability t
10^{-5}	Simulation HD SD	13.9	12	12.3	3+ 4+ 4+
10^{-5}	Analytical HD SD	11.1	12	12.8	4 4 4
10^{-5}	Analytical HD	15	15.5	16.3	3
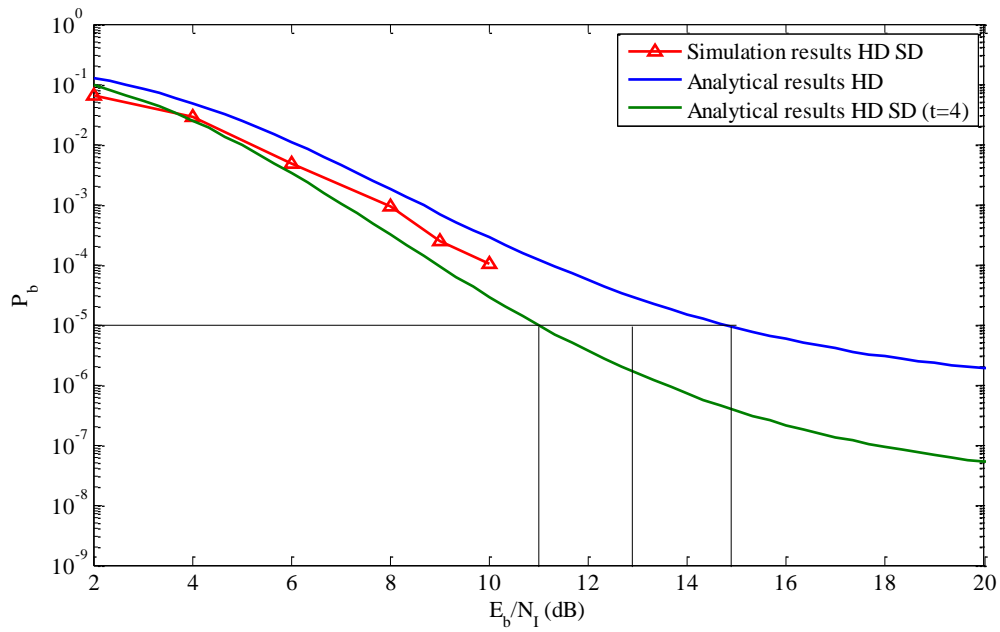
Figure 24.   Probability of bit error for single-symbol 16-FSK with (15, 9) RS encoding in both AWGN and PNI for $\rho = 1$ and $E_b/N_0 = 6.3\,\text{dB}$.

Figure 25.   Probability of bit error for single-symbol 16-FSK with (15, 9) RS encoding in both AWGN and PNI for $\rho = 0.4$ and $E_b/N_0 = 6.3\,\text{dB}$.
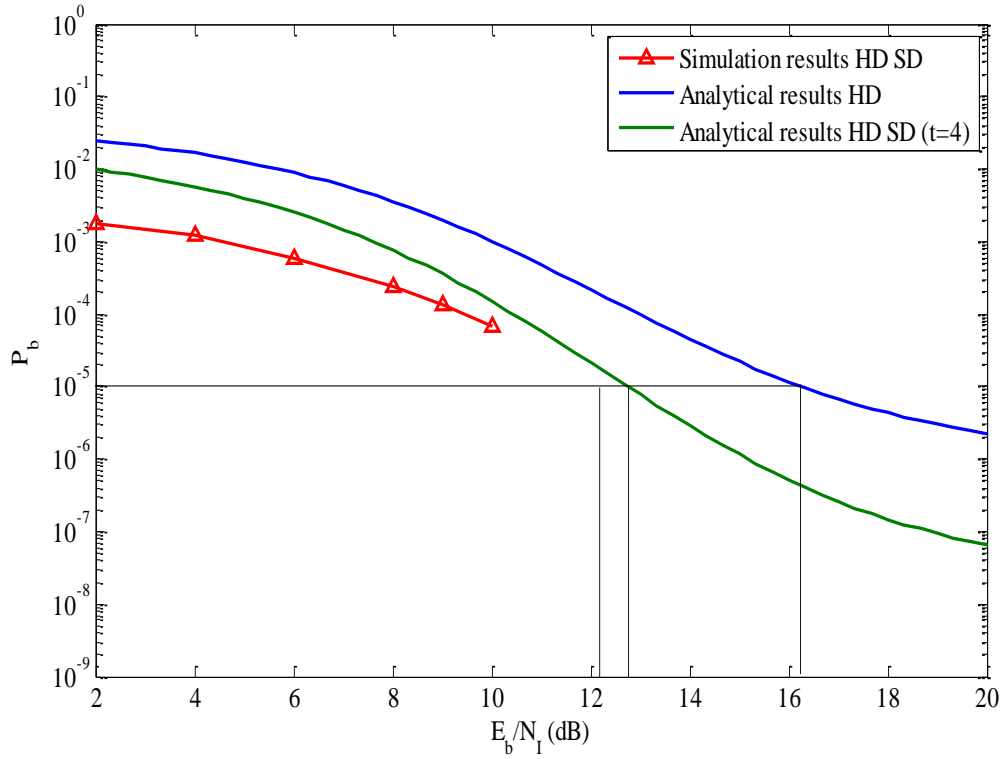
Figure 26. Probability of bit error for single-symbol 16-FSK with (15, 9) RS in both AWGN and PNI for $\rho = 0.2$ and $E_b/N_0 = 6.3\,\mathrm{dB}$

From the preceding results, we see that PNI degrades performance significantly when only HD decoding is used. In order to achieve $P_b = 10^{-5}$, the E_b/N_I required increases as the fraction of time that the interference is on ρ gets smaller. In this case, pulsed jamming is more effective than barrage jamming. For single-symbol 16-FSK and HD SD decoding, performance is improved significantly in PNI as compared to HD decoding, especially for smaller ρ. For $\rho = 0.4$ and 0.2, the coding gains relative to HD decoding are 3.5 dB and 4 dB, respectively. HD SD decoding actually performs better for smaller ρ. This has to do with the change in calculating the reliability information when PNI is present as was discussed at the beginning of the section. The HD SD algorithm has the capability of distinguishing which symbols are jammed, and within a block of ten symbols selected to be reevaluated, the percentage of the jammed symbols that are the most likely to be corrupted increases as ρ gets smaller. In terms of error

correction capability t, HD SD decoding corrects slightly more than three error for the barrage interference and four for $\rho = 0.4$. We note that as ρ decreases, t increases.

Furthermore, during our research for this thesis, we also examined a (15, 7) RS and discovered that for lower code rates, HD SD decoding also improves the performance and the error correction capability of RS codes. The (15, 7) RS code outperforms the (15, 9) RS code, although, with traditional HD decoding the (15, 9) RS code has better performance. The results for a (15, 7) RS code for PNI when $P_b = 10^{-5}$ are summarized in Table 17.

Table 17.   Performance of single-symbol 16-FSK with (15, 7) RS in both AWGN and PNI for $E_b/N_0 = 6.3\,\mathrm{dB}$ when $P_b = 10^{-5}$.

P_b	16 FSK RS (15, 7) $r = 7/15 = 0.47$	E_b/N_I (dB) $\rho=1$	E_b/N_I (dB) $\rho=0.4$	E_b/N_I (dB) $\rho=0.2$	Error Correction Capability t
10^{-5}	Simulation HD SD	12.7	7.8	6.7	4 4 4
10^{-5}	Analytical HD SD	13.3	8.3	12.8	4 4 4
10^{-5}	Analytical HD	19.5	9.4	16.3	3

The preceding analysis was conducted for low E_b/N_0. Next, we performed the analysis and simulations for $E_b/N_0 = 13\,\mathrm{dB}$, which is close to the saturation limit of the performance. This means that if E_b/N_0 is further increased, only insignificant improvement will result for HD decoding, indicating the BER is dominated by the PNI. The probability of bit error in both AWGN and PNI for $\rho = 1$ and 0.4 are shown in Figures 27 and 28, respectively, for $E_b/N_0 = 13\,\mathrm{dB}$. The results are summarized for PNI when $P_b = 10^{-5}$ in Table 18.

Table 18. Performance of single-symbol 16-FSK with (15, 9) RS in both AWGN and PNI for $E_b/N_0 = 13\,\text{dB}$ when $P_b = 10^{-5}$.

| P_b	16 FSK RS (15, 9) $r = 9/15 = 0.6$	E_b/N_I (dB) $\rho = 1$	E_b/N_I (dB) $\rho = 0.4$	Error Correction Capability t
10^{-5}	Simulation HD SD	5.7	7.8	4 4
10^{-5}	Analytical HD SD	5.8	8.3	4 4
10^{-5}	Analytical HD	6.7	9.4	3
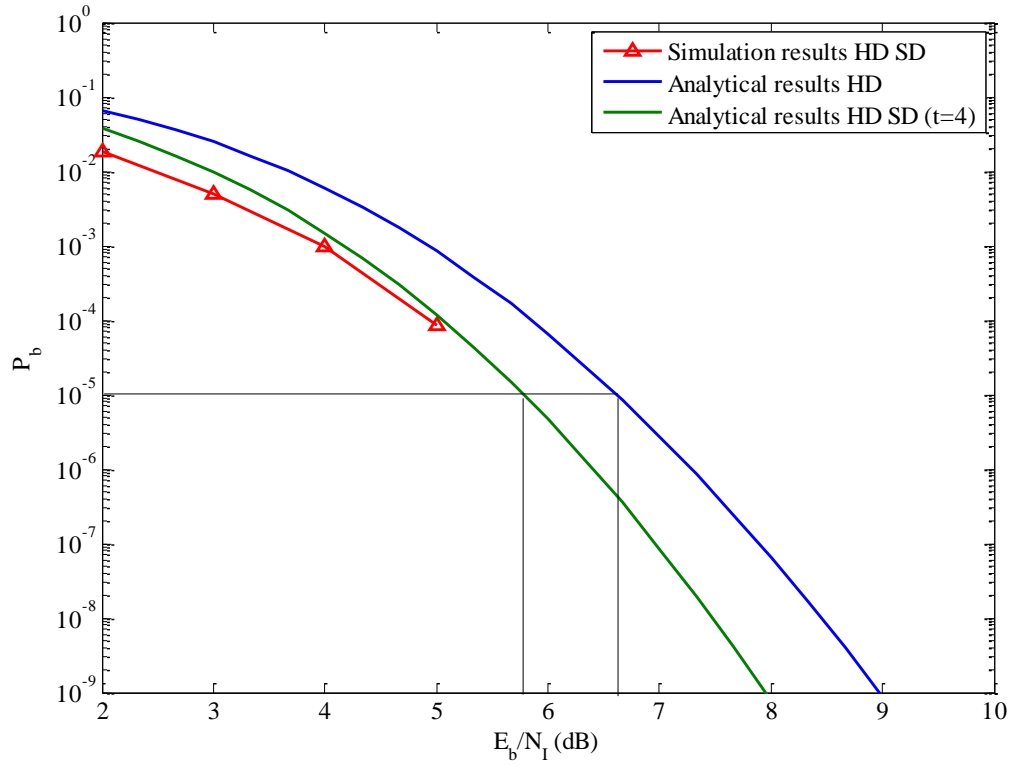
Figure 27. Probability of bit error for single-symbol 16-FSK with (15, 9) RS encoding in both AWGN and PNI for $\rho = 1$ and $E_b/N_0 = 13\,\text{dB}$.
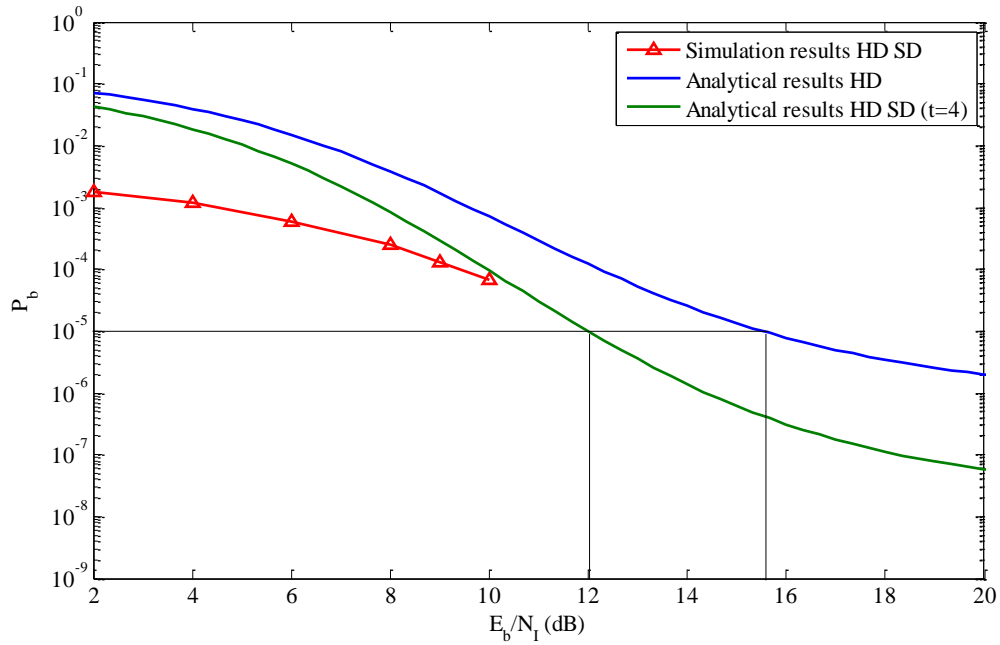
Figure 28.   Probability of bit error for single-symbol 16-FSK with (15, 9) RS encoding in both AWGN and PNI for $\rho = 0.4$ and $E_b/N_0 = 13\,\text{dB}$

Analyzing the data, we see that increased E_b/N_0 improves the performance and degrades the interferer effect. HD SD decoding is effective and, although the coding gains are smaller than for $E_b/N_0 = 6.3\,\text{dB}$, the HD SD algorithm performs slightly better with larger E_b/N_0. Moreover, for $\rho = 0.2$ the performance is below $P_b = 10^{-5}$, which is why simulation results are not shown for this case. Thus, HD SD decoding has even better performance for small ρ. As for $E_b/N_0 = 6.3\,\text{dB}$, the HD SD algorithm is better for lower code rates. A (15, 7) RS code with HD SD decoding outperforms a (15, 9) RS code both in terms of E_b/N_I required for $P_b = 10^{-5}$ and coding gains.

B.   DOUBLE-SYMBOL TRANSMISSION

This section presents the simulation results and the performance analysis for double-symbol transmission and HD SD decoding in both AWGN and PNI. As previously stated, double-symbol transmission allows the use of longer RS block lengths. Specifically, the RS encoder encodes $2m$ bits per code symbol and produces $n = 2^{2m} - 1$ code symbols. In (4.3), P_s is replaced by [30]

$$P_{sDouble} = 2P_s - P_s^2.$$ (3.3)

Both 8-FSK and 16-FSK are examined; however, 32-FSK is not analyzed for the reasons mentioned in previous sections.

1.   8-FSK

For double-symbol 8-FSK, we examine a (63, 39) RS code. The probability of bit error in both AWGN and PNI for ρ = 1, 0.4 and 0.2 are shown in Figures 29, 30 and 31, respectively, for $E_b/N_0 = 6$ dB. This is the E_b/N_0 that yields $P_b = 10^{-8}$ when only AWGN is present. In Table 19, the results are summarized for PNI when $P_b = 10^{-5}$.

Table 19.   Performance of double-symbol 8-FSK with (63, 39) RS encoding in both AWGN and PNI for $E_b/N_0 = 6$ dB when $P_b = 10^{-5}$.

| P_b	8 FSK RS (63, 39) $r = 39/63 = 0.62$	E_b/N_I (dB) $\rho = 1$	E_b/N_I (dB) $\rho = 0.4$	E_b/N_I (dB) $\rho = 0.2$	Error Correction Capability t
10^{-5}	Simulation HD SD	10.7	11.2	10.7	16 16 17
10^{-5}	Analytical HD SD	10.7	11.2	10.7	16 16 17
10^{-5}	Analytical HD	14.2	14.6	15	12

52
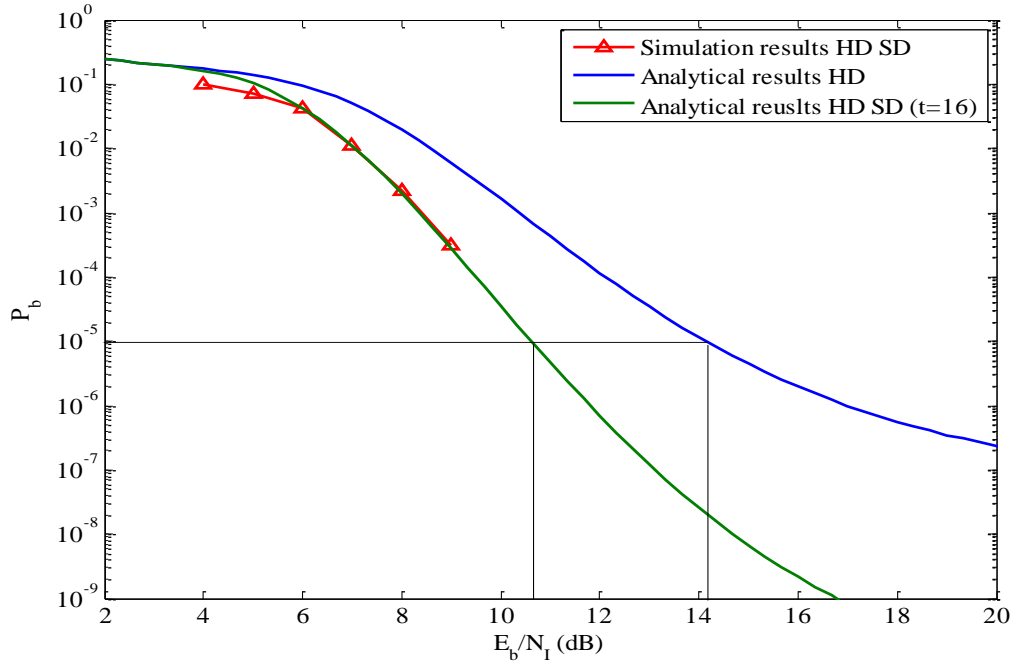
Figure 29.   Probability of bit error for double-symbol 8-FSK with (63, 39) RS encoding in both AWGN and PNI for $\rho = 1$ and $E_b/N_0 = 6$ dB.

Figure 30.   Probability of bit error for double-symbol 8-FSK with (63, 39) RS encoding in both AWGN and PNI for $\rho = 0.4$ and $E_b/N_0 = 6$ dB.

Figure 31. Probability of bit error for double-symbol 8-FSK with (63, 39) RS encoding in both AWGN and PNI for $\rho = 0.2$ and $E_b/N_0 = 6\,\text{dB}$.

As was the case for single-symbol transmission, it is clear that traditional HD decoding performance is degraded as the fraction of time that interference is present is reduced. In this case, this is the best strategy for the jammer since a larger E_b/N_I is present is required for reliable communications. On the other hand, HD SD decoding improves the performance by 3.5, 3.4, and 4.3 dB for values of $\rho = 1$, 0.4, and 0.2, respectively. We see again that HD SD decoding performs better for smaller ρ, and in Figure 31, the same performance as with the barrage noise, shown in Figure 29, is achieved. A (63, 39) RS code with HD SD decoding is able to correct four additional errors for the AWGN case as compared to HD decoding. From Table 19 we see that with HD SD decoding in a PNI environment this advantage is maintained and, for small ρ, is improved.

In addition to a (63, 39) RS code, we also examined a (63, 21) RS code. This code rate with traditional HD decoding could not reach $P_b = 10^{-5}$ but can with HD SD decoding. In the same manner as for single-symbol transmission, we investigated the (63, 39) RS code for $E_b/N_0 = 10$ dB. For $E_b/N_0 > 10$ dB the probability of bit error does not improve significantly. The probability of bit error for double-symbol 8-FSK with a (63, 39) RS code in both AWGN and PNI for ρ = 1, 0.4, and 0.2 and $E_b/N_0 = 10$ dB is shown in Figures 32, 33 and 34, respectively. The effect of PNI is degraded for large E_b/N_0. However, HD SD decoding improves performance by 1, 1.3 and 2.2 dB for ρ = 1, 0.4, and 0.2, respectively. The effectiveness of PNI, contrary to what is obtained with HD decoding, is minimized by HD SD decoding.
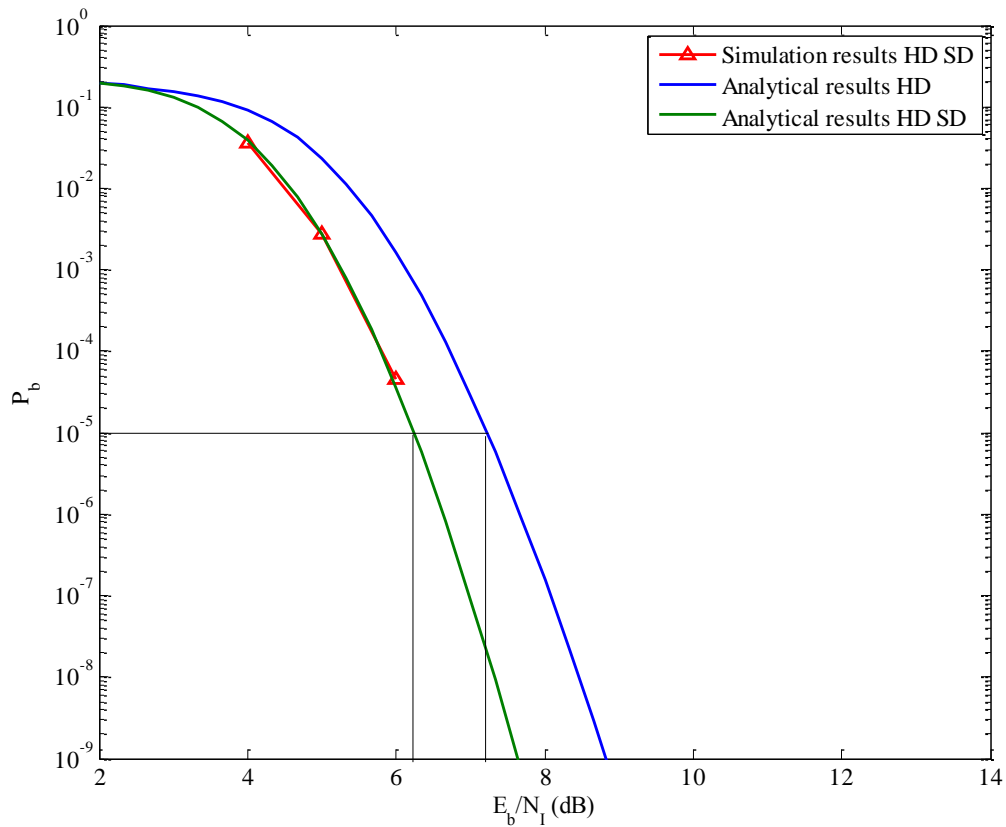
Figure 32.   Probability of bit error for double-symbol 8-FSK with (63, 39) RS encoding in both AWGN and PNI for ρ = 1 and $E_b/N_0 = 10$ dB.
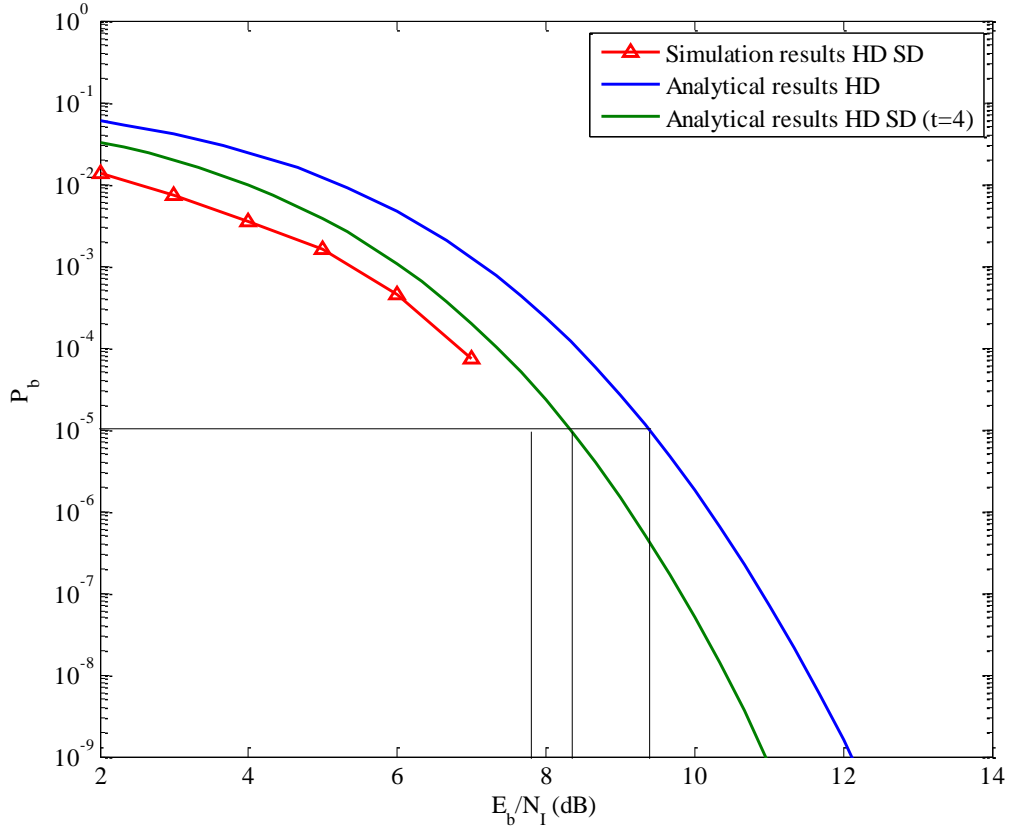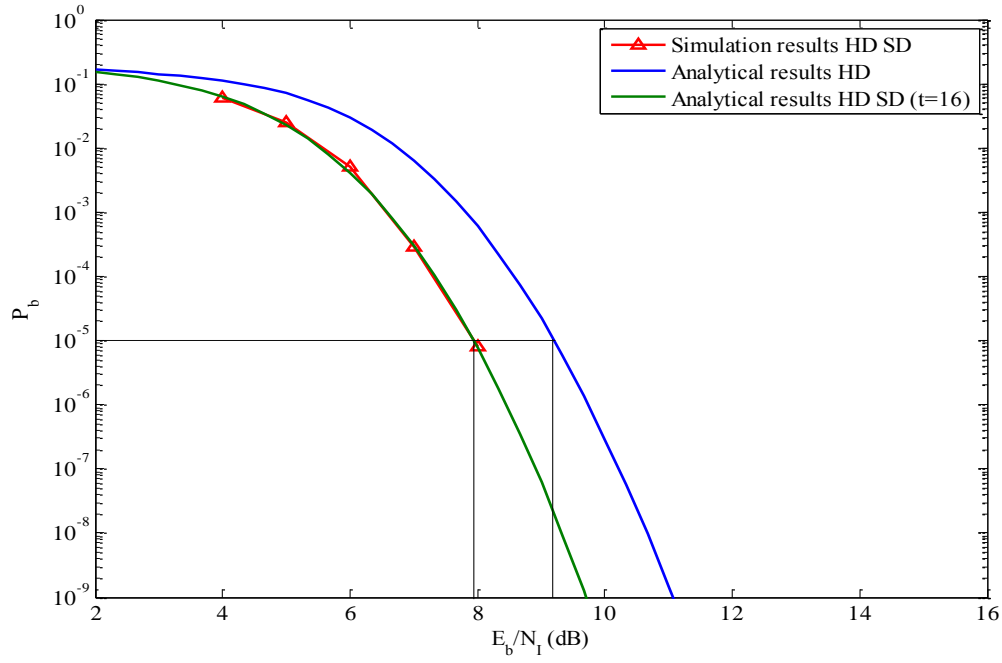
Figure 33.   Probability of bit error for double-symbol 8-FSK with (63, 39) RS encoding in both AWGN and PNI for $\rho = 0.4$ and $E_b/N_0 = 10\,\mathrm{dB}$.

Figure 34.   Probability of bit error for double-symbol 8-FSK with (63, 39) RS encoding in both AWGN and PNI for $\rho = 0.2$ and $E_b/N_0 = 10\,\mathrm{dB}$.

The error correction capability of a (63, 39) RS code with HD SD decoding is the same as in the AWGN case for larger ρ but increases for small ρ. The results are summarized for PNI for PNI when $P_b = 10^{-5}$ in Table 20.

Table 20.   Performance of double-symbol 8-FSK with (63, 39) RS encoding in both AWGN and PNI for $E_b/N_0 = 10\,\text{dB}$ when $P_b = 10^{-5}$.

P_b	8 FSK RS (63, 39) $r = 39/63 = 0.62$	E_b / N_I (dB) $\rho = 1$	E_b / N_I (dB) $\rho = 0.4$	E_b / N_I (dB) $\rho = 0.2$	Error Correction Capability t
10^{-5}	Simulation HD SD	6.3	7.9	8	16 16 17
10^{-5}	Analytical HD SD	6.3	8	8.1	16 16 17
10^{-5}	Analytical HD	7.2	9.2	10.2	12

2.   16-FSK

Next we investigate the performance of double-symbol 16-FSK with HD SD decoding, for a (255, 223) RS code. The performance of coherent double-symbol 16-FSK with (255, 223) RS encoding in both AWGN and PNI for $E_b/N_0 = 4.5$ dB is presented in Figures 35, 36 and 37 for $\rho = 1$, 0.4, and 0.2, respectively. The results are summarized for PNI when $P_b = 10^{-5}$ in Table 21.

Table 21.   Performance of double-symbol 16-FSK with (255, 223) RS encoding in both AWGN and PNI for $E_b/N_0 = 4.5\,\text{dB}$ when $P_b = 10^{-5}$.

| P_b	16 FSK RS (255, 223) $r = 223/255 = 0.87$	E_b / N_I (dB) $\rho = 1$	E_b / N_I (dB) $\rho = 0.4$	E_b / N_I (dB) $\rho = 0.2$	Error Correction Capability t
10^{-5}	Simulation HD SD	12.9	13.6	14.3	21 21 21
10^{-5}	Analytical HD SD	12.9	13.6	14.3	21 21 21
10^{-5}	Analytical HD	17.4	17.8	18.3	16

Figure 35.   Probability of bit error for double-symbol 16-FSK with (255, 223) RS
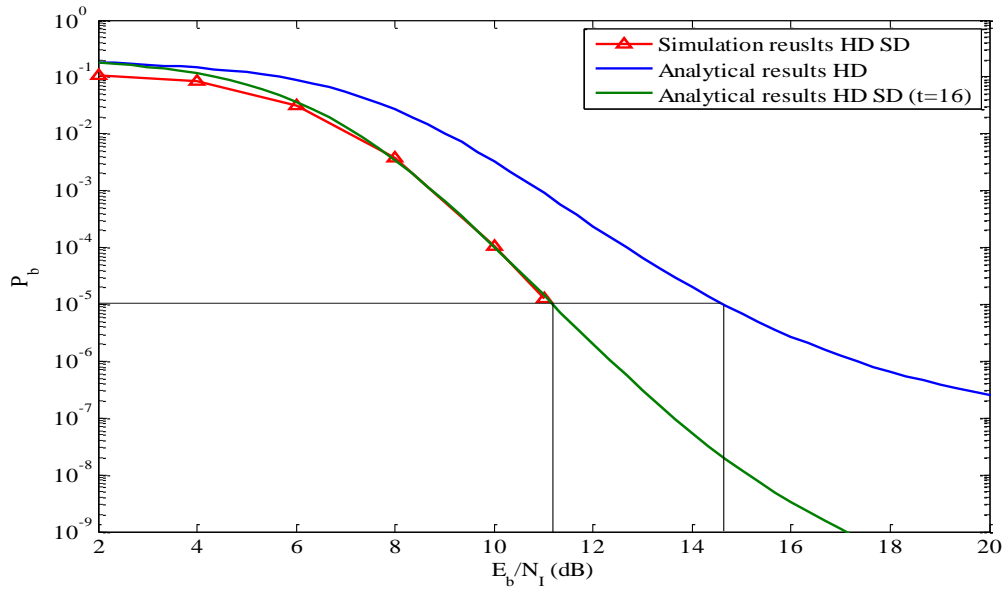encoding in both AWGN and PNI for $\rho = 1$ and $E_b/N_0 = 4.5$ dB.

Figure 36.   Probability of bit error for double-symbol 16-FSK with (255, 223) RS
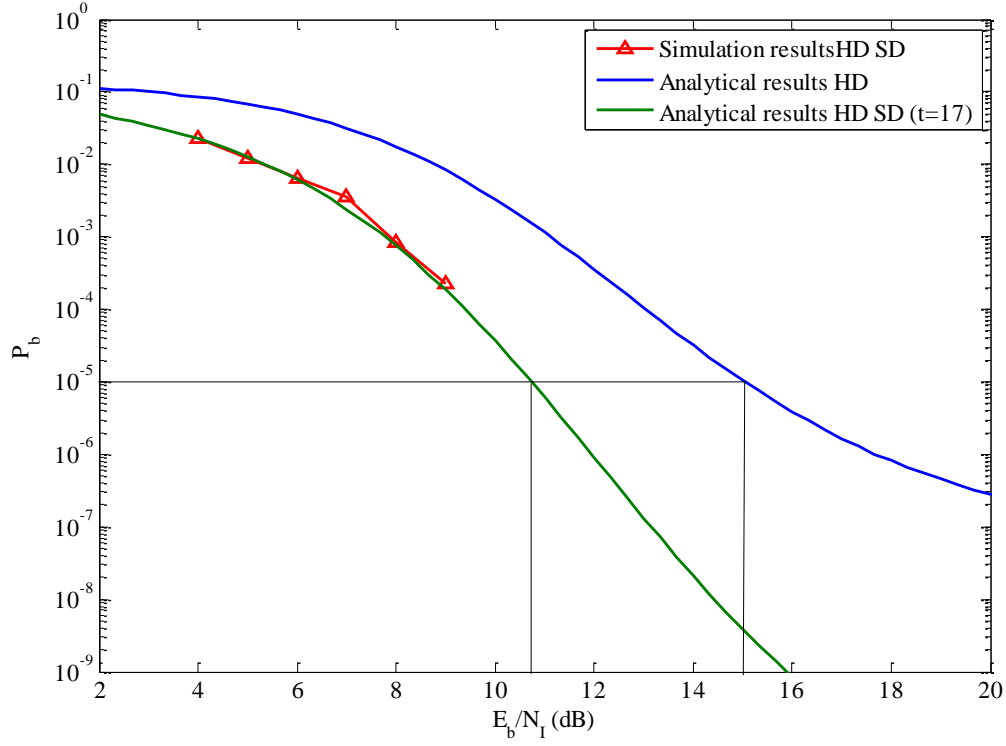encoding in both AWGN and PNI for $\rho = 0.4$ and $E_b/N_0 = 4.5$ dB.

Figure 37.   Probability of bit error for double-symbol 16-FSK with (255, 223) RS encoding in both AWGN and PNI for $\rho = 0.2$ and $E_b/N_0 = 4.5$ dB.

HD SD decoding has significant coding gain over traditional HD decoding, on the order of 4 to 4.5 dB. Furthermore, the error correction capability is improved over the AWGN case; t is increased from four to five. The required E_b/N_I for $P_b = 10^{-5}$ is 12.9, 13.6, and 14.2 dB for $\rho = 1$, 0.4, and 0.2 respectively. Generally, we see that PNI affects double-symbol 16-FSK more than double-symbol 8-FSK for values of E_b/N_0 that yields $P_b = 10^{-8}$ when only AWGN is present. If we compare the barrage noise cases of 8-FSK and 16-FSK, although they use different RS block lengths and code rates and the E_b/N_0 that corresponds to $P_b = 10^{-8}$ in only AWGN is different, we see that 16-FSK requires 2.2 dB more E_b/N_I for $P_b = 10^{-5}$. However, for double-symbol 16-FSK, HD SD decoding does not perform better for small fractions of interference time ρ as we have already seen with single-symbol 16-FSK and double-symbol 8-FSK.

Next, the results of the simulation and analysis of double-symbol 16-FSK with (255, 223) RS encoding for $E_b/N_0 = 10$ dB are presented. In Figures 38, 39, and 40, we see that the required E_b/N_I for $P_b = 10^{-5}$ is 5.13, 7.75 and 9.49 dB for $\rho = 1$, 0.4, and 0.2, respectively. The results are summarized in Table 22.

Table 22.   Performance of double-symbol 16 FSK with (255, 223) RS encoding in both AWGN and PNI for $E_b/N_0 = 10$ dB.

| P_b	16 FSK RS (255, 223) $r = 223/255 = 0.87$	E_b/N_I (dB) $\rho = 1$	E_b/N_I (dB) $\rho = 0.4$	E_b/N_I (dB) $\rho = 0.2$	Error Correction Capability t
10^{-5}	Simulation HD SD	5.1	7.8	9.5	21 21 21
10^{-5}	Analytical HD SD	5.1	7.8	9.5	21 21 21
10^{-5}	Analytical HD	5.6	8.4	10.2	16
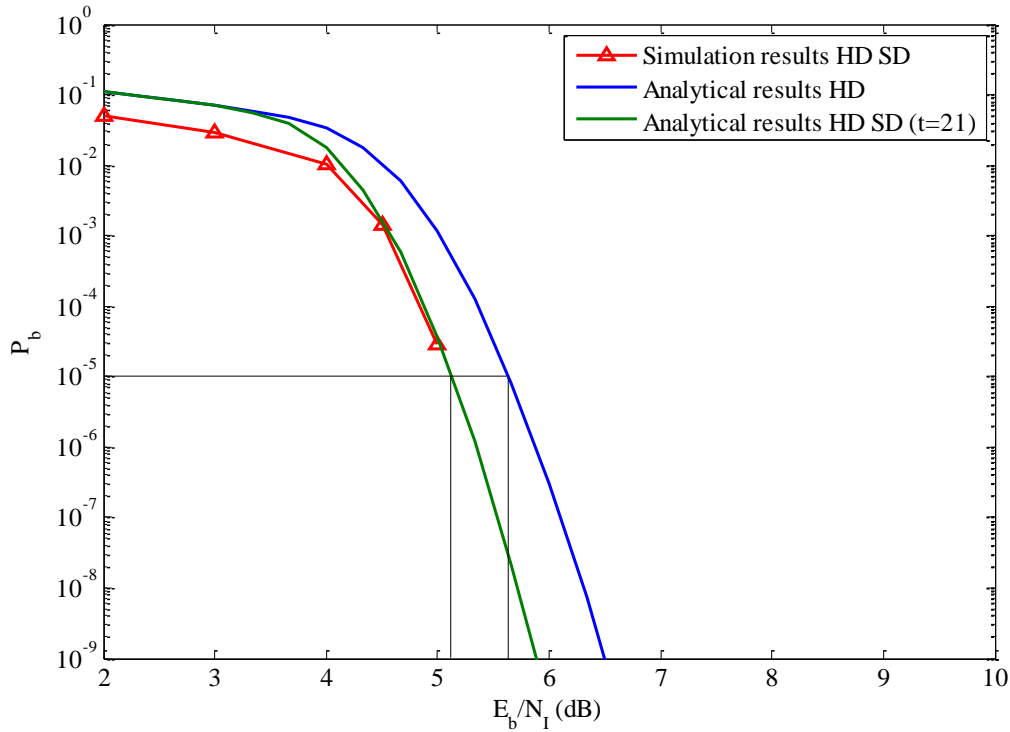
Figure 38.   Probability of bit error for double-symbol 16-FSK with (255, 223) RS encoding in both AWGN and PNI for $\rho = 1$ and $E_b/N_0 = 10$ dB.
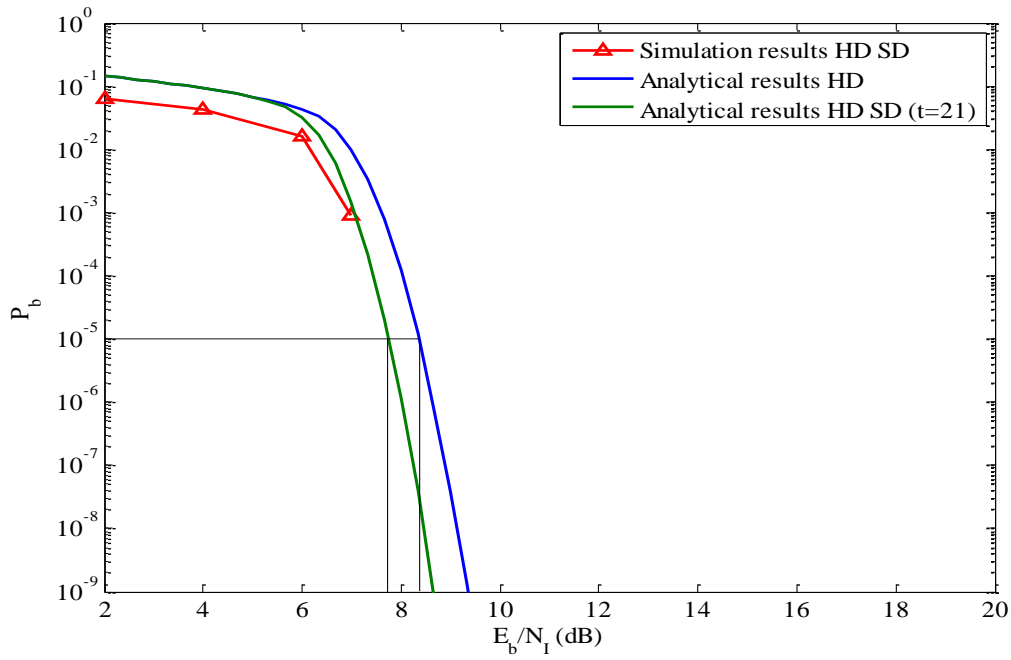
Figure 39.   Probability of bit error for double-symbol 16-FSK with (255, 223) RS encoding in both AWGN and PNI for $\rho = 0.4$ and $E_b/N_0 = 10\,\text{dB}$.
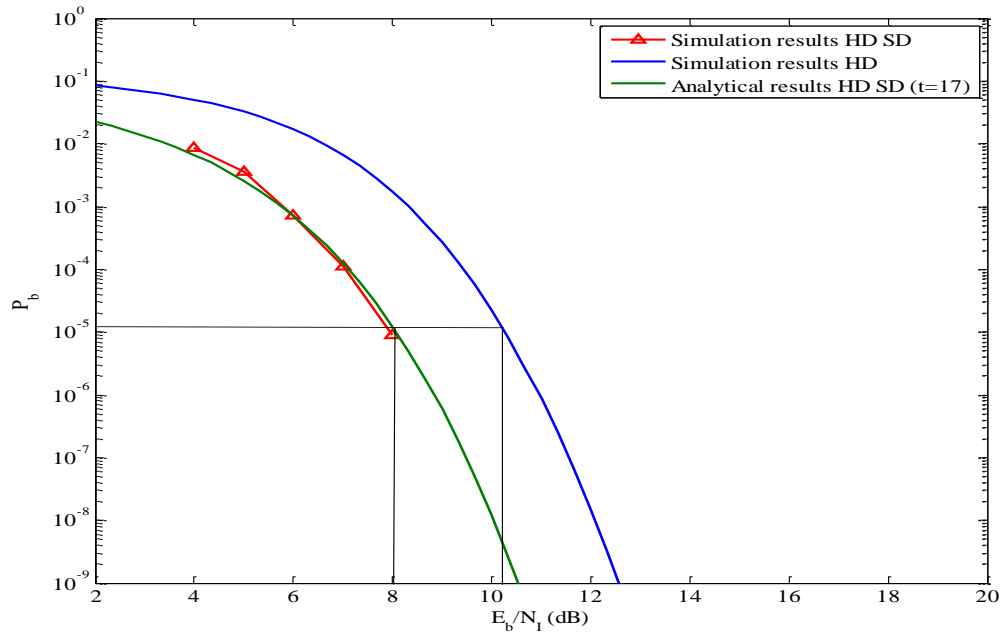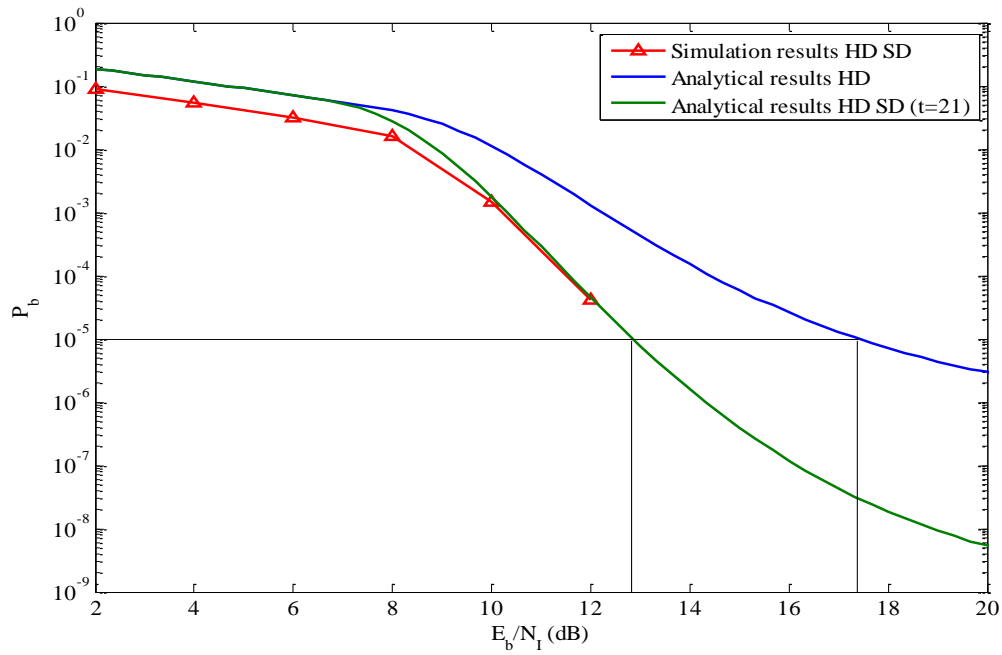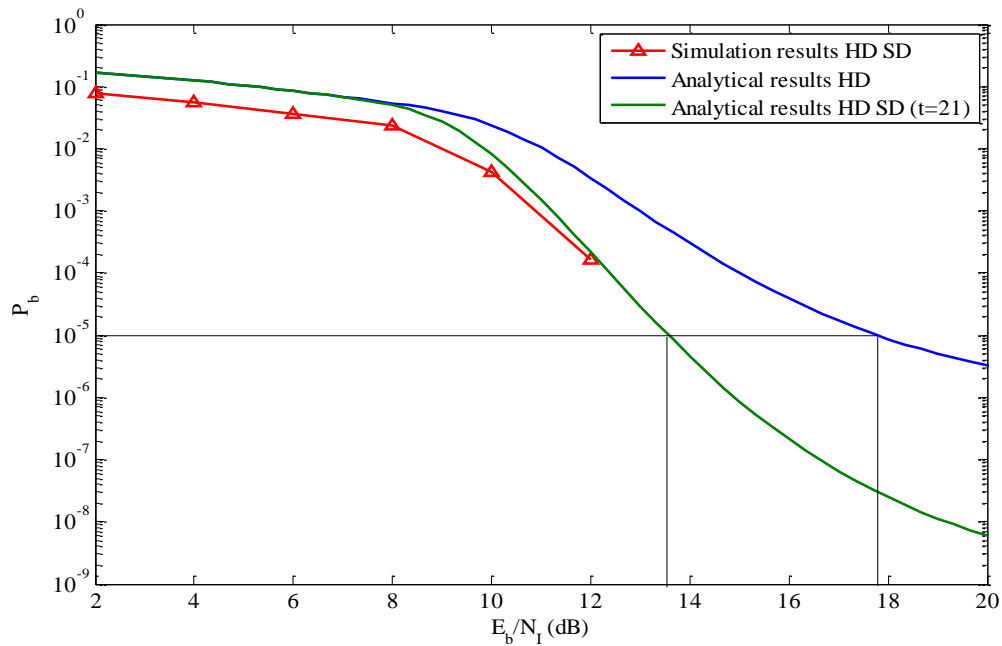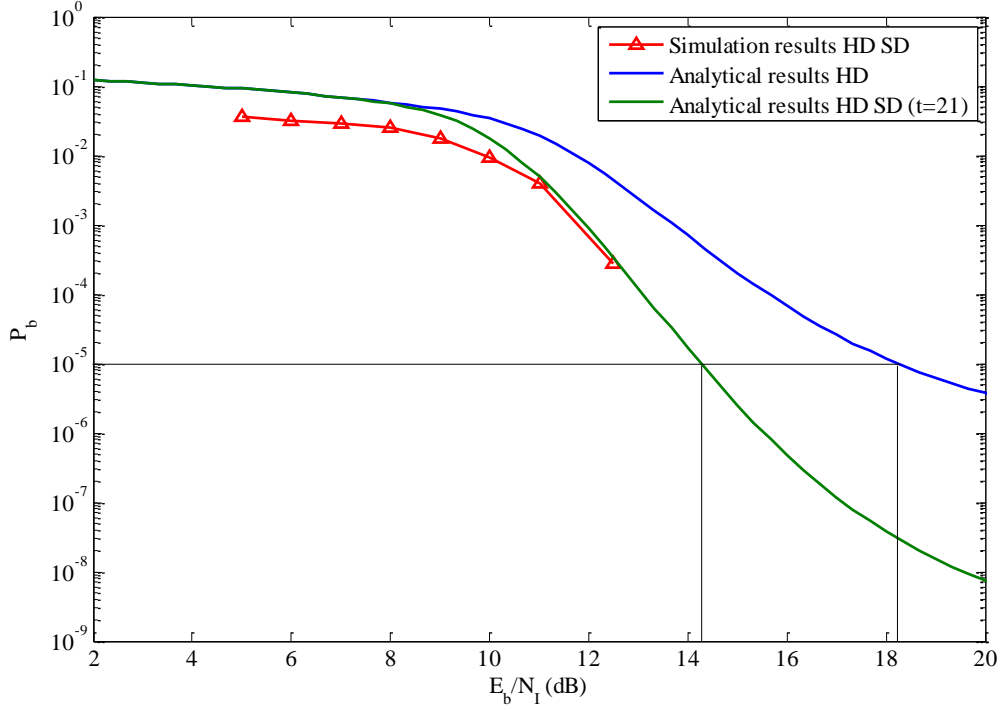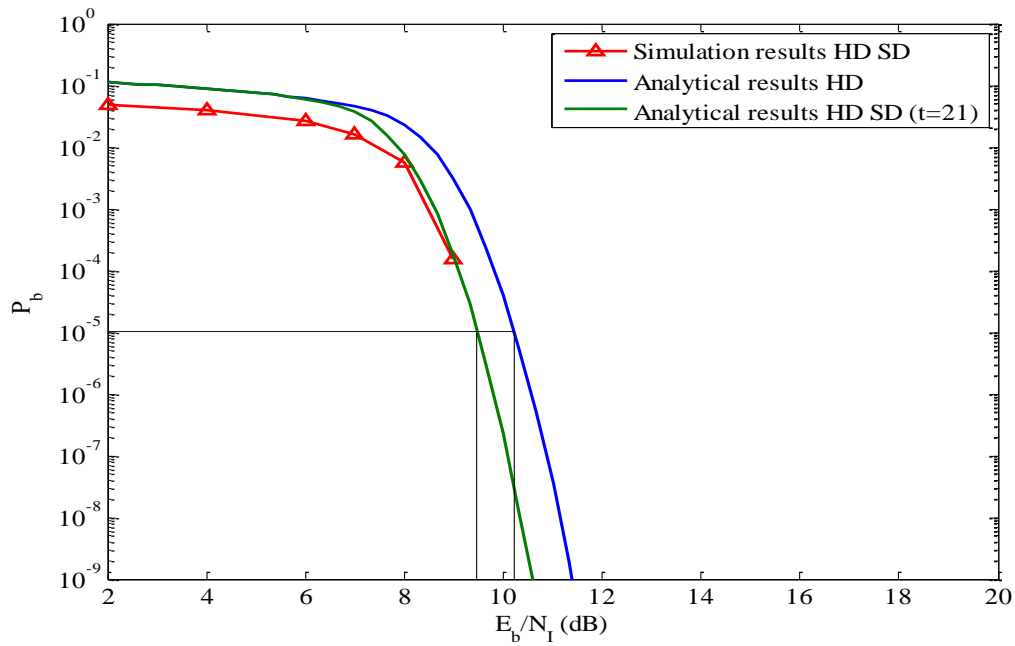

Figure 40.   Probability of bit error for double-symbol 16-FSK with (255, 223) RS in both AWGN and PNI for $\rho = 0.2$ and $E_b/N_0 = 10\,\text{dB}$.

It is obvious that for large E_b/N_0, barrage noise is the least effective interference for double-symbol 16-FSK. On the other hand, as the fraction of time that the interference is on, ρ, gets smaller, the degradation in performance is significant. The coding gains are within a range of 0.5 and 0.8 dB for $0.2 \leq \rho \leq 1$. The HD SD algorithm although it maintains the capability of correcting five more symbol errors per block, however, the coding gains are inversely proportional to E_b/N_0. Thus, low values give greater coding gain.

C. CHAPTER SUMMARY

In this chapter, the effect of AWGN and PNI for MFSK, a power efficient modulation, with hybrid HD SD decoding and coherent demodulation was examined. A significant contribution of this thesis is the examination of the effect of PNI on HD SD decoding. The HD SD decoding algorithm provides significant coding gains over traditional HD decoding and improvement of the error correction capability for Reed Solomon codes. In the event of PNI, the HD SD decoding algorithm increases jamming resistance. The vast improvement compared to only AWGN has to do with how the reliability information was modeled. As was mentioned in the beginning of this chapter, when the SD reliability information is calculated, the conditional PDFs are Gaussian, and the variances are computed using only the effect of AWGN and not PNI.

From the simulation results, it was shown that the HD SD decoding algorithm only works well with single-symbol 16-FSK, double-symbol 8-FSK and double-symbol 16-FSK. The error correction capabilities of the different codes rates examined were the same with only AWGN but in some cases improved for small fractions of interference time ρ. It was also shown that for single-symbol and double-symbol 8-FSK, HD SD decoding provides more robust communications than traditional HD decoding. PNI degrades traditional HD decoding performance as ρ gets smaller for $0.2 \leq \rho \leq 1$, but HD SD decoding achieved performance similar to barrage noise interference, although ρ was 0.2.

Comparing the error correction capability of HD SD decoding with the GS SD algorithm for the (15, 9), (63, 39) and (255, 223) RS codes that were examined in this chapter, we have Table 23.

Table 23.   Comparison of error corrections capabilities.

RS	HD SD t Error Correction	GS SD t Error Correction	HD t Error Correction
(15, 9)	4	3.4	3
(63, 39)	16-17	13.4	12
(255, 223)	21	16.5	16

HD SD decoding significantly increases t compared to both traditional HD and GS SD decoding, especially for double-symbol transmission. This advantage is for medium to high code rates, where the GS SD algorithm is not a powerful tool [13].

In the following chapter, the performance simulation and analysis of MFSK with RS encoding, hybrid HD SD decoding and noncoherent demodulation in AWGN is presented.

THIS PAGE INTENTIONALLY LEFT BLANK

V. PERFORMANCE SIMULATION AND ANALYSIS OF *M*FSK WITH RS ENCODING, HYBRID HD SD DECODING, AND NONCOHERENT DEMODULATION IN AWGN

In this chapter, the performance of *M*FSK with RS encoding and hybrid HD SD decoding for noncoherent demodulation in AWGN is examined. The difference from the simulations of Chapter III is that the receiver does not recover the carrier phase. The demodulation circuitry for noncoherent signal reception is the one that was shown in Figure 4. The performance of noncoherent *M*FSK is worse than for coherent detection. For example, 8-FSK with a (63, 39) RS code and traditional HD decoding for $P_b = 10^{-5}$ requires $E_b/N_0 = 6.8$ dB, while with coherent demodulations $E_b/N_0 = 5.4$ dB, 1.4 dB more, is required. The advantage of the noncoherent demodulation lies in the simplicity of the receiver. The conditional probability density functions for the random variables V_m, $m = 1, 2, ..., M$, that represent the output of the mth branch when the signal corresponding to symbol m is transmitted are modeled as non-central chi-squared probability density functions with two degrees of freedom when the noise is modeled as Gaussian. The performance is presented in two sections, one for single-symbol transmission and one for longer block lengths where two modulation symbols are used to transmit a single code symbol.

A. SINGLE-SYMBOL TRANSMISSION

For noncoherent *M*FSK with HD SD decoding, *M* = 8, 16 and 32 were examined. The channel symbol error probability is given by [22]

$$p_s = \sum_{n=1}^{M-1} \frac{(-1)^{n+1}}{n+1} \binom{M-1}{n} \exp\left[\frac{-nrEs}{(n+1)N_o}\right] \tag{5.1}$$

and the probability of information bit error is given by [7]

$$P_b \approx \frac{n+1}{2n^2} \sum_{i=t+1}^{n} i \binom{n}{i} p_s^{\,i}(1-p_s)^{n-i} \tag{5.2}$$

We know in advance that HD SD does not improve the performance of 32-FSK for the reasons mentioned in Chapter III. However, it was shown that HD SD decoding also does not improve, with the current configuration of the algorithm, the performance even of 8-FSK and 16-FSK. The capability of the decoding scheme is affected by the way that the statistics after the demodulation are modeled. The conditional probabilities for non-central chi-squared probability density functions with two degrees of freedom are in most cases near unity. Even though the HD SD algorithm can select up to ten symbols, the actual number symbols examined are only three or four, and this means that the decoding lists that are created are restricted to between 2^3 and 2^4. Thus, the probability of successfully decoding a received block is reduced significantly.

B.   DOUBLE-SYMBOL TRANSMISSION

Both simulation and analytical results are presented for longer block lengths where two modulation symbols are used to transmit a single code symbol in this section. In this case, (5.1) is used in

$$p_{sDouble} = 2p_s - p_s^2,$$ (5.3)

which is used in (5.2).

1.   8-FSK

Initially, double-symbol 8-FSK was examined for a high rate (63, 53) RS code. As can be seen in Figure 41, when HD SD decoding is used, $E_b/N_0 = 6.3$ dB is required for $P_b = 10^{-5}$. This yields a coding gain of 0.3 dB over HD decoding. The HD SD algorithm can correct one more symbol error per block than HD decoding. The results for a (63, 55) RS code when $P_b = 10^{-5}$ are summarized in Table 24.

Figure 41. Probability of bit error for double-symbol 8-FSK with (63, 53) RS encoding and hybrid HD SD decoding.

Table 24. Performance of double-symbol 8-FSK with (63, 53) RS encoding when $P_b = 10^{-5}$.

P_b	8-FSK RS (63, 53) $r = 55/63 = 0.84$	E_b / N_0 (dB)	Error Correction Capability t
10^{-5}	Simulation HD SD	6.5	6
10^{-5}	Analytical HD SD	6.3	7
10^{-5}	Analytical HD	6.8	5

In Figure 42, the performance for a (63, 47) RS code is shown. Note that by utilizing a code rate near 0.75, performance is improved for HD decoding but much more for HD SD decoding. For $P_b = 10^{-5}$, $E_b/N_0 = 5.3$ dB is required, which yields a coding gain of 0.7 dB. We can observe a vast improvement in the correction capability of the code when HD SD decoding is used; four additional errors per block are corrected. The results for a (63, 47) RS code when $P_b = 10^{-5}$ are summarized in Table 25.

Figure 42.   Probability of bit error for double-symbol 8-FSK with (63, 47) RS encoding
and hybrid HD SD decoding.

Table 25.   Performance of double-symbol 8-FSK with (63, 47) RS encoding
when $P_b = 10^{-5}$.

P_b	8-FSK RS (63, 47) $r = 47/63 = 0.75$	E_b / N_0 (dB)	Error Correction Capability t
10^{-5}	Simulation HD SD	5.9	12
10^{-5}	Analytical HD SD	5.9	12
10^{-5}	Analytical HD	6.6	8

Lastly, we examine double-symbol 8-FSK with a (63, 21) RS code. From Figure 43, we see that for this low code rate, performance is degraded. Nevertheless, the performance with HD SD decoding remains improved compared with HD decoding, and in this case HD SD decoding can correct four additional symbol errors per block. The results for (63, 21) RS encoding when $P_b = 10^{-5}$ are summarized in Table 26.

Figure 43.   Probability of bit error for double-symbol 8-FSK with (63, 47) RS encoding and hybrid HD SD decoding.

Table 26.   Performance of double-symbol 8-FSK with (63, 21) RS encoding when $P_b = 10^{-5}$.

P_b	8-FSK RS (63, 21) $r = 21/63 = 0.33$	E_b / N_0 (dB)	Error Correction Capability t
10^{-5}	Simulation HD SD	7.8	25
10^{-5}	Analytical HD SD	7.8	25
10^{-5}	Analytical HD	8.3	21

2.   16-FSK

The probabilities of bit error for double-symbol 16-FSK and (255, 223), (255, 191) and (255, 83) RS codes were examined. In Figure 44, the simulation and analysis results for a (255, 223) RS code are shown for HD SD and HD decoding. For $P_b = 10^{-5}$,

$E_b/N_0 = 5.0$ dB is required, and HD SD decoding gives a coding gain of 0.3 dB over traditional HD decoding. The HD SD decoding algorithm corrects five more symbol errors per block than HD decoding. The results for (255, 223) RS encoding when $P_b = 10^{-5}$ are summarized in Table 27.

Figure 44.   Probability of bit error for double-symbol 16-FSK with (255, 223) RS encoding and hybrid HD SD decoding.

Table 27.   Performance of double-symbol 16-FSK with (255,223) RS encoding when $P_b = 10^{-5}$.

P_b	16-FSK RS (255, 223) $r = 223/255 = 0.87$	E_b / N_0 (dB)	Error Correction Capability t
10^{-5}	Simulation HD SD	5	21
10^{-5}	Analytical HD SD	5	21
10^{-5}	Analytical HD	5.4	16

In Figures 45 and 46, the probability of bit error for (255, 191) and (255, 83) RS codes are presented. We see that performance improves going from high code rates to medium and then starts degrading for lower code rates.
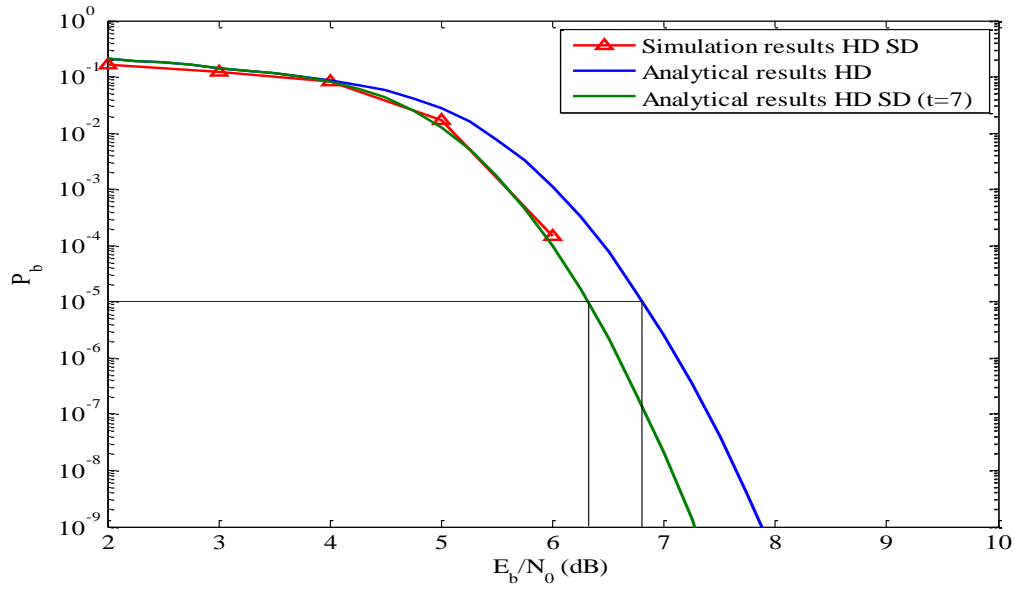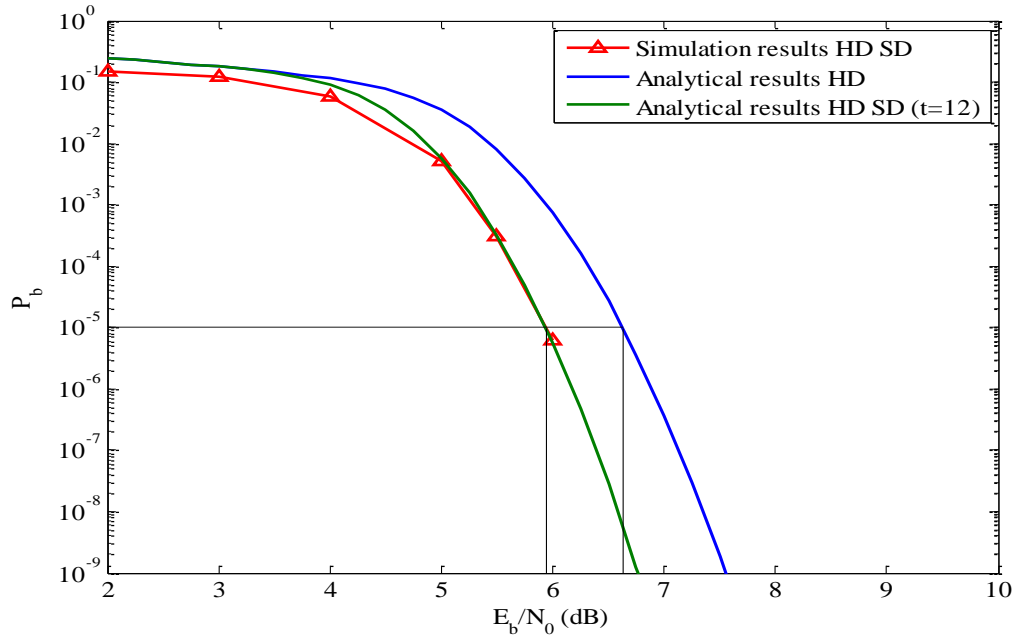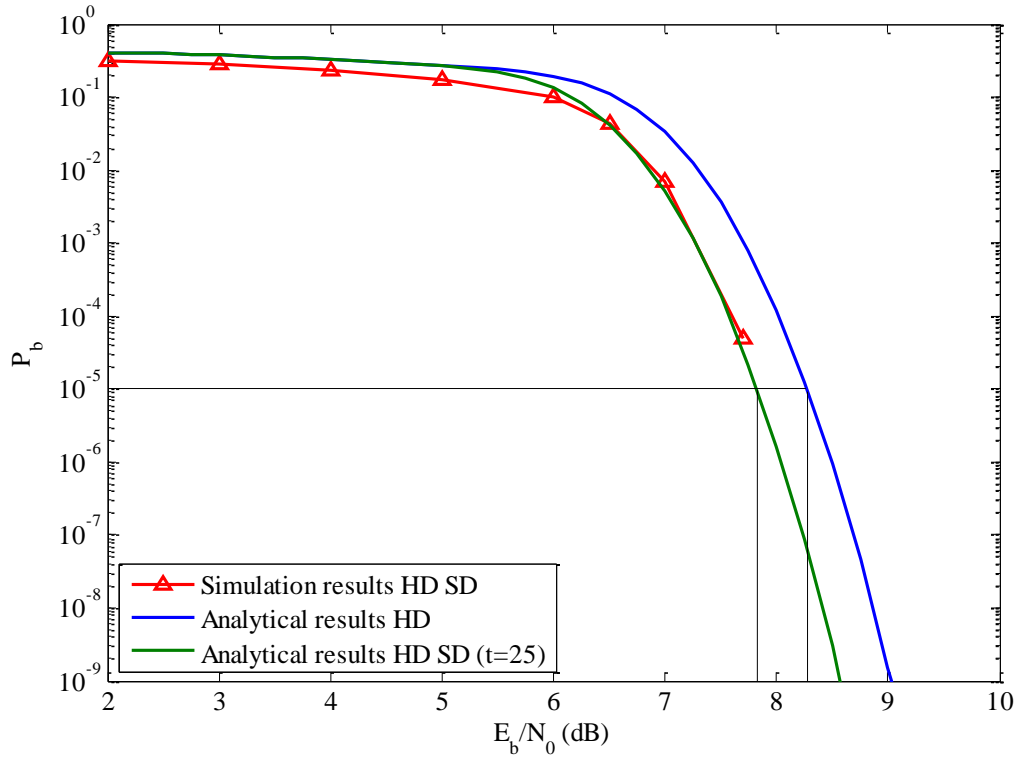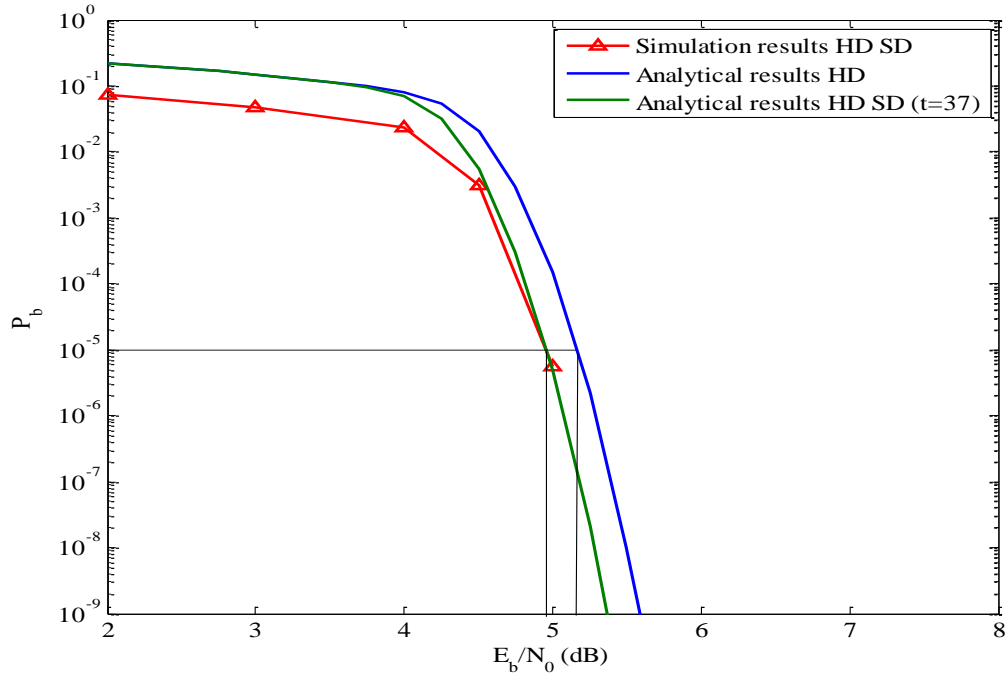

Figure 45.   Probability of bit error for double-symbol 16-FSK with (255, 191) RS encoding and hybrid HD SD decoding.

Table 28.   Performance of double-symbol 16-FSK with (255, 191) RS encoding when $P_b = 10^{-5}$.

P_b	**16-FSK RS (255, 191)** $r = 191/255 = 0.74$	E_b / N_0 **(dB)**	**Error Correction Capability** t
10^{-5}	Simulation HD SD	4.9	37
10^{-5}	Analytical HD SD	4.9	37
10^{-5}	Analytical HD	5.2	32

The (255, 191) RS code has the best performance of all the RS codes of block length 255. For $P_b = 10^{-5}$, $E_b/N_0 = 5.0$ dB is required, and the coding gain is improved by 0.2 dB. The HD SD algorithm significantly extends the error correction capability of traditional HD decoding, correcting five more errors per block. The performance in terms of coding gain over HD decoding is similar to that for coherent demodulation. As already analyzed in Chapter III, the HD SD algorithm provides a small improvement for longer block lengths with 16-FSK, especially when the code rates that have the best performance in terms of required E_b/N_0 are used.

Double-symbol transmission 16-FSK was also examined for a low code rate (255, 83) RS code. As can be seen in Figure 46, for $P_b = 10^{-5}$, $E_b/N_0 = 6.9$ dB is required, which equates to a coding gain of 0.2 dB, although HD SD decoding corrects ten additional symbol errors per block. The results for (255, 83) RS encoding when $P_b = 10^{-5}$ are summarized in Table 29. Furthermore, low code rates have almost 2 dB worse performance from the optimum (255, 191) RS code.

Table 29.   Performance of double-symbol 16-FSK with (255, 83) RS encoding when $P_b = 10^{-5}$.

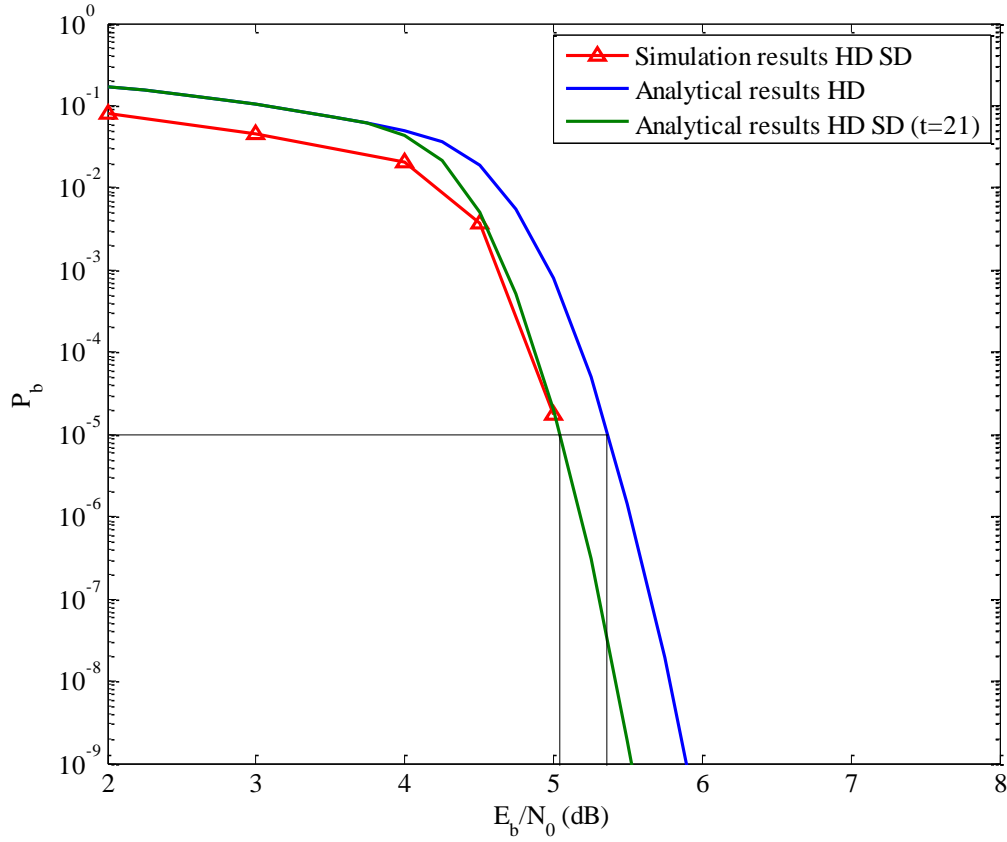| P_b	**16-FSK RS (255, 83)** $r = 83/255 = 0.33$	E_b / N_0 **(dB)**	**Error Correction Capability** t
10^{-5}	Simulation HD SD	6.9	96
10^{-5}	Analytical HD SD	6.9	96
10^{-5}	Analytical HD	7.1	86
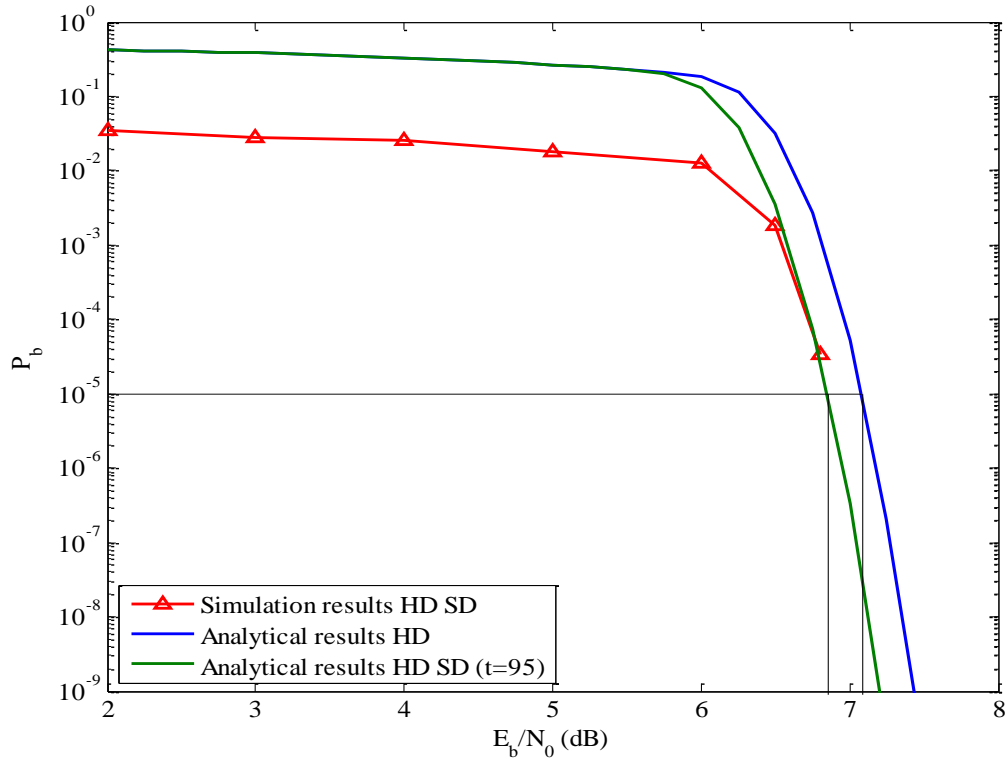
Figure 46.   Probability of bit error for double-symbol 16-FSK with (255, 83) RS encoding and hybrid HD SD decoding.

C.   CHAPTER SUMMARY

In this chapter, the performance of noncoherent MFSK with RS encoding and HD SD decoding was examined in AWGN. Noncoherent demodulation has generally worse performance than does coherent, although in many military communication systems, such as JTIDS/Link–16, noncoherent demodulation is preferred because of the simplicity of the design for the receivers. HD SD decoding cannot currently improve performance with MFSK for single-symbol transmission because the statistics after the demodulator are not modeled as Gaussian RVs as in coherent case. However, the performance of double-symbol 8 and 16-FSK is improved. With 8-FSK, coding gains between 0.2 and 0.5 dB are obtained, and with 16-FSK coding gains between 0.2 and 0.3 dB are obtained. For the same improvement in error correction capability as coherent demodulation, noncoherent

73

demodulation has less coding gain. As was expected, the error correction capability is significantly better than for the GS SD algorithm in many cases, especially for code rates $> 1/3$.

Table 30.   Comparison of error corrections capabilities.

RS	HD SD t Error Correction	GS SD t Error Correction	HD t Error Correction
(63, 53)	6	5.21	5
(63, 47)	12	8.58	8
(63, 21)	25	26.63	21
(255, 223)	21	16.53	16
(255, 191)	37	34.3	32
(255, 83)	96	109.5	86

The performance simulation and analysis of MFSK with RS encoding, hybrid HD SD decoding and noncoherent demodulation in both AWGN and PNI are presented in the next chapter.

VI. PERFORMANCE SIMULATION AND ANALYSIS OF *M*FSK WITH RS ENCODING, HYBRID HD SD DECODING, AND NONCOHERENT DEMODULATION IN AWGN AND PNI

The performance of *M*FSK with RS encoding, HD SD decoding, and noncoherent demodulation in both AWGN and PNI are evaluated in this chapter. The effect of PNI has been addressed in Chapters II and IV. The effect of PNI for $\rho = 1$ (barrage noise), $\rho = 0.4$ and 0.2 are investigated in this thesis. As in Chapter IV, when PNI is present, the SD reliability information is obtained from [2]

$$P_r(T = t_a \mid R = r_\beta) = \frac{f\left(r_\beta \mid t_a\right)}{\sum_{t \in T} f\left(r_\beta \mid t\right)}, \tag{6.1}$$

where in this case the conditional PDFs are non-central chi-squared probability density functions with two degrees of freedom, and the variances are computed by using only the effect of AWGN and not PNI. The symbols received with PNI will have smaller conditional probabilities than the other symbols, and the HD SD decoding algorithm, which selects the ten symbols received with the smallest conditional probabilities, will most likely choose those corrupted by PNI and correct them. As in Chapter IV, it is shown in the following sections that HD SD decoding provides greater coding gains than when only AWGN is present.

Initially, the simulation and analytical results are discussed for single-symbol transmission. Next, results for longer block lengths, obtained by invoking double-symbol transmission, are presented.

A. SINGLE-SYMBOL TRANSMISSION

The channel symbol error probabilities are given by [31]

$$p_s(AWGN) = \sum_{n=1}^{M-1} \frac{(-1)^{n+1}}{n+1} \binom{M-1}{n} \exp\left[\frac{-nrE_s}{(n+1)N_o}\right]$$

$$p_s(AWGN + PNI) = \sum_{n=1}^{M-1} \frac{(-1)^{n+1}}{n+1} \binom{M-1}{n} \exp\left[\frac{-nrE_S}{(n+1)\left(N_0 + \dfrac{N_I}{\rho}\right)}\right], \qquad (6.2)$$

which are used in (2.20), and the probability of information bit error is given by [7]

$$P_b \approx \frac{n+1}{2n^2} \sum_{i=t+1}^{n} i \binom{n}{i} P_s^i (1-P_s)^{n-i}. \qquad (6.3)$$

The simulation results show that, as with AWGN only, hybrid HD SD decoding with the current configuration does not improve the performance for noncoherent MFSK with single-symbol transmission because of the way that the statistics are modeled after the demodulator. A small but insignificant improvement was observed only for 16-FSK.

B.   DOUBLE-SYMBOL TRANSMISSION

The simulation results and the performance analysis of noncoherent MFSK with HD SD decoding in both AWGN and PNI for double-symbol transmission are presented in this section. The difference in the analysis is that P_s in (6.3) is replaced by [30]

$$P_{sDouble} = 2P_s - P_s^2. \qquad (6.4)$$

Contrary to single-symbol transmission, we also examine 8-FSK. However, 32-FSK is not analyzed for the reasons mentioned in previous sections.

1.   8-FSK

Double-symbol 8-FSK was examined for (63, 39) RS encoding, and the probability of bit error in both AWGN and PNI for ρ = 1, 0.4 and 0.2 are shown in Figures 47, 48, and 49, respectively, when $E_b/N_0 = 7.0$ dB. This E_b/N_0 corresponds to

$P_b = 10^{-8}$ when only AWGN is present. The results are summarized in Table 31 for the various values of ρ examined when $P_b = 10^{-5}$.

Table 31. Performance of double-symbol 8-FSK with (63, 39) RS encoding in both AWGN and PNI for $E_b/N_0 = 7$ dB when $P_b = 10^{-5}$.

P_b	8-FSK RS (63, 39) $r = 39/63 = 0.62$	E_b/N_I (dB) $\rho = 1$	E_b/N_I (dB) $\rho = 0.4$	E_b/N_I (dB) $\rho = 0.2$	Error Correction Capability t
10^{-5}	Simulation HD SD	13.9	14.5	14.9	16 16 16+
10^{-5}	Analytical HD SD	13.9	14.5	14.9	16 16 16
10^{-5}	Analytical HD	19.2	19.5	19.8	12
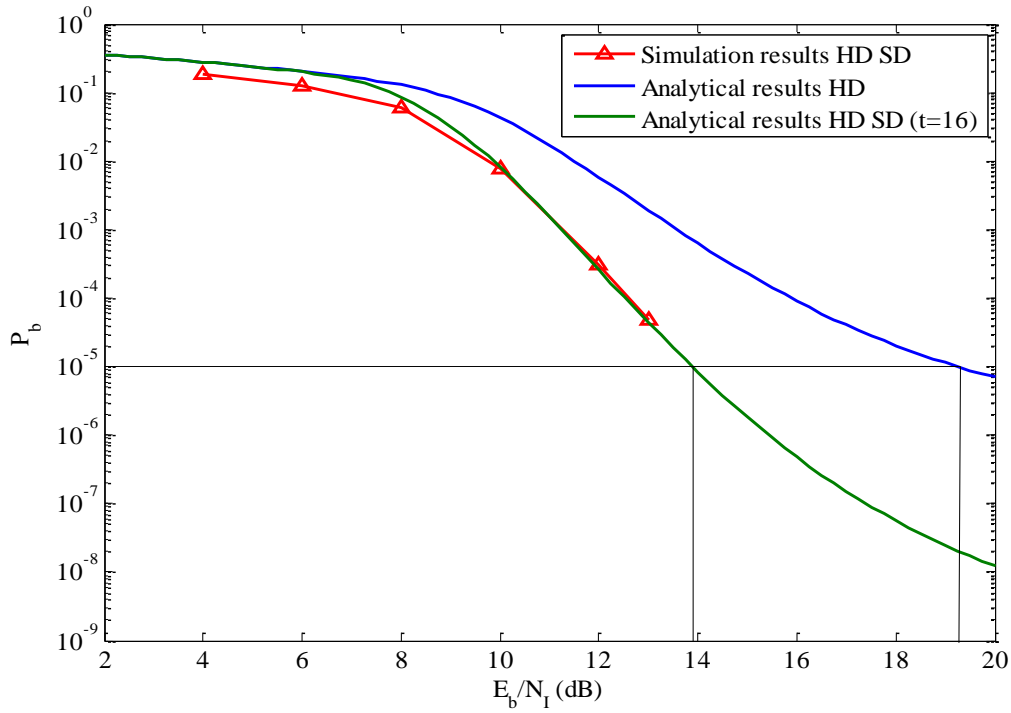
Figure 47. Probability of bit error for double-symbol 8-FSK with (63, 39) RS encoding in both AWGN and PNI for $\rho = 1$ and $E_b/N_0 = 7$ dB.

Figure 48.   Probability of bit error for double-symbol 8-FSK with (63, 39) RS encoding in both AWGN and PNI for $\rho = 0.4$ and $E_b/N_0 = 7$ dB.
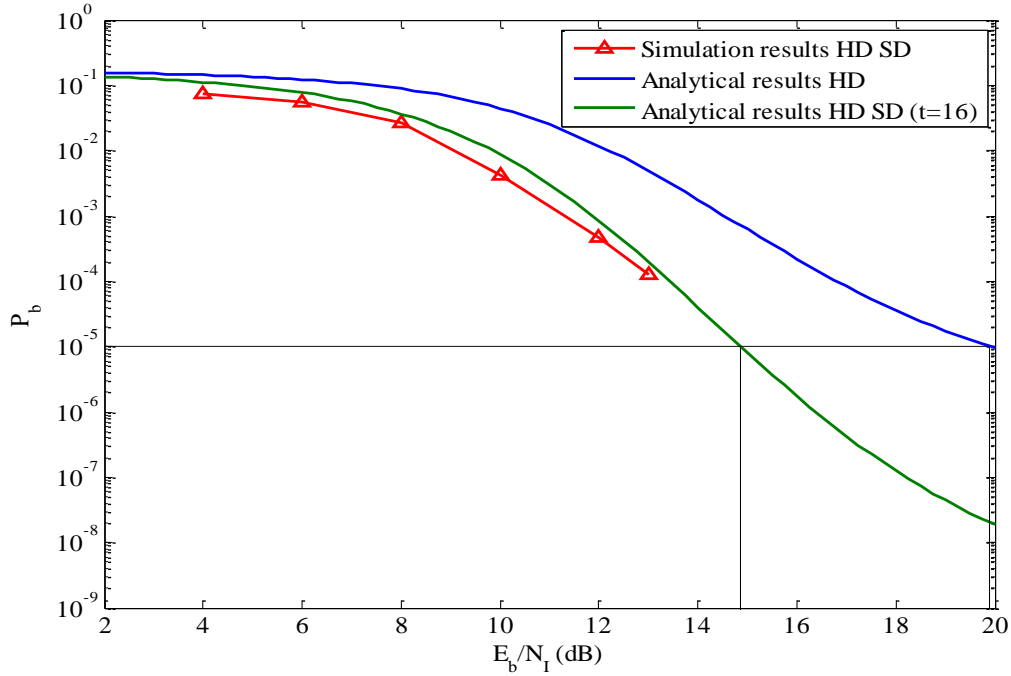
Figure 49.   Probability of bit error for double-symbol 8-FSK with (63, 39) RS encoding in both AWGN and PNI for $\rho = 0.2$ and $E_b/N_0 = 7$ dB.

For noncoherent demodulation, PNI degrades the performance of double-symbol 8-FSK with (63, 39) RS encoding in a manner similar to coherent demodulation as the interference probability ρ gets smaller. In general, noncoherent demodulation has worse performance when PNI is present than coherent demodulation. We examined a (63, 39) RS code with noncoherent demodulation for $E_b/N_0 = 7$ dB, a larger value than for coherent demodulation. For the case of the barrage noise interference, noncoherent demodulation has 5 dB worse performance than coherent demodulation.

From the results shown in Figures 47, 48, and 49, it is obvious that RS encoding in conjunction with double-symbol 8-FSK and hybrid HD SD decoding significantly improves performance when PNI is present. With only traditional HD decoding, $P_b = 10^{-5}$ can barely be achieved. Hybrid HD SD decoding yields coding gains of 5.4, 5.9, and 5.2 dB for ρ = 1, 0.4, and 0.2, respectively, over HD decoding. HD SD decoding significantly increases the error correction capability as in the AWGN only case.

Furthermore, the (63, 39) RS code was also examined for a higher value of $E_b/N_0 = 10$ dB. For $E_b/N_0 \geq 10$ dB, the probability of bit error is not improved significantly, especially when PNI is present. The probability of bit error for double-symbol 8-FSK with a (63, 39) RS code in both AWGN and PNI for ρ = 1, 0.4, 0.2 and $E_b/N_0 = 10$ dB is shown in Figures 50, 51 and 52, respectively. The results are summarized for PNI when $P_b = 10^{-5}$ in Table 32.

Table 32. Performance of double-symbol 8-FSK with (63, 39) RS encoding in both AWGN and PNI for $E_b/N_0 = 10$ dB when $P_b = 10^{-5}$.

| P_b	8 FSK RS (63, 39) $r = 39/63 = 0.62$	E_b/N_I (dB) ρ=1	E_b/N_I (dB) ρ=0.4	E_b/N_I (dB) ρ=0.2	Error Correction Capability t
10^{-5}	Simulation HD SD	8.5	10.3	10.7	16 16 17+
10^{-5}	Analytical HD SD	8.5	10.3	10.8	16 16 17
10^{-5}	Analytical HD	9.5	11.5	12.7	12

Figure 50.   Probability of bit error for double-symbol 8-FSK with (63, 39) RS encoding in both AWGN and PNI for $\rho = 1$ and $E_b/N_0 = 10\,$dB.
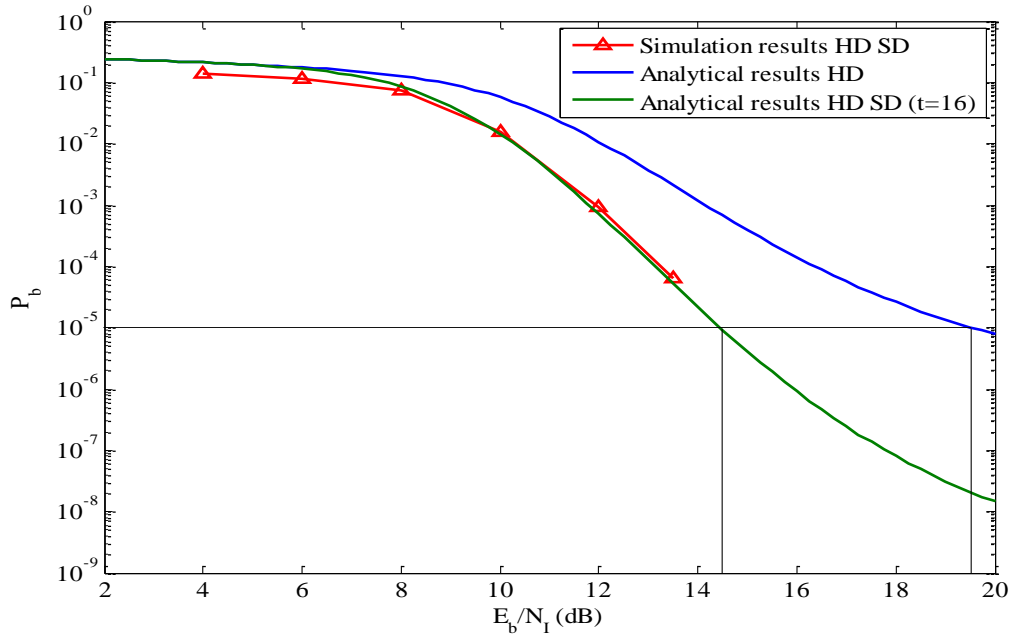

Figure 51.   Probability of bit error for double-symbol 8-FSK with (63, 39) RS encoding in both AWGN and PNI for $\rho = 0.4$ and $E_b/N_0 = 10\,$dB.
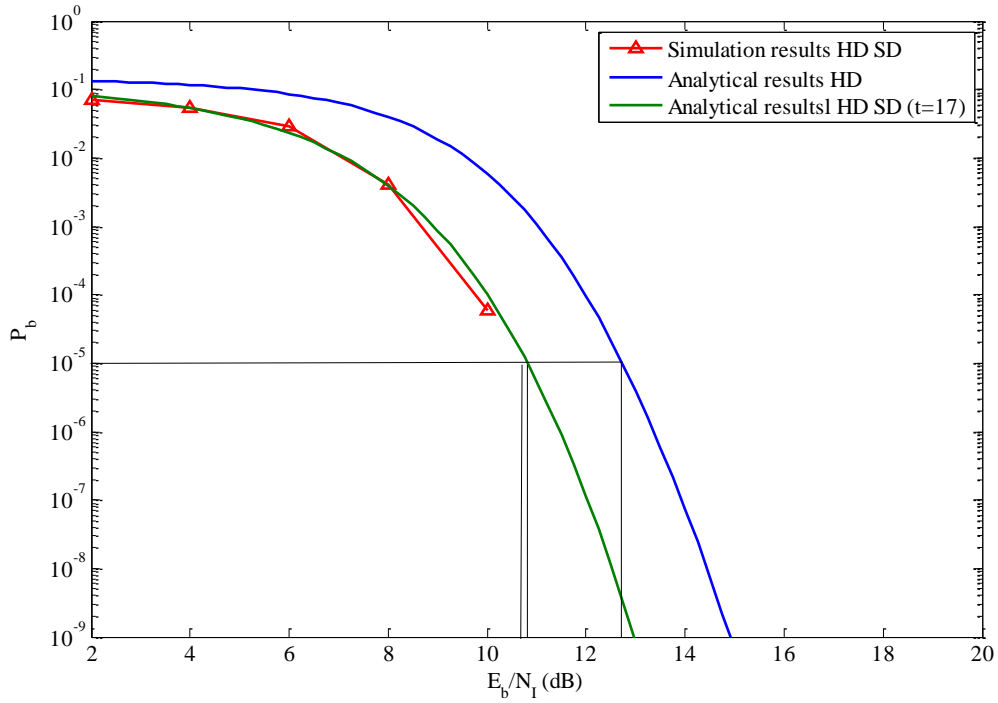
Figure 52.   Probability of bit error for double-symbol 8-FSK with (63, 39) RS encoding in both AWGN and PNI for $\rho = 0.2$ and $E_b/N_0 = 10$ dB.

The effect of PNI is degraded for such a high value of E_b/N_0. However, HD SD decoding improves performance by 1.0, 1.2 and 2 dB for $\rho = 1$, 0.4, and 0.2, respectively, compared to HD decoding. As E_b/N_0 increases, the coding gains become smaller for small probabilities ρ, but PNI is not as effective as with traditional HD decoding. Hybrid HD SD decoding increases the error correction capability t from twelve to sixteen for $\rho = 1$ and 0.4 and seventeen plus (17+) for $\rho = 0.2$. In order to achieve $P_b = 10^{-5}$, $E_b/N_I = 8.5$, 10.3 and 10.7 dB, respectively, is required for $\rho = 1$, 0.4, and 0.2.

2.   16-FSK

Finally, the performance of double-symbol 16-FSK with RS encoding and noncoherent demodulation in both AWGN and PNI was examined. The simulation and

analytical results are shown for a (255, 223) RS code in Figures 53, 54 and 55 for different values of ρ. In Table 33 the results are summarized when $P_b = 10^{-5}$.

Table 33.   Performance of double-symbol 16-FSK with (255, 223) RS encoding in both AWGN and PNI for $E_b/N_0 = 5.3\,\text{dB}$ when $P_b = 10^{-5}$.

P_b	16-FSK RS (255, 223) $r = 223/255 = 0.87$	E_b/N_I (dB) $\rho = 1$	E_b/N_I (dB) $\rho = 0.4$	E_b/N_I (dB) $\rho = 0.2$	Error Correction Capability t
10^{-5}	Simulation HD SD	17.7	17.8	19	26+ 26+ 27
10^{-5}	Analytical HD SD	20	20.5	19	26 26 27
10^{-5}	Analytical HD	-	-	-	16

Figure 53.   Probability of bit error for double-symbol 16-FSK with (255, 223) RS encoding in both AWGN and PNI for $\rho = 1$ and $E_b/N_0 = 5.3\,\text{dB}$.

Figure 54.   Probability of bit error for double-symbol 16-FSK with (255, 223) RS encoding in both AWGN and PNI for $\rho = 0.4$ and $E_b/N_0 = 5.3\,\text{dB}$.
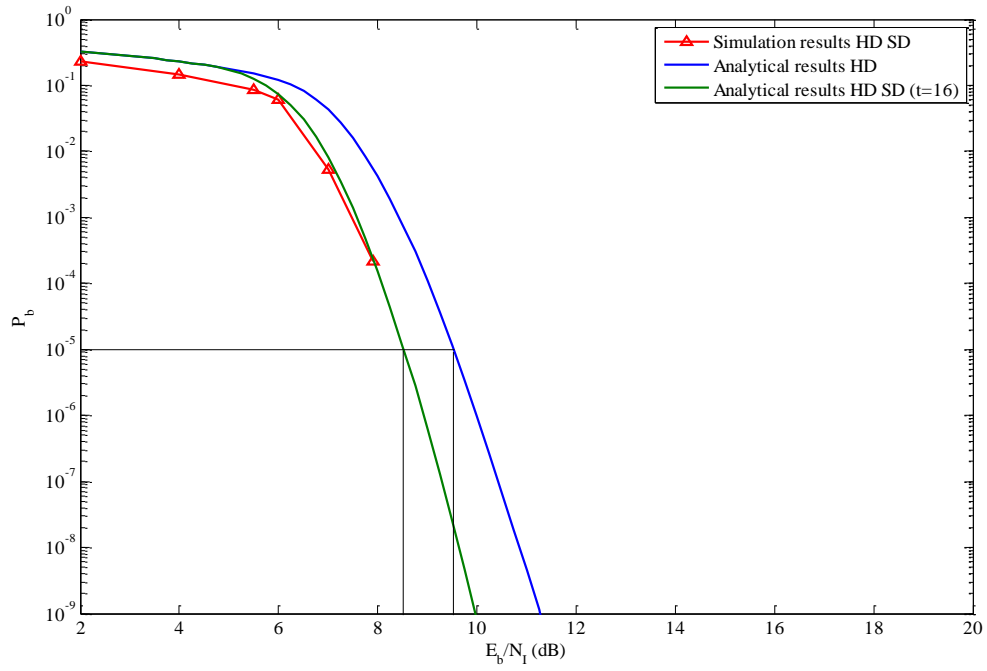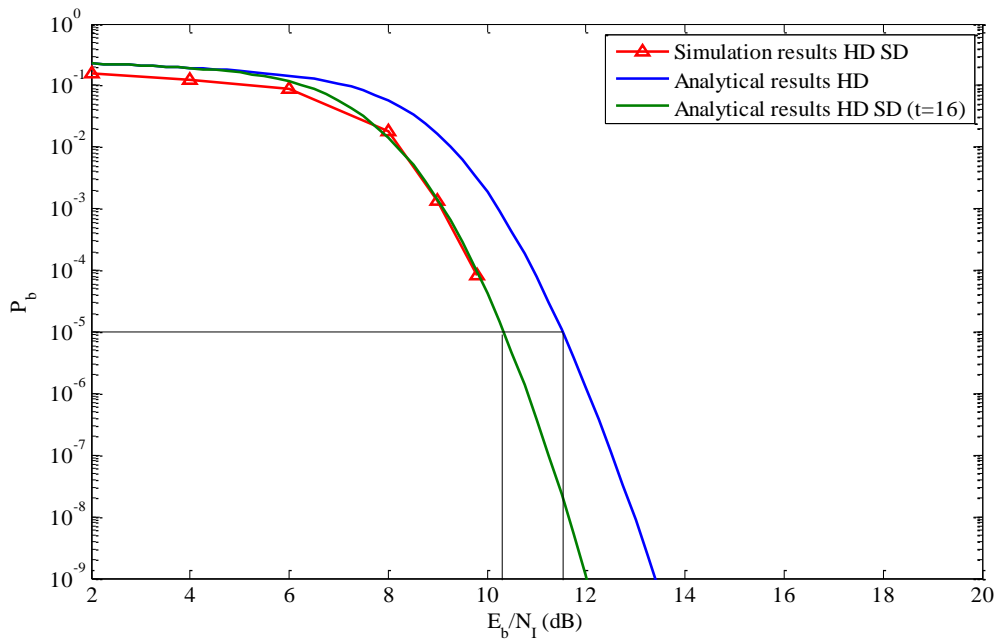

Figure 55.   Probability of bit error for double-symbol 16-FSK with (255, 223) RS encoding in both AWGN and PNI for $\rho = 0.2$ and $E_b/N_0 = 5.3\,\text{dB}$.

HD SD decoding yields much better performance than traditional HD decoding when PNI is present. For double-symbol 16-FSK with (255, 223) RS encoding, $P_b = 10^{-5}$ cannot be achieved with HD decoding when $E_b/N_0 = 5.3$ dB. With HD SD decoding, $P_b = 10^{-5}$ can be obtained when E_b/N_I is 17.7, 17.8, and 19.0 dB for $\rho = 1$, 0.4, and 0.2, respectively, and HD SD decoding increases the error correction capability from five for AWGN only to almost eleven when PNI is present. This significant improvement can be explained by the fact that PNI significantly affects the performance of double-symbol 16-FSK for (255, 223) RS code and HD decoding. Generally, as previously mentioned in Chapter IV, the performances of the higher order modulations are affected much more by PNI for similar E_b/N_0.

Next, the simulation and analysis results of double-symbol 16-FSK with a (255, 223) RS code for $E_b/N_0 = 10$ dB are presented. From Figures 56, 57 and 58, we can see that the required E_b/N_I for $P_b = 10^{-5}$ is 6.8, 9.5 and 11.4 dB for $\rho = 1$, 0.4 and 0.2, respectively. The results are summarized when $P_b = 10^{-5}$ in Table 34.

Table 34.   Performance of double-symbol 16-FSK with (255, 223) RS encoding in both AWGN and PNI for $E_b/N_0 = 5.3$ dB when $P_b = 10^{-5}$.

P_b	16-FSK RS (255, 223) $r = 223/255 = 0.87$	E_b/N_I (dB) $\rho = 1$	E_b/N_I (dB) $\rho = 0.4$	E_b/N_I (dB) $\rho = 0.2$	Error Correction Capability t
10^{-5}	Simulation HD SD	6.8	9.5	11.4	27 28+ 29
10^{-5}	Analytical HD SD	6.8	9.5	11.4	27 28 29
10^{-5}	Analytical HD	10.7	13.9	16.2	16
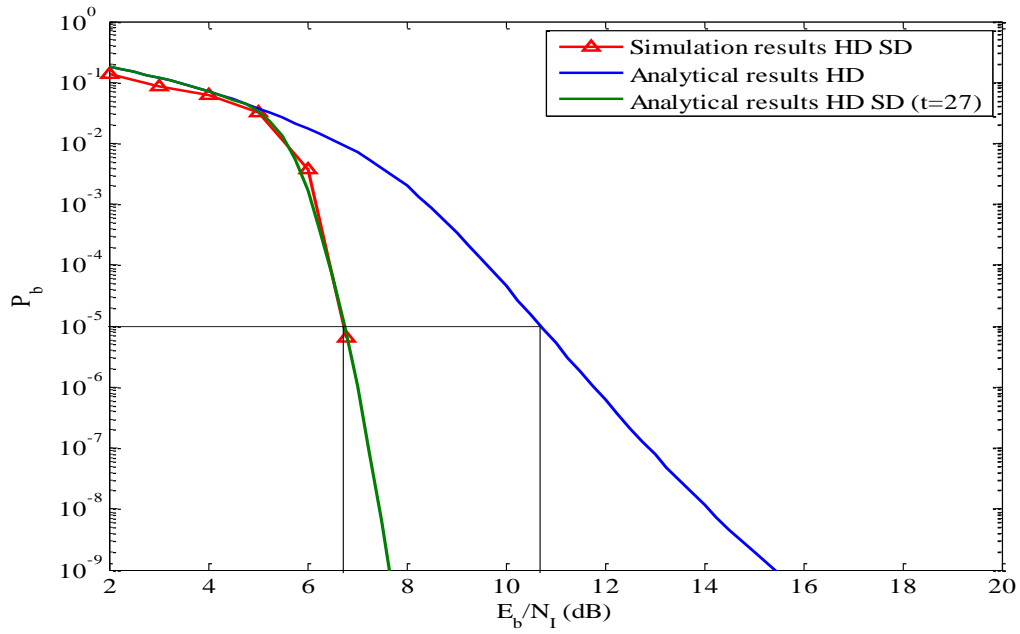
Figure 56.   Probability of bit error for double-symbol 16-FSK with (255, 223) RS encoding in both AWGN and PNI for $\rho = 1$ and $E_b/N_0 = 10\,\text{dB}$.
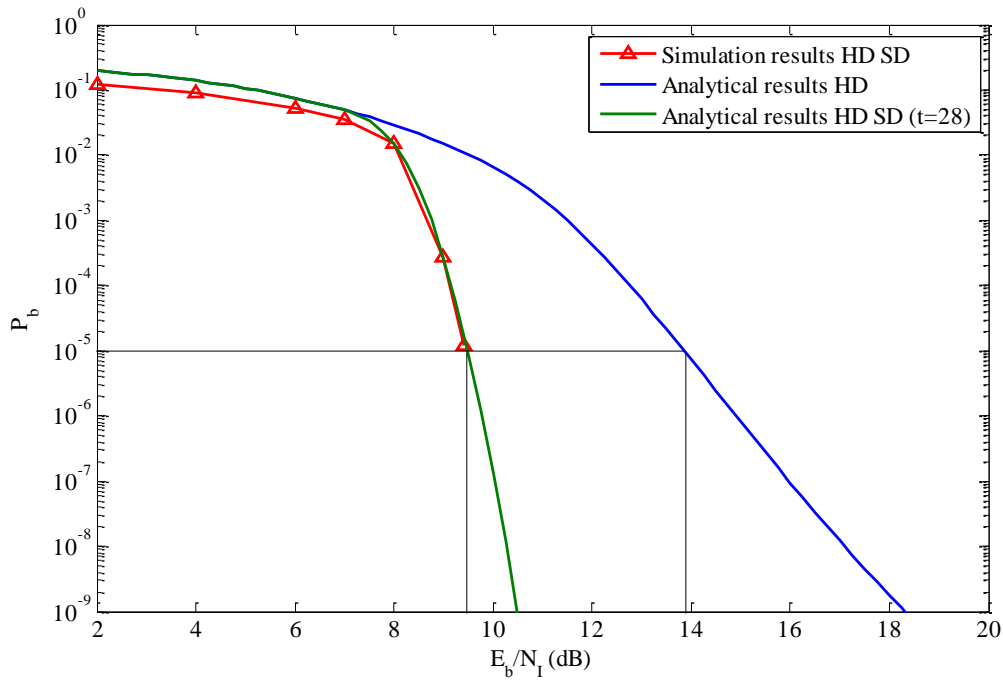
Figure 57.   Probability of bit error for double-symbol 16-FSK with (255, 223) RS encoding in both AWGN and PNI for $\rho = 0.4$ and $E_b/N_0 = 10\,\text{dB}$.
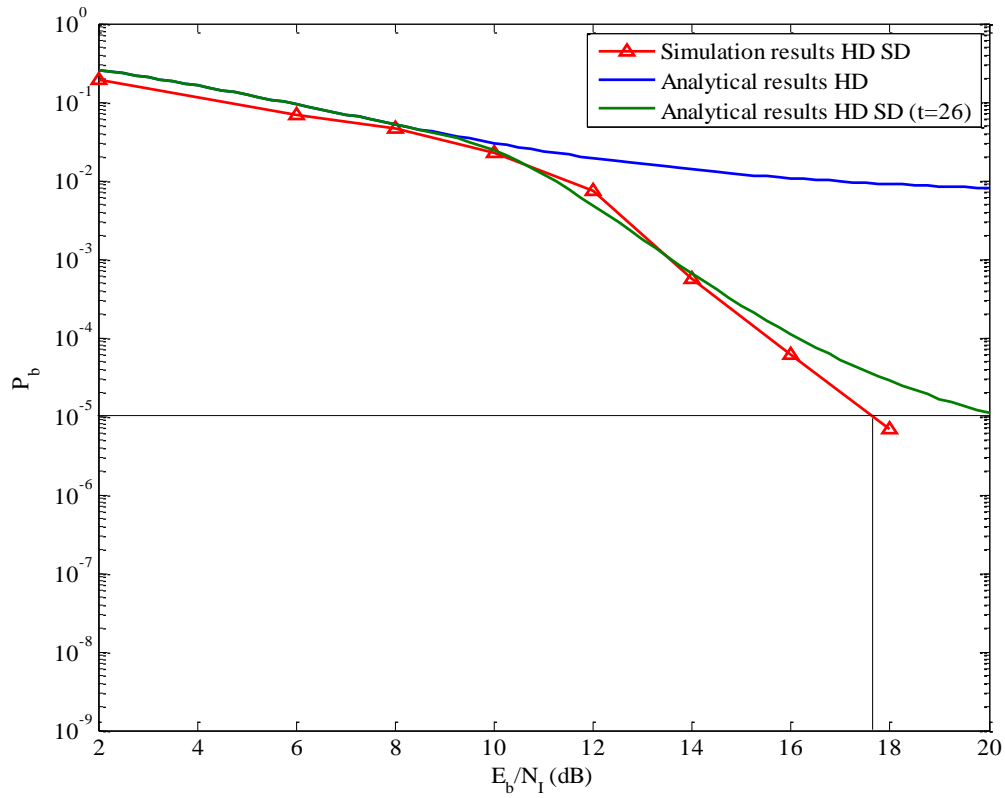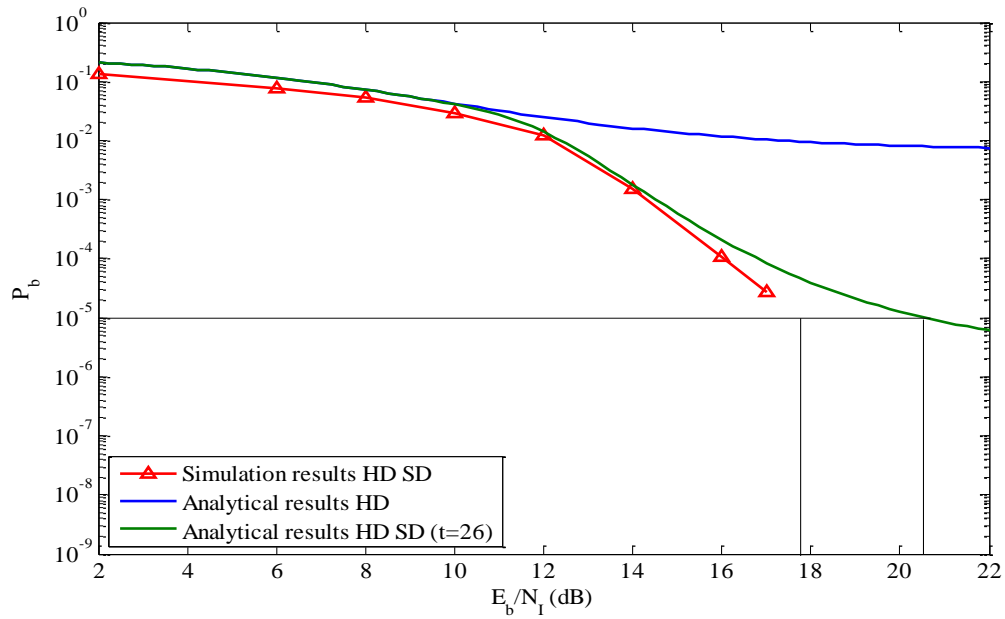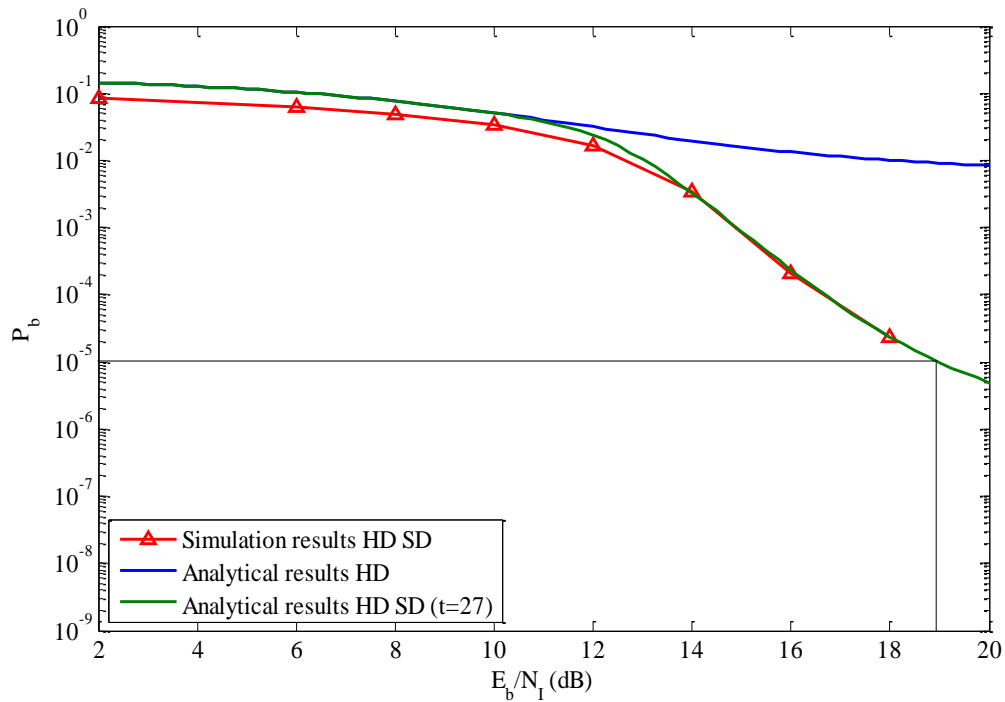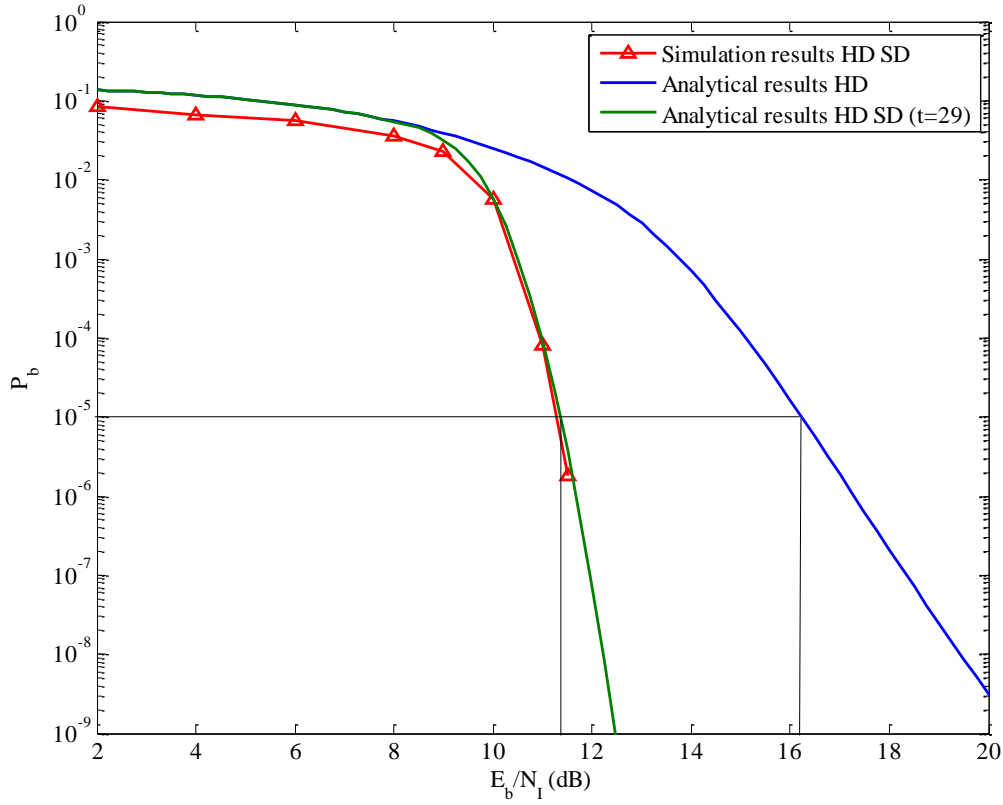
Figure 58.   Probability of bit error for double-symbol 16-FSK with (255, 223) RS encoding in both AWGN and PNI for $\rho = 0.2$ and $E_b/N_0 = 10\,\mathrm{dB}$.

It is obvious that for noncoherent demodulation, a 3 dB increase in E_b/N_0 corresponds to a huge improvement in performance for hybrid HD SD decoding. The coding gains are 3.9, 4.4 and 4.9 dB for $\rho = 1$, 0.4 and 0.2, respectively. Coherent detection with a (255, 223) RS code and HD SD decoding for the same value of E_b/N_0 has significantly less improvement in coding gain compared to traditional HD decoding. Specifically, HD SD decoding corrects eleven, twelve and thirteen more symbol errors per block. This vast improvement is justified by the fact that performance with traditional HD decoding is much worse for noncoherent detection as compared with coherent detection, as can be seen from comparing Tables 22 and 34.

C. CHAPTER SUMMARY

In this chapter, the effect of AWGN and PNI on *M*FSK with hybrid HD SD decoding and noncoherent demodulation was examined. Generally, HD SD decoding significantly improves the performance of noncoherent *M*FSK in a PNI environment. This vast improvement compared to AWGN only has to do with how the reliability information is modeled. As was mentioned at the beginning of this chapter, when the SD reliability information is calculated, the conditional PDFs are non-central chi-squared with two degrees of freedom, and the variances are computed by using only the effect of AWGN and not PNI.

From the simulation results, it was found that the HD SD algorithm can provide performance improvement only for double-symbol 8-FSK and 16-FSK. The error correction capabilities of the different code rates that were examined were generally the same as for AWGN only but in some cases improved for small probabilities of interference. For a (255, 223) RS code an even greater improvement when PNI was present compared to only AWGN is observed. Hybrid HD SD decoding is able to correct ten to thirteen more symbols errors per block than the traditional HD algorithm and five to eight more symbols errors per block when only AWGN is present. Comparing the error correction capability of HD SD decoding with the GS SD algorithm for the code rates (63, 39) and (255, 223) that were presented in this chapter, we have the results in Table 35.

Table 35.   Comparison of error corrections capabilities.

RS	HD SD *t* Error Correction	GS SD *t* Error Correction	HD *t* Error Correction
(15, 9)	4	3.4	3
(63, 39)	16-17	13.4	12
(255, 223)	26-29	16.5	16

The HD SD decoding significantly increases *t* as compared to traditional HD and GS SD decoding, especially for double-symbol transmission. This advantage is obtained for medium to high code rates, where the GS SD algorithm is not a powerful tool [13].

In the following chapter, the application of the results derived in this thesis in order to improve the performance of existing communication systems, such as ALE and JTIDS/LINK-16, is presented.

VII. APPLICATION OF HYBRID HD SD RS DECODING IN ALE AND JTIDS/LINK-16

In this chapter, the application of hybrid HD SD decoding to Automatic Link Establishment (ALE) and JTIDS/LINK-16 is examined. These two systems were chosen because ALE uses orthogonal signaling, specifically 8-FSK, and JTIDS/LINK-16 uses quasi-orthogonal signaling.

A.   AUTOMATIC LINK ESTABLISHMENT (ALE)

Automatic Link Establishment is the de-facto worldwide standard for initiating and sustaining communications using high frequency (HF) radio. HF radio conveys signals via ionospheric propagation, which is a constantly changing medium. ALE provides the capability to selectively call a specific HF station, a group of stations, a net, or a networked station. Automatic Link Establishment provides voice, data, text and internet messaging communication among users. ALE selects the most appropriate frequency to establish a communication link between two users from an available list of frequencies (channels), in which the channels are selected depending on the bit error rate for a specific address. The operators are notified by the system when the link is established, and they can immediately communicate. There is no need for longstanding, repetitive calling on pre-determined time schedules. All ALE users have a unique address in the ALE controller. Some military/commercial HF transceivers are available with ALE options. Amateur radio operators commonly use the PCALE sound card software ALE controller, interfaced to a ham transceiver via RS-232 CAT port, multi-frequency antenna. ALE has the advantage of not requiring expert users to constantly monitor and change the radio frequency manually to compensate for ionospheric conditions or interference. [32]

ALE provides rapid over-the-horizon communications, which is very useful for organizations that are managing widely separated units. It is used by law enforcement units, the coast guard and many other governmental organizations. ALE is also designated by the International Telecommunications Union (ITU) for international

emergency and disaster relief communications. Organizations that use ALE for extraordinary situation response are the Red Cross, FEMA, Disaster Medical Assistance Teams, NATO, the Federal Bureau of Investigation, the United Nations, the State of California Emergency Management Agency (CalEMA), other U.S. States' Offices of Emergency Services or Emergency Management Agencies, and Amateur Radio Emergency Service (ARES) [33]. Furthermore, ALE is going to be integrated into the Joint Tactical Radio System (JTRS). JTRS is the next-generation voice-and-data radio, which is going to be used by the U.S. military in field operations after 2010.

The ALE 2G waveform is 8-FSK and is compatible with 3 kHz single-sideband (SSB) narrowband voice channel transceivers. The orthogonal tones are between 750 and 2500 Hz. The duration of each tone is 8 ms, resulting in a transmitted channel symbol rate of 125 baud and a data rate of 375 bits per second. The ALE 2G data is formatted into 24-bit frames, which consist of a 3-bit preamble followed by three ASCII characters, each seven bits long. ALE 2G uses FEC coding and interleaving in order to improve link reliability and robustness, where the FEC code used is a (24, 12) Golay code. For 8-FSK modulation, the Golay code yields better performance than a (7, 5) RS code.

In this thesis, for ALE 2G we propose (63, 47) RS encoding with double-symbol 8-FSK modulation, coherent demodulation and hybrid HD SD decoding. The performances of the proposed and existing ALE 2G waveforms in AWGN are shown in Figure 59. The yellow line represents the performance of the existing ALE 2G waveform, and $E_b/N_0 = 7.0$ dB for $P_b = 10^{-5}$ is required. The blue line represents the performance of double-symbol 8-FSK with (63, 47) RS encoding, coherent demodulation and traditional HD decoding. For $P_b = 10^{-5}$, the required E_b/N_0 is 5.4 dB. Finally, the red and the green lines represent the simulation and analytical performances, respectively, of the proposed waveform, which requires $E_b/N_0 = 4.6$ dB for $P_b = 10^{-5}$. Hence, hybrid HD SD decoding provides a coding gain of approximately 3.5 dB over the existing ALE 2G waveform. Additionally, the proposed waveform requires 65% less bandwidth since the alternative system uses a higher code rate of $r = 0.746$ as compared to $r = 0.5$ for the (24, 12) Golay code.
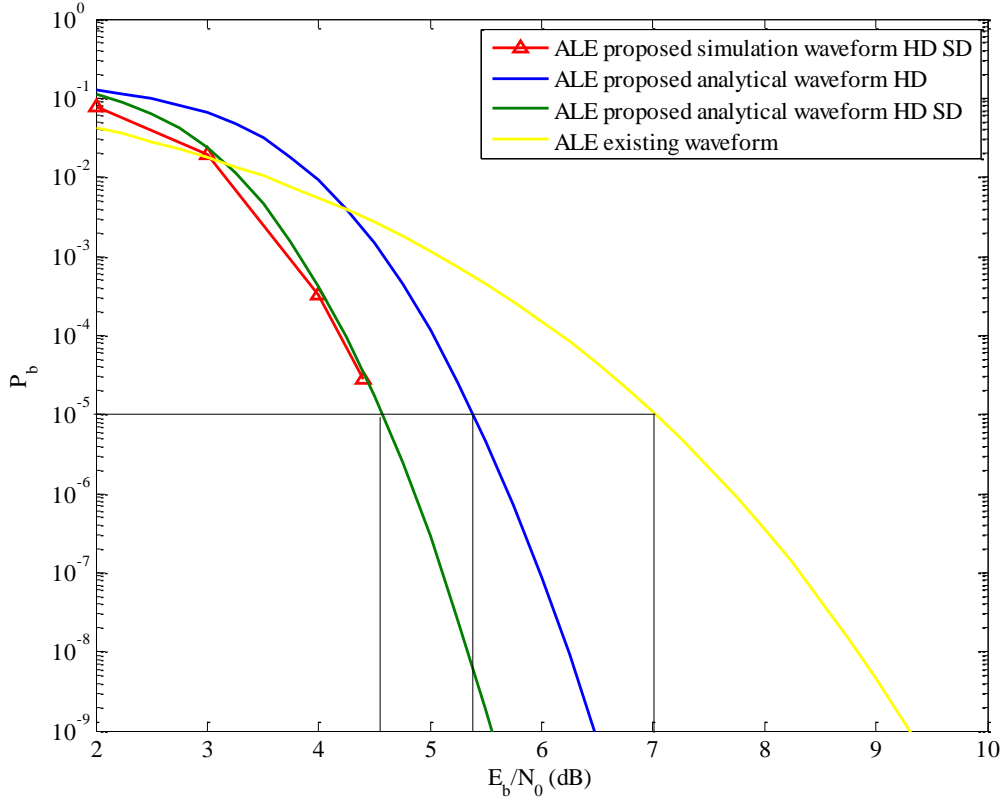
Figure 59.   Performances of the proposed and existing ALE waveforms for coherent demodulation in AWGN.

The performances of the existing ALE 2G and the proposed waveform when PNI is present when $E_b/N_0 = 10$ dB are shown in Figure 60. The triangles represent the simulation results for the proposed waveform, and the solid lines represent the analytical results for the existing ALE 2G waveform. The red, green and blue lines are the results for $\rho = 1$, 0.4 and 0.2, respectively, and correspond to coding gains of 4.2, 4.3, and 5.6 dB as compared to the existing waveform, respectively, when $P_b = 10^{-5}$. It is interesting that the results are the same for $\rho = 0.2$ and $\rho = 0.4$ (blue and green lines overlay). The implication is that the proposed waveform is more resistant to PNI than the existing ALE 2G.

91
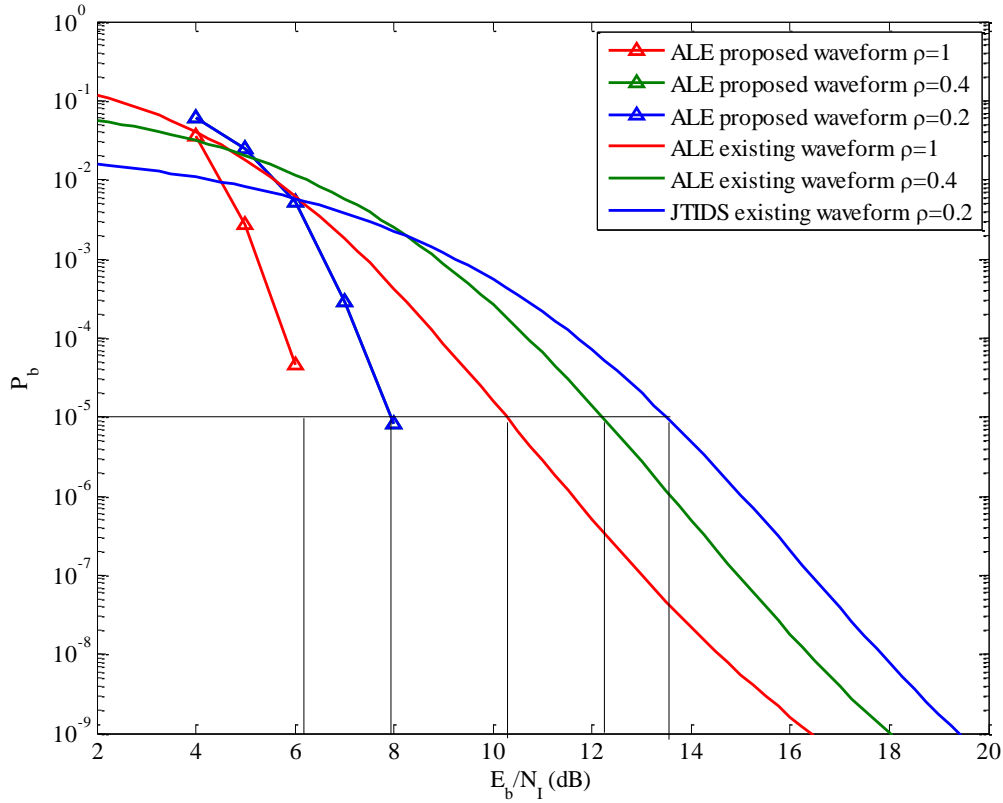
Figure 60.   Performances of the proposed and existing ALE waveforms for coherent demodulation in AWGN and PNI.

B.   JTIDS/LINK-16

Link-16/JTIDS operates in the L-band and is a system designed to withstand hostile interference. It uses a combination of time-division multiple access, frequency-hopping (FH), direct sequence spread spectrum (DSSS), Reed-Solomon encoding, and a 32-ary modulation scheme known as cyclic code-shift keying (CCSK). The CCSK modulation produces a 32-chip sequence to represent each 5-bit symbol. Prior to transmission, the CCSK sequence is converted to a DSSS signal via BPSK spreading using a 32 chip pseudo-noise sequence, and the individual chips are transmitted using minimum-shift keying modulation.

JTIDS is the communication component of Link-16. The JTIDS system hops over 51 different frequency bins at a rate of around 77,000 hops/s. The hop frequencies are in

the ultra HF band and range from 969 MHz to 1,206 MHz at 3 MHz intervals with two sub-bands centered at 1,030 MHz and 1,090 MHz excluded for IFF. The chip rate is 5.0 Mchips/s. [34]

One of the primary drawbacks to Link-16/JTIDS is limited data throughput, which reduces its effectiveness for the transmission of bulk data such as Intelligence, Surveillance and Reconnaissance (ISR) imagery or live video feeds. This constrains its usage to situational awareness functions, command and control, low data rate ISR functions, and weapons guidance. [34]

For Link-16/JTIDS we propose double-symbol 8-FSK modulation with (63, 47) RS encoding, noncoherent demodulation and hybrid HD SD decoding. Noncoherent demodulation is currently preferred for FH systems with fast hop rates. The performances of the proposed and existing waveforms are shown in Figure 61. The yellow line represents the analytical approximation for the existing waveform as derived in [24], [34]. The red and green lines represent the simulation and analytical results, respectively, for the proposed waveform. Lastly, the blue line represents the analytical results for the proposed waveform with traditional HD decoding.

We recognize that a hardware change to an existing system is not efficient and cost effective, especially for a system such as Link-16/JTIDS that was designed decades ago, but the intention is to depict the advantage of double-symbol transmission, RS encoding, and hybrid HD/SD decoding, especially when PNI is present. As can be seen in Figure 61, the proposed waveform yields a coding gain of approximately 2.1 dB for $P_b = 10^{-5}$ as compared to the existing Link-16/JTIDS waveform.
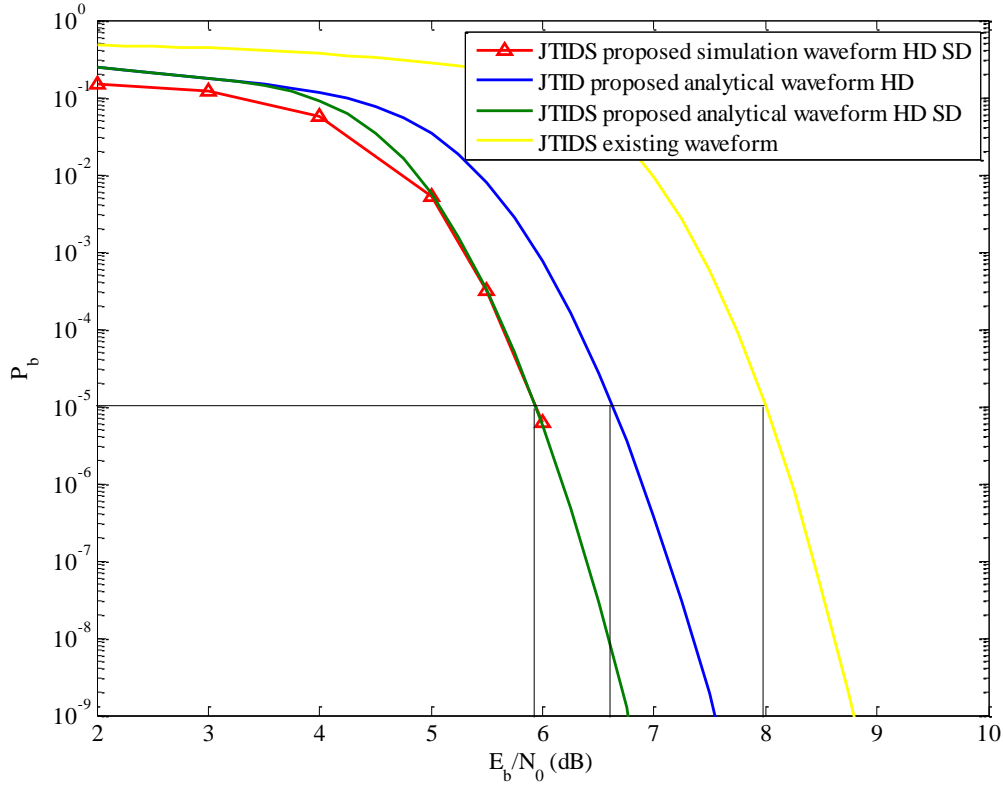
Figure 61.   Performances of the proposed and existing Link-16/JTIDS waveforms for noncoherent demodulation in AWGN.

8-FSK modulation requires less bandwidth than 32-ary CCSK [20, 21]. If we also take in consideration the higher code rate $r = 0.746$ of the proposed system as compared to the rate $r = 0.484$ of the existing one, we can easily see that in an era of increased bandwidth requirements for military users, the proposed waveform is much more efficient in terms of throughput than the existing one. As far as PNI is concerned, the performances of the proposed and existing Link-16/JTIDS waveforms in AWGN and PNI when $E_b/N_0 = 10$ dB are shown in Figure 62.
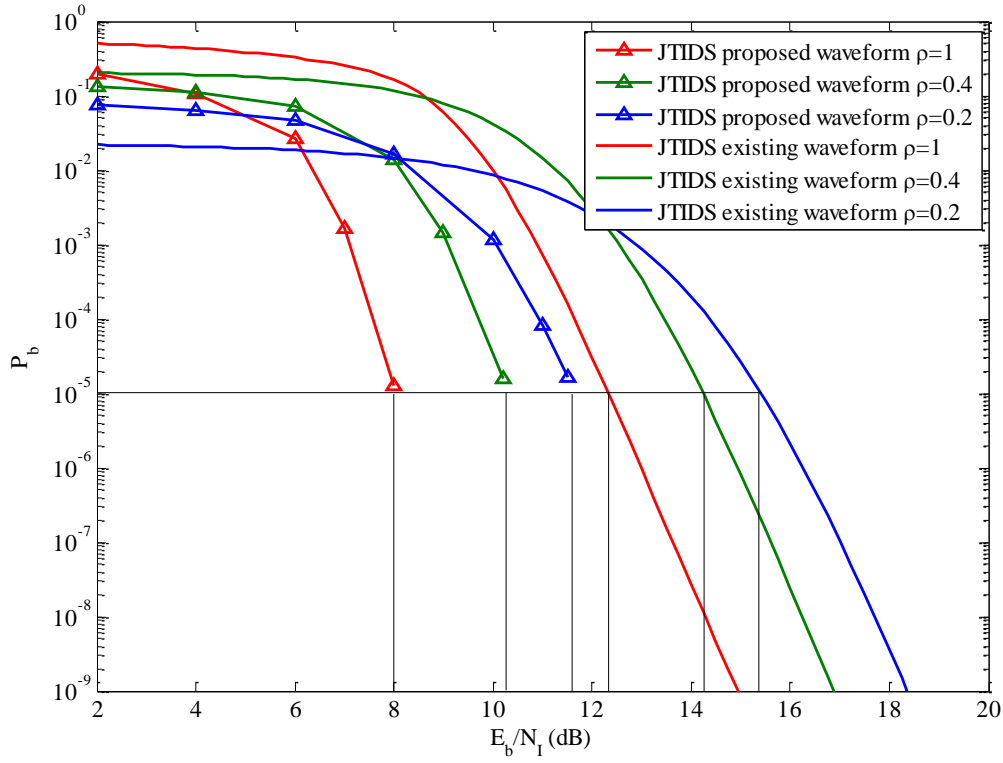
Figure 62.   Performances of the proposed and existing Link-16/JTIDS waveforms for noncoherent demodulation in AWGN and PNI.

In Figure 62 the triangles represent the simulation results for the proposed waveform (double-symbol 8-FSK with (63, 47) RS encoding and hybrid HD SD decoding), and the straight lines present the analytical results for the existing Link-16/JTIDS waveform. The red, green and blue lines represent the results for PNI with ρ = 1, 0.4 and 0.2, respectively, where it can be seen that the proposed waveform yields a coding gain of approximately 4.0 dB for $P_b = 10^{-5}$. Clearly, the proposed waveform yields increased resistance to PNI as compared to the existing Link-16/JTIDS waveform.

C.   CHAPTER SUMMARY

In this chapter, alternative waveforms were proposed for ALE 2G and Link-16/JTIDS utilizing double-symbol 8-FSK, RS encoding and hybrid HD SD decoding. The results showed significant improvement in both performance and bandwidth requirements, especially when PNI is present.   Hybrid HD SD decoding provides significant improvement as compared to the error correction capability of traditional HD RS decoding. Since the proposed waveforms utilize RS codes, and both ALE 2G and Link-16/JTIDS will be integrated into JTRS, they could decrease the complexity of the JTRS receivers and also significantly improve performance.

The last chapter of this thesis provides a summary of the conclusions made in previous chapters, as well as recommendations for future work.

VIII. CONCLUSIONS AND FUTURE WORK

A. CONCLUSIONS

The implementation of hybrid HD SD decoding for MFSK was presented in this thesis. The error correction capability of traditional HD decoding was extended by utilizing the soft decision reliability information of the channel for MFSK modulation, a power efficient modulation technique. Previously, HD SD decoding had only been shown to work with bandwidth efficient modulation techniques.

Initially, coherent demodulation was examined for AWGN both by simulation and analysis. For only AWGN and single-symbol transmission, HD SD decoding improves the performance only for $M = 16$ and for medium and low code rates for the reasons explained in Chapter III. The coding gains compared to traditional HD decoding was between 0.65 and 1.2 dB for medium and low code rates, respectively. HD SD decoding performs better with longer block lengths and double-symbol MFSK. For longer block lengths, HD SD decoding is limited to $M = 8$ and 16. As was discussed for $M = 32$, about twenty more symbol errors per block must be corrected in order to improve the performance only 0.2 dB. Additionally, for such large block lengths, the decoding time is increased dramatically.   The coding gains for double-symbol transmission were between 0.2 and 0.8 dB, depending on the order of the modulation and the code rate.

Coherent demodulation was also examined for both AWGN and PNI. In this case, the soft decision reliability information utilized was modified. Specifically, when the statistics of the channel are calculated, the effect of PNI is ignored. In that way, the HD SD algorithm is able to distinguish the jammed symbols from the unjammed ones. The improvement in performance is significant. The results also depend on the value of E_b/N_0 . A value of E_b/N_0 that corresponds to $P_b = 10^{-8}$ when only AWGN is present was examined as well as a larger E_b/N_0 . The achieved coding gains were almost 5 dB at times. HD SD decoding was able to correct more symbol errors per block for smaller

probabilities of interference ρ. It is interesting that for single-symbol and double-symbol 8-FSK, HD SD decoding performs better for smaller probabilities ρ, and for these cases the jammer loses the advantage that it has with traditional HD decoding.

Noncoherent demodulation for AWGN and PNI was also examined. Two significant observations are that HD SD decoding for noncoherent demodulation improves the performance only for double-symbol transmission. This is related to the different SD statistics used. Second, for a (255, 223) RS code in AWGN and PNI, HD SD decoding offers a vast performance improvement compared to the traditional HD algorithm. In general, and for all the other cases, HD SD decoding with noncoherent demodulation provides improvement similar to that obtained with coherent demodulation. The error correction provided is slightly less than for the coherent case.

B.   FUTURE RESEARCH AREAS

HD SD decoding in the event of a decoding failure selects n symbols received with low probabilities and creates new code symbol estimates by utilizing the channel statistics and selecting the symbol received with the second highest conditional probability. In this way, when a failure occurs, up to 2^n possible decoding lists are created. In previous research [2], [3], a maximum of $n = 9$ was used. Throughout this thesis, $n = 10$ was utilized. We could increase this more, but this would dramatically increase decoding time.

For future work, we suggest further increasing n in combination with the parallel programming capabilities of Matlab. When the 2^n possible iterations are calculated we can break the matrix into smaller matrices that use different HD RS decoders. This could decrease decoding time significantly. Furthermore, as we have seen, the HD SD algorithm does not perform very efficiently with short block lengths, even though all the incorrectly received symbols can be examined. This means that, for smaller block lengths, the correct symbol may not be the one with second highest conditional probability, but may be the third or even fourth. Other possible future work could be to change the base number 2 in the HD SD algorithm. For the single symbol-transmission and $M = 8$, we tried 3^6 iterations, but the algorithm still did not work efficiently.

Finally, it would be interesting to examine the performance in a PNI environment for even smaller probabilities of interference. In this thesis, we used $\rho = 1, 0.4$ and 0.2.

THIS PAGE INTENTIONALLY LEFT BLANK

LIST OF REFERENCES

[1]   C. Shannon, "A mathematical theory of communication," *Bell System Technical Journal*, vol. 27, pp. 379–423 (Part I) and pp. 623–656 (Part II), 1948.

[2]   J. Caldwell, "*M*-ary hyper phase shift keying with forward error correction coding," PhD dissertation, Naval Postgraduate School, Monterey, CA, 2009.

[3]   J. Caldwell and C. Robertson, "*M*-ary hyper phase-shift keying with Reed Solomon encoding and soft decision reliability information," *Proceedings IEEE Military Communications Conference,* Oct. 2009.

[4]   C. Wilson, "Network centric operations: Background and oversight issues for Congress," *CRS Report for Congress* (CRS RL32411), Mar. 2007.

[5]   C. Kopp, "Network Centric Warfare Fundamentals—Part 3" [Online]. Available at: http://www.ausairpower.net/NCW-101-3.pdf (accessed January 16, 2010).

[6]   S. Lin and D. Costello, *Error Correction Coding*. 2nd ed., New Jersey: Prentice Hall, 2004.

[7]   R. C. Robertson, class notes for EC4580 (Error Correction Coding), Department of Electrical and Computer Engineering, Naval Postgraduate School, Monterey, CA, 2007 (unpublished).

[8]   D. Gorenstein and N. Zierler, "A class of error correcting codes in *pm* symbols," *Journal of the Society of Industrial and Applied Mathematics,* vol. 9, pp. 207–214, June 1961.

[9]   G. D. Forney, "On decoding BCH codes," *IEEE Transactions on Information Theory,* vol. IT-11, pp. 549–557, October 1965.

[10]   R. T. Chien, "Cyclic decoding procedure for the Bose-Chaudhuri-Hocquenghem Codes," *IEEE Transactions on Information Theory,* vol. IT-10, pp. 357–363, October 1964.

[11]   E. R. Berlekamp, "Nonbinary BCH Decoding," *Proceedings International Symposium Information Theory*, San Remo, Italy, 1967.

[12]   J. L. Massey, "Shift register synthesis and BCH decoding," *IEEE Transactions on Information Theory,* vol. IT-15, Number 1, pp. 122–127, Jan. 1969.

[13]   V. Guruswami and M. Sudan, "Improved decoding of Reed-Solomon and algebraic-geometric codes," *IEEE Transactions on Information Theory*, vol. 45, no. 5, pp. 1757–1767, 1999.

[14]   M. Sudan, "Decoding of Reed Solomon codes beyond the error-correction Bound," *Journal of Complexity,* vol. 13, pp. 180–193, 1997.

[15]   R. Koetter and A. Vardy, "Algebraic Soft-Decision Decoding of Reed-Solomon Codes," *IEEE Transactions on Information Theory*, vol. 49, no. 11, pp. 2809–2825, 2003.

[16]   R. Roth and G. Ruckenstein, "Efficient decoding of Reed-Solomon codes beyond half the minimum distance," *IEEE Transactions on Information Theory*, vol. 46, pp. 246–257, Jan. 2000.

[17]   D. Augot and A. Zeh, "On the Roth and Ruckenstein equations for Guruswami-Sudan algorithm," *Proceedings of the IEEE ISIT Conference*, 2008.

[18]   X. Wu and P. Siegel, "Efficient root-finding algorithm with application to list decoding of algebraic-geometric codes," *IEEE Transactions on Information Theory*, vol. 47, pp. 2579–2587, Sep. 2001.

[19]   V.Guruswami and A.Rudra, "Limits to List Decoding Reed Solomon Codes," *IEEE Transactions on Information Theory,* vol. 52, pp. 3642–3649, August 2006.

[20]   B. Sklar, *Digital Communications. Fundamentals and Applications*, 2nd ed. Upper Saddle River, NJ: Prentice Hall PTR, 2001.

[21]   J. G. Proakis and M. Salehi, *Digital Communications*, 5th ed. New York: McGraw-Hill Higher Education, 2008.

[22]   R. C. Robertson, class notes for EC4550 (M-ary Digital Communication Systems), Department of Electrical and Computer Engineering, Naval Postgraduate School, Monterey, CA, 2007 (unpublished).

[23]   D. Lekkakos, "Performance Analysis of a Link-16/JTIDS Compatible Waveform Transmitted Over a Channel with Pulse-Noise Interference," Master's thesis, Naval Postgraduate School, Monterey, CA, 2008.

[24]   AHA Application Note, "Primer: Reed-Solomon Error Correction Codes (ECC)," Comtech AHA Corporation subsidiary of Comtech Telecommunications Corporation [Online]. Available at: http://www.csupomona.edu/~jskang/files/rs1.pdf (accessed March 2, 2010)

[25]   J. Sylvester, "Reed Solomon Codes," Elektrobit (EB) Corporation [Online]. Available at: http:// www.aha.com/pubs/anrs01_0404.pdf (accessed March 5, 2010)

[26]   A. Duggan and A. Barg, "Performance Analysis of Algebraic Soft-Decision Decoding of Reed–Solomon Codes," *IEEE Transactions on Information Theory*, vol. 54, no. 11, pp. 5012–5018, 2008.

[27]   N. Chen and Z. Yan, "Complexity analysis of Reed-Solomon decoding over GF (2^m) without using syndromes," *EURASIP Journal on Wireless Communication and Networking*, Article 843634, 2008.

[28]   W. W. Peterson, "Encoding and error-correction procedures for Bose-Chaudhuri codes," *IRE Transactions on Information Theory*, vol. IT-6, pp. 459–470, 1960.

[29]   G. Clark and J. Cain, *Error-Correction Coding for Digital Communication*. New York: Plenum Press, 1981.

[30]   J. Caldwell and C. Robertson, "*M*-ary Hyper Phase Shift Keying with Reed Solomon Encoding and Soft Decision Reliability Information," *Proceedings. IEEE Military Communications Conference,* Oct. 2009.

[31]   R. C. Robertson, class notes for EC3510 (Digital Communications), Department of Electrical and Computer Engineering, Naval Postgraduate School, Monterey, CA, 2009 (unpublished).

[32]   Department of Defense Interface Standard, "MIL STD 188-141B," March 1999.

[33]   B. Crystal B, and A. Barrow., "ALE for Emergency / Disaster Relief Communications," 2007 [Online]. Available at: http://www.hflink.com/garec/garec2007/index_files/v3_document.htm (accessed March 18, 2010)

[34]   R. C. Robertson, class notes for EC4560 (Spread Spectrum Communications), Department of Electrical and Computer Engineering, Naval Postgraduate School, Monterey, CA, 2007 (unpublished).

[35]   C.-H. Kao, "Performance Analysis of JTIDS/Link-16-type Waveform Subject to Narrowband Waveform over Slow, Flat Nakagami Fading Channels," *Proc. IEEE MILCOM,* Nov. 2008.

[36]   *J. Caldwell an*d C. Robertson, "Long Block Length Reed S*olomon Coded M-ary Hyper Phase Shift Keying," Proceedings of Asilomar Conference on Signals, Systems, and Computers,* Oct. 2008.

THIS PAGE INTENTIONALLY LEFT BLANK

INITIAL DISTRIBUTION LIST

1. Defense Technical Information Center
   Ft. Belvoir, Virginia

2. Dudley Knox Library
   Naval Postgraduate School
   Monterey, California

3. Professor R. Clark Robertson, Chairman
   Department of Electrical and Computer Engineering
   Naval Postgraduate School
   Monterey, California

4. Associate Professor Frank Kragh
   Department of Electrical and Computer Engineering
   Naval Postgraduate School
   Monterey, California

5. Professor Roberto Cristi
   Department of Electrical and Computer Engineering
   Naval Postgraduate School
   Monterey, California

6. Embassy of Greece
   Office of Naval Attaché
   Washington, District of Columbia

7. LT Konstantinos Spyridis
   Hellenic Navy General Staff
   Athens, Greece